博士論文番号：1381202

(Doctoral student number)

Molecular mechanism of sodium acetate tolerance caused by the Thr255Ala mutation in the yeast ubiquitin ligase Rsp5p

Watcharawipas Akaraphol

Nara Institute of Science and Technology

Graduate School of Biological Sciences

Prof. Hiroshi Takagi

Submitted on 2017/01/23

TABLE OF CONTENTS

ABSTRACT

Protein ubiquitination is one of the fundamental cellular processes for regulating cellular activities at the post-translational level through protein modification by the small regulatory protein ubiquitin. This process is catalyzed by series of enzymatic reactions, the final step of which requires ubiquitin ligase. The essential protein Rsp5, which is a homologous to the E6AP carboxyl terminus (HECT)-type ubiquitin ligase of the yeast *Saccharomyces cerevisiae*, as well as its human orthologue Nedd4, play important roles in the regulation of diverse cellular processes, such as environmental stress responses, nutrient signal transduction, quality control of plasma membrane proteins, intracellular protein trafficking, and potentially monovalent cation homeostasis through the interaction and ubiquitination of various substrate proteins. Rsp5 recognizes the substrate through the interaction between its WW domains and PY motifs in the substrate. However, in most cases, the substrates of Rsp5 do not contain the PY motifs, and thus, Rsp5 utilizes the PY-motif containing adaptor proteins to mediate the interaction with different substrates. Precise substrate recognition via the WW domains of Rsp5 and various adaptor proteins is necessary because this leads to specific protein ubiquitination and cellular responses. Recently, my lab discovered that the substitution of a conserved Thr255 to Ala (T255A) in the WW1 domain of Rsp5 confers tolerance to sodium acetate (NaAc) stress on *S. cerevisiae* cells (Wijayanti *et al., J. Biochem.,* 2015). This finding raised the novel possibility that Rsp5 and its substrate recognition are involved in NaAc stress responses. Acetate is one of the fermentation inhibitors generated during the pretreatment of lignocellulosic biomass from highly acetylated hemicellulose and has been shown to inhibit growth and reduce ethanol production in *S. cerevisiae*. The recent report reveals that the presence of Na^+, but not K^+, provides a synergistic inhibitory effect to acetate. This raises the significance of NaAc stress in bioethanol production from lignocellulosic biomass. Here, I aimed to elucidate the molecular mechanism underlying NaAc stress tolerance, which is potentially useful for breeding industrial bioethanol yeasts.

First, a newly found T255A mutation in the *RSP5* gene was phenotypically and genetically characterized. The T255A mutant specifically increased the tolerance to NaAc, but not to NaCl or acetic acid, indicating that NaAc stress responses were unique and different from that of NaCl or acetic acid. To determine whether the T255A mutation is gain- or loss-of-function, the NaAc tolerant phenotype of the T255A mutant was compared with that of the Ala401Glu (*rsp5*^{A401E}) and Leu733Ser (*rsp5*^{L733S} or *rsp5-1*) mutants, both of which are classified as loss-of-function *rsp5* mutants. As A401E and L733S mutants were more sensitive to NaAc, the T255A mutation was regarded as gain-of-function. In diploid cells, the heterozygous T255A mutant grew similar to the wild-type strain under NaAc stress conditions, whereas the homozygous T255A mutant exhibited higher NaAc tolerance, indicating that the T255A mutation is recessive. Based on these results, it was suggested that Rsp5 ubiquitination activity is required for NaAc tolerance, and it appears that the recessive allele of *rsp5*^{T255A} specifically enhances this phenotype by unknown mechanism(s).

To find a clue to molecular mechanisms by which the T255A mutation confers NaAc tolerance, I focused on genetic interaction with the high osmolarity glycerol (HOG) signaling pathway. Activation of the Hog1 mitogen-activated protein kinase (MAPK) is the key to hyperosmotic stress responses, as well as to Na^+ or acetate stress responses, through

intracellular glycerol accumulation that counteracts with loss of cytoplasmic water. Here, in my study, genetic analysis revealed that the NaAc tolerance increased by the T255A mutation was fully abrogated by disruption of the *HOG1* gene or the *PBS2* gene, which encodes a MAPK kinase (MAPKK) upstream of Hog1. This result indicates that the NaAc tolerance of the T255A mutant is dependent on the Hog1 MAPK signaling. To determine whether the T255A mutation enhances activation of Hog1, western blot analysis was performed to detect the phosphorylated form of Hog1 under NaAc stress conditions. The result showed that the T255A mutation did not affect the timing and the intensity of Hog1 phosphorylation triggered by NaAc stress, suggesting that it functions at the downstream level of Hog1. To identify the downstream target of Hog1, three putative ones were tested: (i) *FPS1*, encoding an aquaglyceroporin channel involved in acetate uptake; (ii) *NHA1*, encoding a Na^+/H^+ antiporter required for Na^+ extrusion under acidic conditions; (iii) *ENA1*, *ENA2*, and *ENA5* (*ENA1/2/5*), encoding P-type ATPase Na^+ extrusion pumps crucial for long-term maintenance of cation homeostasis. As a result, the triple disruption of the *ENA1/2/5* genes strongly suppressed the NaAc tolerance of the T255A mutant, although disruption of the *FPS1* or *NHA1* gene did not affect the phenotype of wild-type and T255A mutant cells. This result suggests that the NaAc tolerance of the T255A mutant is dependent on the Ena1/2/5 Na^+ extrusion system and is mostly involved in Na^+ tolerance in the presence of acetate. Therefore, I further focused on the analysis of intracellular Na^+ contents using the inductively coupled plasma mass spectrometry (ICP-MS). As expected, the steady-state level of intracellular Na^+ content in the T255A mutant was significantly lower than that of the wild-type strain under NaAc stress conditions, and this difference was cancelled when the *ENA1/2/5* genes were disrupted, as well as in the *HOG1*-deleted cells. Based on these data, it was concluded that the T255A mutation alleviates NaAc stress via positively regulating Na^+ extrusion through Ena1/2/5.

Although the target of Rsp5 is still unknown, in many cellular processes, adaptor proteins mediate the function of Rsp5. Thus, genetic screening was performed to identify the adaptor proteins required for the NaAc tolerance of the T255A mutant. Among known Rsp5 adaptor proteins, Bul1 and Bul2 (Bul1/2), Art1, and Rim8 were found to be involved in the NaAc tolerance of the T255A mutant. Most notably, disruption of the *RIM8* gene severely abolished the NaAc tolerance and increased the intracellular Na^+ content of the T255A mutant under NaAc stress condition. As previously reported, yeast cells lacking *RIM8* exhibit a defect in Ena1 trafficking to the plasma membrane under NaCl stress condition. Hence, together with my findings, this emphasizes the role of Rim8 in Na^+ detoxification system. Rsp5 is known to physically interact and ubiquitinate Rim8. However, in my study, Rim8 ubiquitination and its interaction with Rsp5 were not necessary for the NaAc tolerance, suggesting that Rsp5 functions at the downstream level of Rim8. Recent studies reported that Rim101 complex downstream of Rim8 also plays a role in proper accumulation of Ena1 at the plasma membrane and the ubiquitination activity of Rsp5 is essential for the formation of Rim101 complex. Thus, it is intriguing to hypothesize that if the T255A mutant positively affects either its interaction or ubiquitination toward an unidentified target in the Rim101 complex, leading to enhanced Ena1/2/5 trafficking to the plasma membrane.

Elucidation of this molecular mechanism will contribute to better understanding how the Nedd4-family ubiquitin ligases recognize their substrate for cellular responses to environmental changes, as well as to improvement of industrial yeast strains for bioethanol production.

CHAPTER I
INTRODUCTION

1. Bioethanol production from lignocellulosic biomass and its related stresses

Bioethanol is one of the most important alternative transportation fuels due to its environmental friendliness. At present, major biomass utilized in the bioethanol production is mainly relied on food crops such as sugar cane and corn grain (Sánchez and Cardona, 2008). However, there has been a growing concern regarding an intervention between food and energy sectors since sugar cane and corn grain are also utilized for food production. For decades, many attempts have been employed to develop economically effective bioethanol production system using non-edible biomasses which are lignocellulosic materials e.g. corn stover, corn fiber, rice straw, bagasse, and wheat straw. Lignocellulosic biomass is the promising resource for bioethanol production since it consists up to 70% carbohydrates in the forms of cellulose and hemicellulose and is potentially cheaper than sugar cane and corn grain (Zaldivar *et al*., 2001). However, both cellulose and hemicellulose form close complex with lignin in the plant cell wall. To open this structure, dilute acid hydrolysis is employed due to economic reasons together with stream explosion, liquid hot water, etc (Balat *et al*., 2008). By these methods, not only sugars but also various compounds are generated (Palmqvist and Hahn-Hägerdal, 2000). Many of them are derived from the breakdown of sugars (e.g. furfural, hydroxymethylfurfural (HMF), formic acid, levulinic acid, and acetic acid). Some of them are phenolic compounds derived from the degradation of lignin (e.g. vanillin and 4-hydroxybenzoic acid) (Figure 1). These compounds have been shown to be the fermentation inhibitors in many studies (Klinke *et al*., 2004). For examples, furfural and HMF have been shown to reduce enzymatic and biological activity which in turn induce oxidative stress via the generation of reactive oxygen species (ROS) as well as cause the breakdown of DNA (Modig *et al*., 2002; Khan and Hadi, 1994). Vanillin has also been shown to repress the translation in yeast cells and cause the activation of Yap1 which might be related to oxidative stress response (Nguyen *et al*., 2014). Unlike the generation of furan and phenolic compounds which can be reduced via the process optimization, acetic acid is released from hemicellulose which is highly acetylated (Almeida *et al*., 2007). Thus, acetate always exists in lignocellulosic hydrolylates over 10 g/L at pH 5-6 (Klinke *et al*., 2004; Palmqvist and Hahn-Hagerdal, 2000). Acetate has been shown to inhibit growth and fermentation ability of the budding yeast *Saccharomyces cerevisiae* in many studies (Bellissimi *et al*., 2009; Almeida *et al*., 2007; Pampulha and Loureire-Dias, 1989). Therefore,

development of industrial yeast strains with acetate tolerance could be one of the promising strategies for improving bioethanol production from lignocellulosic biomass. The following section will be focused on the toxicity of acetate and adaptive mechanisms of yeast cells to acetate stress.

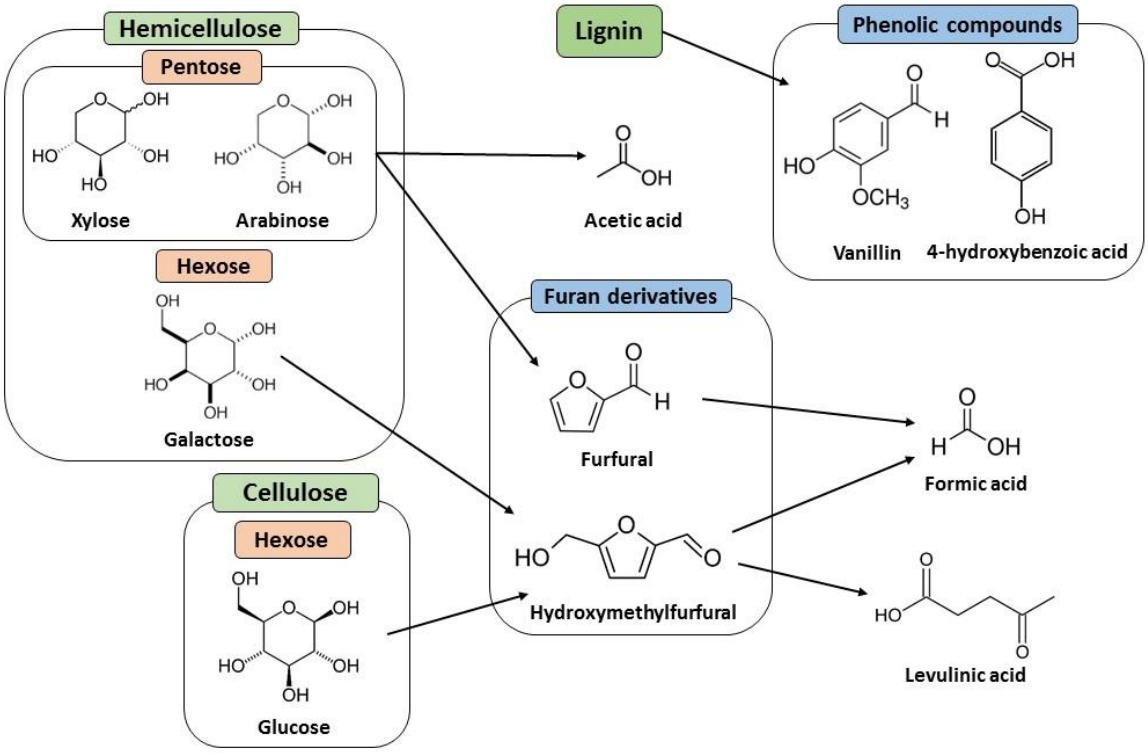

Figure 1. Fermentation inhibitors generated from the pretreatment of lignocellulosic biomass (Adapted from Takagi, H. and Kitagaki, H. (2015). *Stress Biology of Yeasts and Fungi*. Tokyo: Springer.)

2. Acetate stress: toxicity and adaptive mechanisms of yeast cells

Acetic acid is one of the common weak organic acids that are intrinsically produced by yeast *S. cerevisiae* and other microorganisms. These compounds determine the flavor of their products such as wine and vinegar (Vilela-Moura *et al*., 2011; Mas *et al*., 2014). In addition, it has been believed that yeasts compete with acetic acid bacteria which convert ethanol to acetic acid in their natural habitats (Mollapour and Piper, 2006). Furthermore, together with sulfite, acetic acid and other weak organic acids, including benzoic acid and sorbic acid, are widely used as the preservative for foods and beverages (Piper 2011). The resistance to weak organic acids of yeasts such as *S. cerevisiae* and *Zygosaccharomyces bailii* can be the major determinant

for food spoilage (Mollapour *et al*., 2008). Therefore, the adaptation responses to weak organic acids especially acetic acid have been intensively studied.

In solution, acetic acid exists in the forms of undissociated and dissociated molecules in the pH-dependent equilibrium that is determined by its p*K*a value (4.75). The undissociated form of acetic acid increases as the pH decreases from its p*K*a. When acetic acid is added in to the medium, it can enter yeast cells either by direct diffusion across the plasma membrane or facilitated diffusion via Fps1, aquaglyceroporin channel (Mollapour and Piper, 2007). Once acetic acid is in the cytoplasm, it dissociates to acetate anion and proton due to the near-neutral pH in the cytoplasm. The released protons cause a long-term decrease in the intracellular pH known as intracellular acidification (Stratford *et al*., 2013; Ullah *et al*., 2012). Consequently, the activity of metabolic functions (Orij *et al*., 2012; Pearce *et al*., 2001), signal transduction (Dechant *et al*., 2010), protein interaction (Young *et al*., 2010), and cell division rate (Orij *et al*., 2012) are affected, leading to growth inhibition. Therefore, Pma1, the plasma membrane H^+-ATPase which functions in pumping intracellular protons out of the cells and maintaining cytosolic pH is strongly required for growth recovery under acetic acid conditions (Ullah *et al*., 2012) (Figure 2). In addition to Pma1, the vacuolar proton pump (V-ATPase) also contributes to cytosolic pH homeostasis by collecting protons inside the vacuole and possibly by targeting Pma1 to the plasma membrane (Martinez-Munoz and Kane, 2008; Smardon and Kane, 2014). However, the role of V-ATPase under acetic acid condition is still unclear. The acetate anions released also cause an increase in internal turgor pressure and exert growth inhibitory actions (Ullah *et al*., 2012). In addition, the ATP required for plasma membrane ATPases to pump protons and acetate anions out of the cells and the inhibition of glycolytic enzymes is postulated to be the cause of the depletion of intracellular ATP pool (Holyoak *et al*., 1996). Furthermore, acetic acid also inhibits the uptake of some nutrients including histidine, leucine and glucose, which might be a result of the decreased levels of intracellular ATP as well as the decreased expression of some nutrient transporter genes such as *HXT1*, *HXT3*, or *BAP2* (Ding *et al*., 2013). Acetic acid at sublethal concentration also induces programmed cell death (Ludovico *et al*., 2002). Hence, *S. cerevisiae* has evolved a sophisticated molecular mechanism to cope with this acetic acid stress through an action of stress-activated mitogen activated protein kinase (SAPK) pathway also known as high osmolarity glycerol (HOG) signaling pathway (Mollapour and Piper, 2006). In unstressed cells, a sub-fraction of Hog1 mitogen-activated protein kinase (MAPK) is physically bound to the N-terminal cytosolic domain of Fps1. Once the HOG signaling is activated by acetic acid stress, this sub-fraction of Hog1 becomes active and

phosphorylates Fps1. This process leads to the ubiquitination of phosphorylated Fps1 and finally its degradation in the vacuole, thereby, renders acetate resistance to yeast cells (Mollapour and Piper, 2007) (Figure 2). In addition, yeast cells also employ the transcription activator Haa1 to regulate gene expression under acetic acid stress conditions (Mira *et al.*, 2011; Fernandes *et al.*, 2005) (Figure 2). So far, many downstream genes of Haa1 have been identified through searching the *cis*-acting Haa1-responsive element (HRE) in the promoter regions, thus, forming the Haa1 regulon (Mira *et al.*, 2011). Among the genes regulated by Haa1, *TPO2* and *TPO3* which encode the drug: H^+ antiporters have been shown to play an important role for exporting acetate anion out of the cells (Fernandes *et al.*, 2005). Furthermore, *SAP30*, encoding a component of histone deacetylase Rpd3L complex, and *HRK1*, encoding a protein kinase crucial for reducing intracellular acetate contents, have been found to provide the strongest protective effect against acetic acid stress (Mira *et al.*, 2010). Moreover, *SPI1* and *YGP1*, encoding the cell wall proteins, potentially play a protective role against the re-entry of acetic acid by direct diffusion (Fernandes *et al.*, 2005; Simoes *et al.*, 2006; Mira *et al.*, 2011). Indeed, the constitutively *HAA1*-overexpressing *S. cerevisiae* laboratory strain and industrial strain Ethanol Red® (ER HAA1-OP) showed higher tolerance to acetic acid and better fermentation ability under acetic acid stress than did the wild-type strain (Tanaka *et al.*, 2012; Inaba *et al.*, 2013). Therefore, the disruption of *FPS1* or the overexpression of *HAA1* could be considered as the promising strategy for developing acetate-tolerant yeasts useful for bioethanol production.

Interestingly, pH condition in lignocellulosic hydrolysate can be varied due to the type of biomass. It has been described that the pH of lignocellulosic hydrolysate after pretreatment is about 5 to 6, which is higher than p*K*a of acetic acid (4.75) (Klinke *et al.*, 2004; Palmqvist and Hahn-Hagerdal, 2000). Thus, under this condition, acetate is largely present in a deprotonated form which shows less inhibitory effect than does its protonated form (Mollapour *et al.*, 2009). However, its counter ions (e.g. Na^+ and K^+) play an important role in the toxicity of acetate at higher pH. A recent report reveals that the presence of Na^+, but not K^+, has a synergistic inhibitory effect to acetate (Peña *et al.*, 2013). Nevertheless, the precise molecular mechanism has not been elucidated. Notably, either the amplification of *ENA1/2/5* tandem gene cassette encoding P-type ATPase Na^+ pumps in the genome of *S. cerevisiae* or the overexpression of *ENA2* from the 2-micron plasmid can improve cell growth under acetate stress in the presence of Na^+ (Gilbert *et al.*, 2009; Peña *et al.*, 2013). In terms of application, this raises a significance of sodium acetate (NaAc) stress in the bioethanol production from lignocellulosic biomass. Therefore, the next step to be considered is to breed yeast strains with

tolerance to NaAc stress. Since Na^+ monovalent cation comes to play a synergistic role with acetate stress, the following section will be described about the toxicity of Na^+ ions and adaptive responses of yeast cells under Na^+ stress conditions.

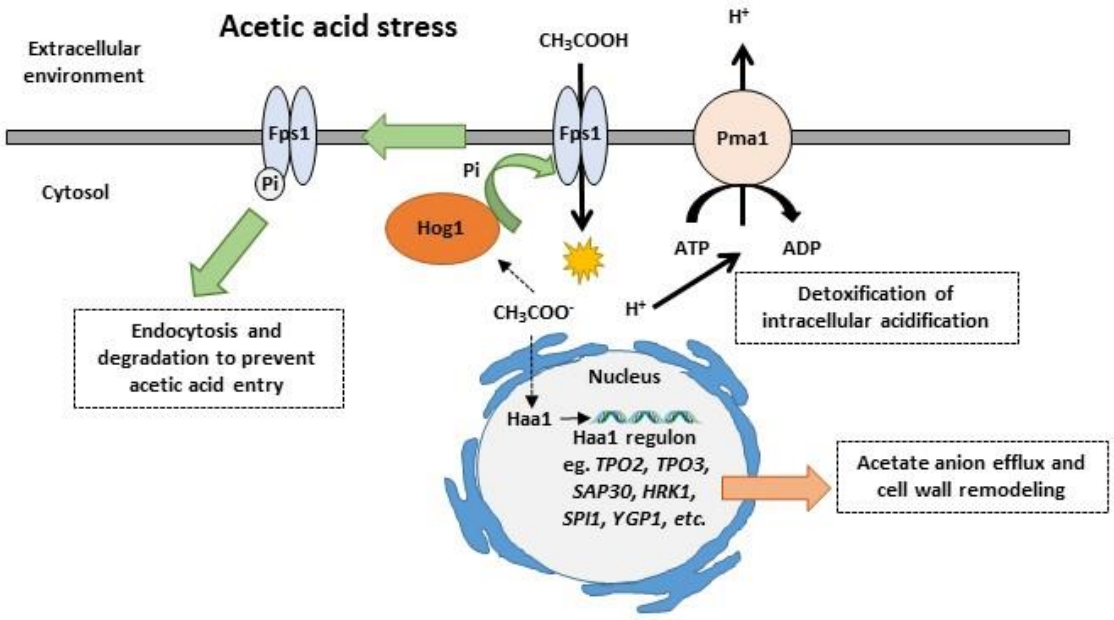

Figure 2. Schematic diagram representing adaptive responses to acetic acid stress
(Adapted from Takagi, H. and Kitagaki, H. (2015). *Stress Biology of Yeasts and Fungi*. Tokyo: Springer.)

3. Na^+ stress: toxicity and adaptive mechanisms of yeast cells

Na^+ cations itself are toxic to yeast cells as demonstrated by NaCl stress (Serrano, 1996). At a high NaCl concentration, significant extracellular amount of Na^+ enters the cells and consequently an equivalent intracellular amount of K^+ must leave to maintain an electroneutrality within the cells, leading to the increase in intracellular Na^+ concentration and the decrease of intracellular K^+/Na^+ ratio (Ariño *et al*., 2010). High intracellular Na^+ concentration is inhibitory to various cellular enzymatic activities, such as *HAL2* nucleotidase (Murguía *et al*., 1996), whereas proper intracellular K^+ concentration is required for several enzyme functions (Lapathitis and Kotyk, 1998). In addition, a high extracellular Na^+ concentration also causes osmotic stress to yeast cells by inducing the loss of intracellular water (Hohmann, 2002). Therefore, to cope with the toxic Na^+ cations, yeast cells have developed sophisticated adaptive mechanisms which mainly involve the production of glycerol for

counteracting changes in osmolarity and the balance of intracellular cations, which requires the series of plasma membrane and organellar ion transporters.

As shown in Figure 3, in *S. cerevisiae*, the Na^+ ions can enter the cells through various transporters mainly by displacing the K^+ ions. First, the high-affinity K^+ transport Trk1/Trk2 system has been shown to transport Na^+, even though the affinity is much lower (Haro and Rodríguez-Navarro, 2002). Second, the non-specific cation transport system named NSC1 for non-specific cation channel which accounts for the low-affinity K^+ transport has been reported to be involved in Na^+ uptake (Gómez et al., 1996). In addition, the Pi-Na^+ symporter Pho89 is the only one sodium-dependent phosphate transporter, the expression of which is specifically induced by phosphate limitation and alkaline pH (Martinez and Persson, 1998; Serrano *et al.*, 2002). Thus, under a high extracellular Na^+ concentration, the Na^+ ions are likely to enter the cells via these systems. Due to its toxicity, the accumulation of Na^+ inside the cells must be avoided. Thus, surplus Na^+ has to be extruded out of the cells in order to maintain high intracellular K^+/Na^+ ratio. This extrusion is known as the detoxification system which consists two kinds of plasma membrane transporters including the Na^+/ H^+ antiporter Nha1 and the P-type ATPase Na^+ pumps Ena system (Ariño *et al.*, 2010). The plasma membrane H^+-ATPase Pma1 is important for maintaining the proton gradient across the plasma membrane required for secondary transport such as that mediated by Nha1. In addition, the toxic Na^+ ions in the cytosol can be sequestered in the vacuole via the activity of Nhx1 and Vnx1, the two Na^+/ H^+ antiporters located in endosomal and vacuolar membranes, respectively (Ariño *et al.*, 2010). Indeed, their activities require the proton gradient across cytosol and endosomal or vacuolar compartments, which is maintained by the V-ATPase activity (Kane 2007).

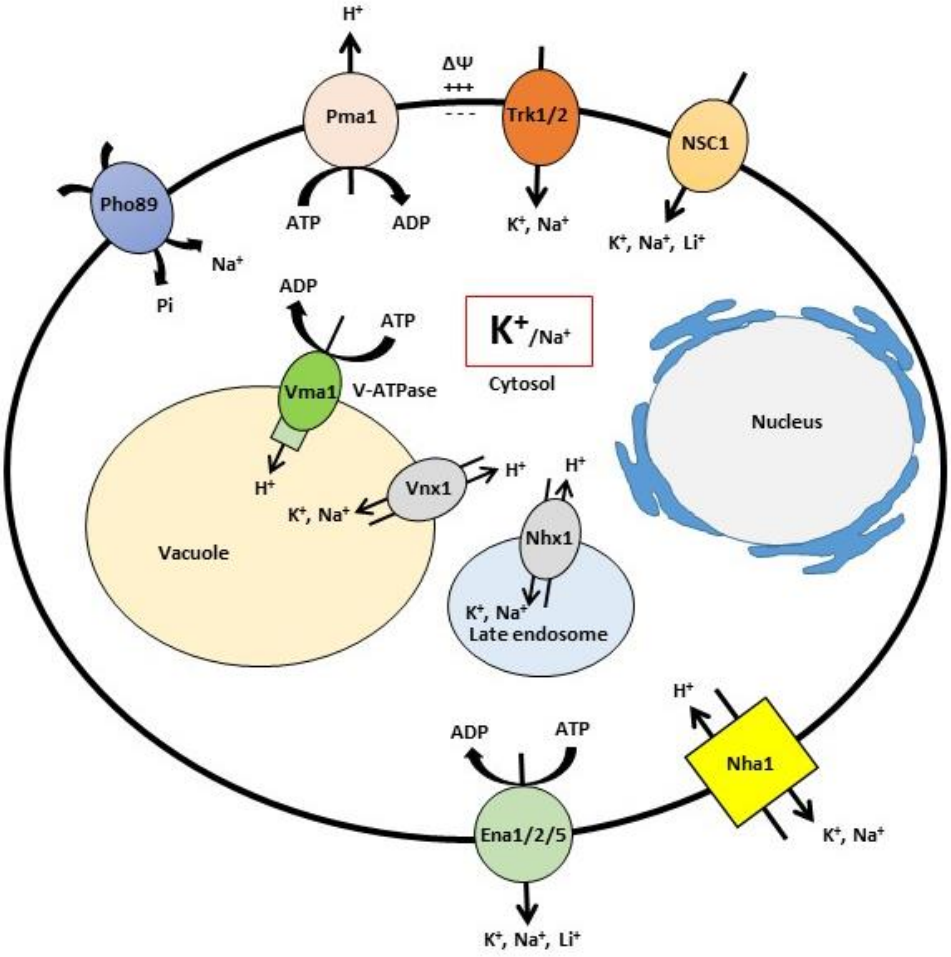

Figure 3. Schematic diagram representing proteins involving in Na^+ transport (Adapted from Ramos, J., Sychrová, H., and Kschischo, M. (2016). *Yeast Membrane Transport*. Cham: Springer.)

4. High osmolarity glycerol (HOG) signaling

The high osmolarity glycerol (HOG) signaling pathway is one of the five MAPK cascades in *S. cerevisiae*, the other four of which include the cell wall integrity pathway, the spore wall assembly pathway, the filamentous/invasive growth pathway, and the pheromone response pathway (Posas *et al*., 1998). The HOG MAPK signaling cascade is essential for yeast cells to adapt to high osmolarity environments including high sugar and high salt concentrations. The HOG signaling is composed of two branches conventionally known as Sln1 and Sho1 branches (Figure 4). The Sln1 branch begins with the modified version of bacterial two component system Sln1-Ypd1-Ssk1. Sln1 is the histidine kinase (HK) which acts as an osmosensor. Under normal condition, Sln1 is active and auto-phosphorylates its HK domain. The phosphate is then transferred from His in auto-phosphorylation sites to Asp in its receiver

(REC) domain. Further phosphorelay reactions occur from the REC domain of Sln1 to His site in Ypd1 and then to Asp site in Ssk1 (Saito, 2001; 2003). Thus, Ssk1 is phosphorylated and inactive. Ssk1 is an activator of Ssk2 and Ssk22 MAPKKK when only it is unphosphorylated or dephosphorylated. Under high osmotic conditions, Sln1 is inactivated, although the inactivation mechanism is still unclear. It has been previously proposed that this may occur through changes in plasma membrane fluidity and turgor pressure which induce conformational changes of Sln1, leading to its inactivation (Reiser *et al*., 2003). Once Sln1 is inactive, the phosphorelay reaction to Ssk1 is disrupted, causing significant accumulation of unphosphorylated Ssk1 which further activates Ssk2 and Ssk22 MAPKKK. Ssk2 and Ssk22 are redundant and composed of an N-terminal auto-inhibitory domain (AID) and C-terminal catalytic kinase domain (KD). The mechanism in which unphosphorylated Ssk1 activates Ssk2 and Ssk22 is through its binding to AID, thereby opening the KD of Ssk2 and Ssk22. Activated Ssk2 and Ssk22 MAPKKK then initiates the phosphorylation cascade to Pbs2 MAPKK and finally to Hog1 MAPK on Thr174 and Tyr176 (Maeda *et al*., 1995). In addition to Ssk2 and Ssk22, Pbs2 MAPKK can also be activated by Ste11 MAPKKK which belongs to Sho1 branch. The Sho1 branch requires Msb2, Hkr1, Sho1, Cdc42, Ste50, Ste20, Cla4, Opy2, and Ste11 for transmitting the signal (Posas and Saito, 1997; Posas *et al*., 1998; Raitt *et al*., 2000; Reiser *et al*., 2000; Tanaka *et al*., 2014). Msb2 and Hkr1 are transmembrane mucin-like glycoproteins without enzymatic activity (Cullen *et al*., 2004). They serve as the osmosensors, together with the transmembrane protein Sho1. Once Sho1 branch is activated, the Ste11 MAPKKK is recruited to the plasma membrane by the adaptor protein Ste50 which binds to both Ste11 and Opy2 located on the plasma membrane. The Pbs2 MAPKK is recruited to the plasma membrane by binding to the Src homology 3 (SH3) domain of Sho1 via its proline rich motif. It is likely that the complex containing Ste11 and Pbs2 is formed. Then, the p21-activated kinase (PAK)-family protein kinases Ste20 and Cla4, which are associated with Cdc42, phosphorylate Ste11. The Ste11 MAPKKK subsequently activates Pbs2, leading to Hog1 activation.

Once Hog1 is activated, major fraction of phosphorylated Hog1 enters the nucleus to elicit its activity for controlling gene expression. Some fraction of phosphorylated Hog1 associates with the plasma membrane and performs cytosolic functions. The major task of Hog1 as reflected on its name is to increase the accumulation of glycerol as a compatible solute in response to hyperosmotic stress. The increase in intracellular glycerol can be achieved by: 1) inducing the expression of genes involved in glycerol production including *GPD1*, *GPP1*, and *GPP2*; 2) inducing the expression of Stl1 active glycerol uptake system; 3) increasing the

activity of glycolytic enzyme phosphofructo-2-kinase; 4) controlling the function of Fps1 aquaglyceroporin channel to limit the loss of glycerol (Hohmann, 2009). Previous studies have shown that acetate stress at pH 6.8 exhibits growth inhibitory effect and triggers Hog1 MAPK phosphorylation which leads to the upregulation of *GPD1* mRNA level and consequently causes the increased accumulation of intracellular glycerol (Mollapour and Piper, 2006; Mollapour *et al*., 2009). Thus, these studies indicate that one of the acetate stress responses at higher pH is to increase intracellular osmolarity via the accumulation of glycerol, which allows the cells to counteract the loss of intracellular water.

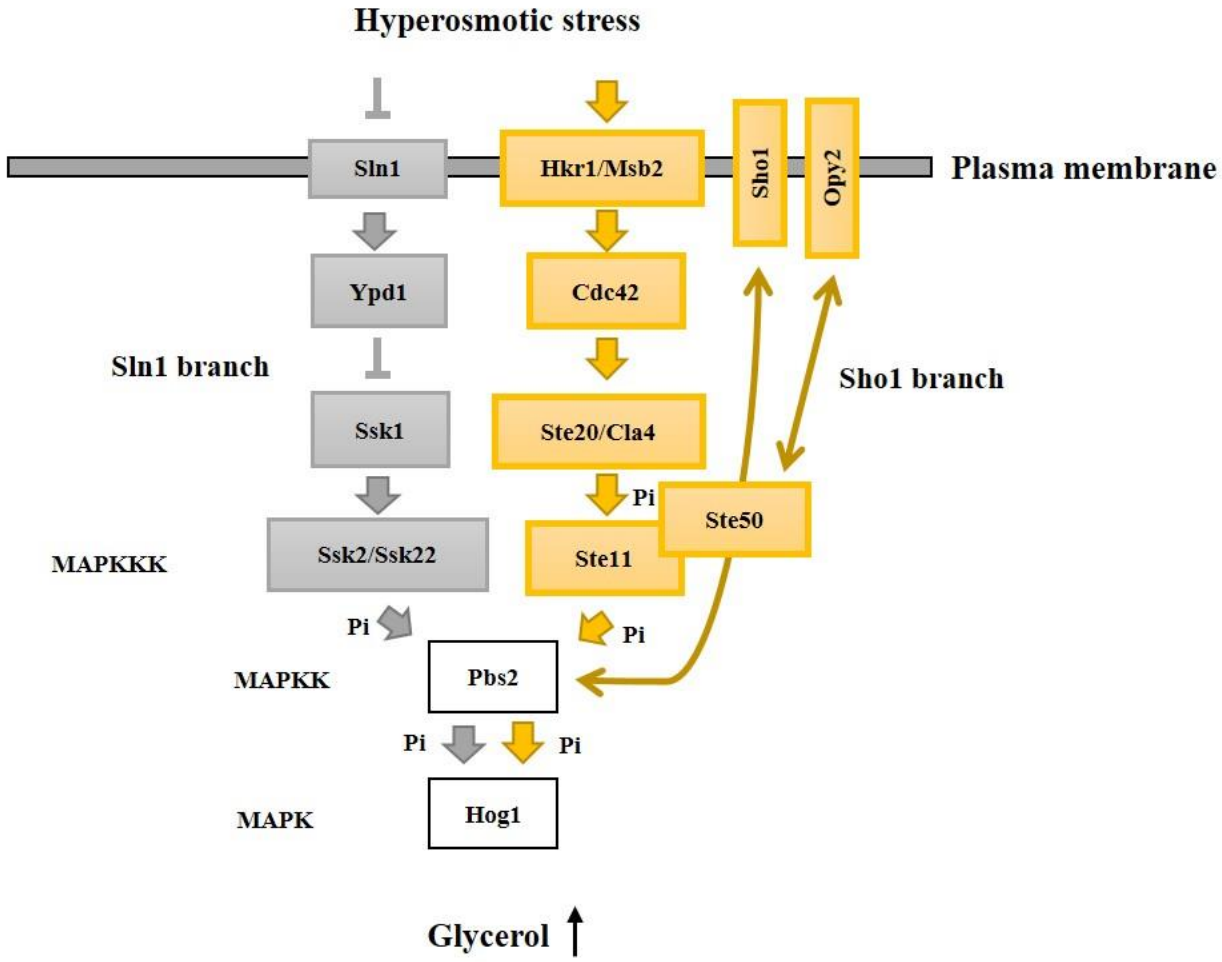

Figure 4. Schematic diagram representing HOG signaling pathway (Adapted from Saito and Tatebayashi, 2004; Hohmann, 2009)

5. Ena ATPases and their regulations

The Ena proteins are known as P-type ATPases that couple ATP hydrolysis with the transport of alkaline metal cations including Na^+, Li^+, and K^+. Their genes exist in tandem repeats in the chromosome IV of *S. cerevisiae* and the number varies strain by strain from one

to five genes. For example, *S. cerevisiae* BY4741 strain possesses three genes including *ENA1*, *ENA2*, and *ENA5*. They are identical in the number of amino acids (1,091 residues) and share very high homology (>97% nucleotide identity). They are believed to perform similar functions despite it is also reported that by the *in vitro* study, overexpressed Ena1 preferentially transports Na^+ whereas Ena2 is more specific toward Li^+ (Wieland *et al*., 1995). Thus, the differential function of each Ena remains to be clarified. The existence of *ENA* genes is known to be important for the salt tolerance phenotype of *S. cerevisiae* since the deletion of the entire cluster (Δ*ena1-5*) results in the strong sensitivity toward salt stresses including NaCl and LiCl (Haro *et al*., 1991; Garciadeblas *et al*., 1993; Rodriguez-Navarro *et al*., 1994; Posas *et al*., 1995; Wieland *et al*., 1995). In addition, recent studies have shown that either the amplification of the copy number of *ENA1/2/5* gene cluster or the overexpression of *ENA2* improves NaAc tolerance (Gilbert *et al*., 2009; Peña *et al*., 2013).

In terms of their expression, under non-stress condition, expression levels of *ENA1*, *ENA2*, and *ENA5* are very low and known as basal levels. However, under stress conditions including osmotic, salt and alkaline pH stresses, the expression level of *ENA1* is significantly up-regulated whereas that of *ENA2* and *ENA5* are not affected (Mendoza *et al*., 1994; Márquez and Serrano, 1996; Lamb *et al*., 2001). Thus, *ENA1* has been much studied on the transcriptional regulation which integrates at least five signal transduction pathways on its promoter. They are composed of Hog1 MAPK, calmodulin/calcineurin, Rim101, Snf1, and TOR pathways (Ruiz and Ariño, 2007). Under the salt stress and osmotic stress conditions, *ENA1* is principally regulated by Hog1 MAPK and calmodulin/calcineurin pathways while Snf1 and TOR pathways give little contribution (Márquez and Serrano, 1996; Alepuz, Cunningham, and Estruch, 1997; Proft and Serrano, 1999; Crespo *et al*., 2001). Under alkaline pH stress condition, the expression of *ENA1* is mainly controlled by calmodulin/calcineurin, Rim101, and Snf1 pathways (Lamb *et al*., 2001; Serrano *et al*., 2002; Lamb and Michell, 2003; Platara *et al*., 2006). Importantly, the transcriptional regulation of *ENA1* by Hog1 is achieved by the phosphorylation of bZip transcription factor Sko1, which converts the Sko1-Ssn6-Tup1 complex from the repressor to the transcriptional activator for *ENA1* (Proft and Struhl, 2002). Furthermore, Hog1 is involved in the recruitment of the histone deacetylase complex Rpd3-Sin3 to the promoter of *ENA1* where this complex facilitate the association of RNA polymerase II, resulting in the transcriptional activation (De Nadal *et al*., 2004).

In terms of post-transcriptional regulations, so far there are three studies involving in the trafficking of Ena1. First, the study by Wadskog *et al.* (2006) identifies that the product of

SRO7/SOP gene (homolog of the *Drosophila* Lgl tumor suppressor gene) involves in the specific sorting of Ena1 to the plasma membrane. This gene putatively encodes the protein involved in exocytic docking and fusion of the Golgi-derived vesicles with the plasma membrane. Thus, the deletion of *SRO7* causes Ena1 mis-localization and finally targeting to the vacuole for degradation. This vacuolar targeting is mediated by multivesicular bodies (MVB) sorting pathway which requires the ubiquitin ligase activity by Rsp5. Second, the study by Logg *et al*. (2008) shows that Ena1 is mis-localized in several *vps* mutants although some Ena1 can still be targeted to the plasma membrane. Third, the study by Marques *et al*. (2015) shows that some of the Vps proteins in Logg's study (also known to be endosomal sorting complexes required for transport (ESCRT) components), which interact with Rim101 complex and associated components, play a role in the proper Ena1 accumulation on the plasma membrane. Among deletion mutants of these encoding genes, the *rim8* mutant shows very strong phenotypes regarding the salt sensitivity and the defect in Ena1 accumulation on the plasma membrane. Rim8 is known as an adaptor protein of Rsp5. Therefore, it seems that the ubiquitination system principally mediated by Rsp5 possibly plays a role in the regulation of the plasma membrane trafficking of Ena ATPases. I will further focus on the ubiquitination system, Rsp5 and its adaptor proteins, particularly Rim8.

6. Protein ubiquitination

Protein ubiquitination is one of the fundamental cellular processes for regulating cellular activities at the post-translational level through protein modification by the small regulatory protein ubiquitin. Ubiquitination is known to play a role in various cellular processes such as protein degradation and trafficking, regulation of cell cycle and/or apoptosis as well as array of signal transductions (Hershko and Ciechanover, 1998; Mukhopadhyay and Riezman, 2007). Ubiquitin is the highly conserved 76 amino acid-containing protein. This ubiquitination process occurs in a multi-step cascade (Figure 5). At the first step, ubiquitin is activated in an ATP-dependent manner by the E1 activating enzyme. Then the thioester bond formation occurs between the C-terminal glycine residue of ubiquitin and a cysteine in the active center of E1. Next, the activated ubiquitin is transferred to a cysteine residue located in the active center of the E2 conjugating enzyme. After that, the active ubiquitin is prompt to be transferred to the target protein with the aid of the E3 ubiquitin ligase. Ligation of ubiquitin with the target protein occurs via isopeptide bond which is formed between the C-terminal glycine residue of ubiquitin

and the lysine residues of the target protein or another ubiquitin, if poly-ubiquitin chain is formed.

The E3 ubiquitin ligases have an important role in recognition of a specific target or substrate protein in a particular condition. The E3 ubiquitin ligases can be categorized into two types including really interesting new genes (RING)-finger type (Jackson *et al*., 2000) and homologous to E6-AP carboxy terminus (HECT) type (Huibregtse *et al*., 1995). There are many HECT-type E3 ubiquitin ligases in *S. cerevisiae* including Rsp5, Ufd4, Tom1, Hul4, and Hul5 (Wang *et al*., 1999). However, the sole essential HECT-type E3 ubiquitin ligase in Nedd4 family found in *S. cerevisiae* is Rsp5 which plays diverse roles in regulation of various cellular processes.

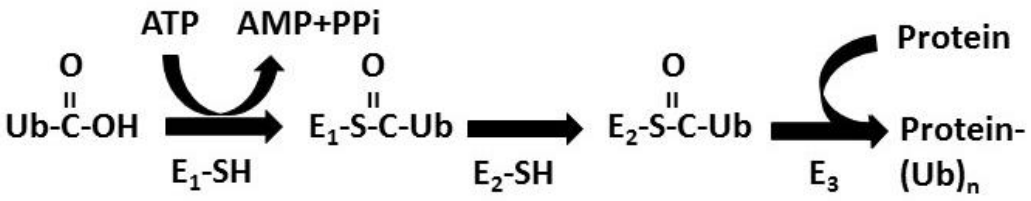

Figure 5. Protein ubiquitination cascade (modified from Hershko and Ciechanover, 1998).

7. The E3 ubiquitin ligase Rsp5

Rsp5 (Reverses Spt$^-$ phenotype protein 5) is originally isolated as a mutated gene to suppress *SPT3* mutations that negatively affect the gene expression (Winston, 1993, personal communication to SGD). Rsp5 is the orthologue of the human Nedd4 E3 ubiquitin ligase in *S. cerevisiae*, implicating its important roles in regulating various physiological processes in cells such as signal transduction (Dunn and Hicke, 2001), quality control of plasma membrane proteins (Shiga *et al*., 2014), and intracellular trafficking (Jarmoszewicz *et al*., 2012) through the interaction and ubiquitination of various substrate proteins. Rsp5 is composed of the N-terminal Ca^{2+}-dependent phospholipid membrane binding (C2) domain, the three substrate recognition (WW) domains (commonly referred to two conserved tryptophan residues in the domains), and the C-terminal catalytic ubiquitin ligase (HECT) domain (Rotin and Kumar, 2009).

The C2 domain consists of approximately 130 amino acids and is normally regulated by the Ca^{2+} ions (Nalefski and Falk, 1996; Hurley and Misra, 2000). It is important for the ability of Rsp5 to electrostatically interact with either plasma membrane or endosomal membrane (Cho,

2001). The interaction occurs via the positively-charged basic amino acids in the C2 domain and the negatively-charged phosphorylated phosphatidylinositol on the membrane. It has been shown that the mutations of five lysine residues to glutamine abolish this electrostatic interaction and negatively affect the localization of Rsp5 to endosomal membranes (Dunn *et al*., 2004). This implies the role of the C2 domain in MVB sorting pathway (Dunn *et al*., 2004). Moreover, previous study also points out the role of the C2 domain in endocytosis pathway. Notably, the truncation of the C2 domain affects the endocytosis of the general amino acid permease Gap1 without affecting its ubiquitination and also causes the defect in fluid phase endocytosis (Springael *et al*., 1999a).

The WW domain consists of approximately 40 amino acid residues initially described by Sudol (1996). Basically, the structure of the WW domain is predicted to be three-stranded anti-parallel β-sheets which form a hydrophobic pocket (Macias *et al*., 1996). Generally, the binding motifs for the WW domain are categorized into four groups based on its specificity (Bedford *et al*., 2000). Group I recognizes the PXY, LPXY, and PPXY motifs. Group II and III bind the PPLP and PPR motif, respectively. Group IV recognizes the motif containing phosphoserine and phosphothreonine followed by proline (Lu *et al*., 1999). There are three WW domains in Rsp5 referred as WW1, WW2, and WW3, which are categorized as Group I. The WW domains of Rsp5 play an important role in substrate recognition and binding through the interaction with the PXY, LPXY, and PPXY motifs, so called PY motifs, exist in the substrate protein. In many cases, the substrate proteins of Rsp5 do not contain the PY motifs (Gupta *et al*., 2007). Thus, the PY motif-containing adaptor proteins are required for mediating the interaction between Rsp5 and various substrate proteins.

The HECT domain, which accounts for the ubiquitination activity of Rsp5, is composed of approximately 350 amino acid residues. The important residue in this catalytic domain is Cys777, which is the point for thioester formation with ubiquitin. Thus, the mutation of Cys777 to Ala (C777A) abolishes the overall ubiquitination activity of Rsp5 (Huibregtse *et al*., 1995). In addition, the mutation of Leu733 to Ser (L733S), known as *rsp5-1* (temperature-sensitive allele), has been described to cause the defect in ubiquitin-thioester formation and decrease the stability of Rsp5 at restrictive temperatures (>35˚C) (Wang *et al*., 1999).

8. Roles of Rsp5 and their ubiquitin-mediated regulations

The essential role of Rsp5 is attributed to its activity in the regulation of the *OLE1* gene expression via ubiquitination-mediated proteolytic processing of endoplasmic reticulum (ER)-

localized Spt23 and Mga2 transcription activators (Zhang *et al*., 1999; Hoppe *et al*., 2000; Shcherbik *et al*., 2003; 2004). The *OLE1* gene encodes Δ9 fatty acid desaturase which is essential for unsaturated fatty acid biosynthesis (Stukey *et al*., 1989). In *S. cerevisiae*, major saturated fatty acyl-CoA are palmityl-CoA and stearyl-CoA, which are converted to palmitoleoyl-CoA and oleoyl-CoA by the activity of Δ9 fatty acid desaturase (Stukey *et al*., 1989). These two unsaturated fatty acyl-CoAs are the initial sources of various unsaturated fatty acids that are necessary for maintaining membrane integrity and fluidity (Stukey *et al*., 1989). Since Rsp5 regulates the maturation of Spt23 and Mga2 transcription activators which also control the transcription of several genes involving in lipid biosynthesis; thus, Rsp5 is believed to play an important role in lipid homeostasis in *S. cerevisiae* (Kaliszewski and Żołądek, 2008). In addition to its essential function, Rsp5 performs several functions which can be categorized based on its locations including plasma membrane, internal membrane compartments, cytoplasm, and nucleus.

1) Plasma membrane

Rsp5 is known to down-regulate various plasma membrane transporters for nutrients and ions as well as receptors. This downregulation is a part of both protein quality control mechanisms where plasma membrane proteins are misfolded (e.g. in response to heat stress) and regulatory mechanisms where transporters are endocytosed to restrict their activity or receptors are degraded for their desensitization. For example, the ubiquitination by Rsp5 mediates the endocytosis of the general amino acid permease Gap1 in response to shifting from poor nitrogen source to ammonium ions (Springael *et al*., 1999b) and in response to environmental stresses such as ethanol, H_2O_2, high temperature, and LiCl (Shiga *et al*., 2014). It has been shown that Gap1 remains stable on the plasma membrane under ethanol stress in the stress hypersensitive *rsp5*^{A401E} mutant (Shiga *et al*., 2014). Moreover, the endocytosis of the uracil permease Fur4 (Galan et al., 1996; Hein and Andre, 1997), the maltose permease Mal61 (Medintz *et al*., 1998), the hexose transporter Hxt6/7 (Krampe *et al*., 1998; Nikko and Pelham, 2009), the tryptophan permease Tat2 (Beck *et al*., 1999), the zinc transporter Zrt1 (Gitan and Eide, 2000), and the divalent cation transporter Smf1 (Sullivan *et al*., 2007) is regulated by the ubiquitination by Rsp5 in response to various stimuli. However, the role of Rsp5 in regulation of the monovalent cation transporters Ena1/2/5 has not been elucidated. The internalization of the pheromone receptor Ste2 after pheromone sensing is also controlled by the ubiquitination mediated by Rsp5 as a part of its desensitization (Dunn and Hicke, 2001). In addition, Rsp5

ubiquitin ligase activity is shown to be important for fluid phase endocytosis (Dunn and Hicke, 2001). Generally, Lys63-linked poly-ubiquitination mediated by Rsp5 is involved in the endocytosis process (Hicke, 2001). However, a recent study also shows that a fraction of the plasma membrane H^+-ATPase Pma1 is mono-ubiquitinated by Rsp5, leading to its internalization and vacuolar degradation, in response to the loss of V-ATPase activity (Smardon and Kane, 2014). Thus, not only Lys63-linked poly-ubiquitination, but also mono-ubiquitination, play a role in the endocytosis process.

2) Internal membrane compartments

Sorting of proteins to vacuole either from Golgi apparatus or from the plasma membrane relies on MVB sorting pathway which requires mono-ubiquitination (Katzmann *et al*., 2001; Reggiori and Pelham, 2001; Urbanowski and Piper, 2001; Morvan *et al*., 2004). The ubiquitination activity of Rsp5 has been shown to be crucial for proper sorting of the vacuolar carboxypeptidase S (Cps1) to the MVB vesicles (Dunn *et al*., 2004). Moreover, mutation in either WW3 domain of Rsp5 or PPXY motif of Sna3, an Rsp5 adaptor protein, as well as its Lys63-linked poly-ubiquitinated lysine residue causes the mislocalization of Sna3 to multiple mobile vesicles, which prevents its sorting to MVB or endosome pathway (Stawiecka-Mirota *et al*., 2007). In addition to regulation at the plasma membrane, the ubiquitination by Rsp5 is also known to regulate the sorting of Gap1 at the Golgi apparatus (Helliwell *et al*., 2001).

3) Cytoplasm

Heat shock is known to induce protein misfolding of not only plasma membrane proteins but also cytosolic proteins. Rsp5 has been shown to play a major role in recognition and ubiquitination of cytosolic misfolded proteins such as the pyruvate kinase Cdc19, the pyruvate decarboxylase Pdc1, and the translation release factor 1 Sup45, leading to their degradation by proteasome (Fang *et al*., 2014). The mechanism of recognition is either via direct interaction between the WW domains of Rsp5 and the PXY motifs of substrates or via the aid of the Hsp40 co-chaperone Ydj1 which binds the cytosolic misfolded proteins and contains the PXY motif (Fang *et al*., 2014). The Ydj1-binding motif and the PXY motif in the cytosolic proteins have been suggested as the heat-inducible degrons which are hindered when the protein is correctly folded and opened when heat induces its misfolding (Fang *et al*., 2014).

4) Nucleus

The nuclear functions of Rsp5 can be categorized into the regulation of transcription, RNA biogenesis/export, and chromatin assembly. First, Rsp5 is known to control transcription through its ability to ubiquitinate and target Rpb1, the large subunit of RNA polymerase II, for proteasomal degradation under stress conditions (Wang *et al*., 1999). The WW2 or WW3 domain of Rsp5 recognizes the PXY motif located in the C-terminal domain of Rpb1 (Wang *et al*., 1999; Beaudenon *et al*., 1999) and this recognition also requires RNA polymerase II degradation factor (Def1) for recruiting Rsp5 to Rpb1, thereby facilitating the ubiquitination and subsequent degradation of Rpb1 (Reid and Svejstrup, 2004). Thus, this negative regulation of general transcription through the ubiquitination and degradation of RNA polymerase II is probably important for cells to redirect adaptive response under stress conditions.

Second, Rsp5 is involved in controlling RNA biogenesis and export. This function is initially supported by the evidence that poly(A)$^+$ RNA is accumulated in the nuclei of *rsp5-1* mutant cells at the restrictive temperature (Rodriguez *et al*., 2003). Later on, Rsp5 is found to play a role in the ubiquitination and degradation of Hpr1 (Gwizdek *et al*., 2005), of which function is implicated in transcription elongation, transcription-dependent recombination, and mRNA export (Zenklusen *et al*., 2002; Strasser *et al*., 2002). In addition, *rsp5-3* mutant, which possesses three mutations in the catalytic HECT domain, is shown to have increased nuclear accumulation of tRNA and defects in the export of mRNA as well as pre-ribosomal subunits (Neuman *et al*., 2003). Furthermore, *rsp5-19*, which possesses the P418L mutation in the WW3 domain, shows an increase in the fidelity of translation which is primarily due to the increased nuclear accumulation of tRNA (Kwapisz *et al*., 2005). In terms of stress responses, Rsp5 regulates stress response genes through the regulation of mRNA export of *HSF1*, encoding transcriptional activator responsible for heat shock responses and *MSN2/4*, encoding transcriptional activator responsible for general stress responses (Haitani *et al*., 2006; Haitani and Takagi, 2008). It has been shown that in the stress hypersensitive *rsp5*^{A401E} mutant, the *HSF1* and *MSN2/4* mRNA are restricted in the nucleus under both non-stress and stress conditions including temperature upshift from 25˚C to 37˚C and exposure to 10% ethanol (Haitani and Takagi, 2008).

Third, Rsp5 plays a role in the regulation of chromatin condensation and assembly. This function is demonstrated by the evidence that Rsp5 and anaphase promoting complex (APC) act together in chromatin condensation and assembly processes with the aid of the E2 enzyme Ubc7 (Altheim and Schultz, 1999; Harkness *et al*., 2002; Arnason *et al*., 2005). In summary,

Rsp5 involves and plays important physiological roles in various cellular processes at different locations under both non-stress and stress conditions.

9. Rsp5 adaptors

To catalyze the ubiquitination on a particular substrate, the E3 ubiquitin ligase Rsp5 has to interact with the substrate through the interaction between the WW domains of Rsp5 and the PY motifs located in the substrate. However, most of the Rsp5 substrates do not contain the PY motifs (Gupta *et al*, 2007). This suggests that Rsp5 interacts with the substrate either via non-PY motifs or by the assistance of the PY-motif containing adaptors (Tables 1 and 2) (Léon and Haguenauer-Tsapis, 2009). The evidence supporting the existence of the Rsp5 adaptors originates from the identification of Bsd2 and Tre1/2, which contain the PY motifs, as the proteins required for the ubiquitination of the divalent cation transporter Smf1 (Liu *et al*., 1997; Hettema *et al*., 2004; Stimpson *et al*., 2006). In addition, Bsd2, but not Tre1/2, is found to be crucial for ubiquitination and trafficking of the precursor of the vacuolar enzyme Phm5 (Polyphosphatase) (Hettema *et al*., 2004). This suggests that combination of adaptors can also affect the substrate specificity by Rsp5. In addition, many Rsp5 adaptor proteins are identified, including Bul1/2 (Soetens *et al*., 2001; Liu *et al*., 2007), Ear1 and its homologue Ssh4 (Léon *et al*., 2008), as well as the arrestin-related trafficking adaptor (ART) protein family members consisting of Art1 to Art9 (Lin *et al*., 2008). The functions of each adaptor protein have been elucidated. The Ear1/Ssh4 homologous proteins function as the Rsp5 adaptors in the intracellular trafficking from Golgi apparatus to vacuole. It has been shown that Ear1/Ssh4 are required for the vacuolar trafficking of the siderophore transporter Sit1 and also the proper sorting of the uracil transporter Fur4 to MVB (Léon *et al*., 2008). Bul1/2 are known to facilitate the endocytosis of many plasma membrane proteins. For an example, they mediate interaction between Rsp5 and the general amino acid permease Gap1. This interaction is required for poly-ubiquitination of Gap1 at the plasma membrane, leading to its endocytosis in response to ammonium addition (Soetens *et al*., 2001; Liu *et al*., 2007). However, it has recently been shown that the poly-ubiquitination and endocytosis of Gap1 are mediated in a Bul1/2-independent manner under environmental stresses such as ethanol, H_2O_2, high temperature, and LiCl (Shiga *et al*., 2014). For the ART protein family, a recent study showed that Rsp5 and the ART proteins form the network for plasma membrane protein quality control system. This system functions to eliminate misfolded and non-functional proteins out of the plasma

membrane and prevent their aggregation, thereby maintain the plasma membrane integrity under proteotoxic stress, such as heat shock (Zhao *et al*., 2013).

Table 1. Lists of Rsp5 adaptor proteins, conserved domains, and their locations

Adaptor protein	Conserved domain	Location
Bsd2	TM	Golgi-endosome
Tre1/2	TM, TFR dimer, PA	Golgi-endosome
Ear1/Ssh4	TM, B30.2/SPRY	Golgi-endosome
Bul1/2	Bul1 N-terminus, Bul1 C-terminus	Plasma membrane, Golgi-endosome
Bul3	Bul1 N-terminus	-ND-
Art1	Arrestin N-terminus	Plasma membrane
Art2	Arrestin C-terminus	Plasma membrane
Art3	Arrestin N-terminus, Arrestin C-terminus	-ND-
Art4	Arrestin N-terminus, Arrestin C-terminus	Plasma membrane
Art5	Arrestin C-terminus	Plasma membrane
Art6	Arrestin C-terminus	-ND-
Art7	Arrestin N-terminus, Arrestin C-terminus	-ND-
Art8	Arrestin C-terminus	Plasma membrane
Art9 (Rim8)	Arrestin N-terminus, Arrestin C-terminus	Plasma membrane
Art10	-ND-	-ND-

Note: TM=Predicted transmembrane domain, TFR dimer=Transferrin receptor-like dimerization domain, PA=protease-associated domain, B30.2/SPRY=B30.2 and/or SP1a/RYanodine receptor domain, and ND=Not determined (Information was obtained from *Saccharomyces* Genome Database (SGD) and Lauwers *et al*., 2010.)

Table 2. Functions of Rsp5 adaptor proteins

Transporter (Substrate)	Condition of vacuolar targeting	Rsp5 adaptor protein
Can1 (arginine)	Cycloheximide	Art1
Ctr1 (copper)	Substrate excess	Bul1, Bul2
Fur4 (uracil)	Cycloheximide	Bul1, Bul2, Art1, Art2, Art8, Bsd2, Ear1, Ssh4
	Substrate excess	Bul1, Bul2, Art1, Art2, Art8, Bsd2
Gap1 (amino acids)	Ammonium or substrate excess	Bul1, Bul2, Ear1, Ssh4
Hxt6 (hexoses)	Cycloheximide	Art8
	Substrate excess	Art4
Itr1 (inositol)	Substrate excess	Art5, Bsd2
Lyp1 (lysine)	Cycloheximide	Art2
	Substrate excess	Art1
Mup1 (methionine)	Substrate excess	Art1
Sit1 (ferroxiamines)	Absence of substrate	Ssh4, Ear1, Tre1, Tre2
Smf1 (manganese)	Substrate excess	Bsd2, Tre1, Tre2
	Stresses	Art2, Art8, Bsd2, Tre1, Tre2, Ear1, Ssh4
Tat2 (tryptophan)	Cycloheximide	Bul1, Bul2, Art2, Art8, Bsd2
	Substrate excess	Bul1, Bul2, Art1, Art2, Art8, Bsd2
Pma1 (proton)	Loss of V-ATPase	Art9 (Rim8)

(This table was modified from Lauwers *et al*., 2010.)

10. Rim8 and its roles in Rim signaling and as an Rsp5 adaptor

RIM8, systematically known as *ART9*, is composed of 1,629 bp, which encodes 542 amino acid residues with the molecular weight of approximately 61 kDa. The structure of Rim8 consists of N-terminal arrestin domain from residue 39-201 and C-terminal arrestin domain from residue 259-394, as well as ESCRT interacting domain from residue 519-537. Rim8 is known as the essential component of the Rim signaling pathway (Figure 6) which responds to external alkalization. In the Rim signaling, it has initially been shown that Rim8 interacts with Rsp5 *in vitro* via the PXY motif (506-508) and is mono-ubiquitinated by Rsp5 *in vivo* at Lys521

(Herrador *et al*., 2010). However, the mono-ubiquitination of Rim8 is dispensable for the Rim signaling. Notably, its mono-ubiquitination is strongly dependent on the binding to Vps23, the ESCRT-I subunit. Later on, the molecular mechanism of Rim8 mono-ubiquitination has been clarified that the ubiquitin E2 variant (UEV) domain of Vps23 prevents K63-linked polyubiquitination of Rim8 (Herrador *et al*., 2013). Therefore, the binding of Vps23 not only facilitates the ubiquitination of Rim8, but also directs Rim8 mono-ubiquitination. One year later, it has been shown that the level of Rim8 mono-ubiquitination is also regulated by the deubiquitination mediated by Doa4 (Obara and Kihara, 2014). In this study, it is also shown that the ubiquitination by Rsp5 is essential for the Rim signaling. Thus, in addition to Rim8, Rsp5 catalyzes the ubiquitination of unknown target(s) which could be downstream of Rim8. These unknown target(s) remain to be identified (Obara and Kihara, 2014). In the same year, another group has reported that Rsp5 and its adaptor Rim8 mediate ubiquitination of Pma1, which leads to its endocytosis and degradation in response to the loss of V-ATPase activity (Smardon and Kane, 2014). This suggests that Rsp5-Rim8 has a novel role in the regulation of plasma membrane protein trafficking besides the well-established role of Rim8 in the Rim signaling. Recently, two studies have been published. One study has expanded the regulation of Rim8 in the Rim signaling. It has been shown that Rim8 is subjected to phosphorylation at 17 serine/threonine residues from residue 228-256 by casein kinase 1 (CK1). This phosphorylation of Rim8 provides the inhibitory mechanism that prevents the interaction between Rim8 and Rim21 at acidic pH (Herrador *et al.*, 2015). However, conformational change of Rim21 can override the inhibitory effect of Rim8 phosphorylation at alkaline pH, allowing the activation of the Rim signaling (Herrador *et al.*, 2015). The other study has shown that Rim8 and the Rim-ESCRT complex are required for the proper trafficking of Ena1 to the plasma membrane under NaCl stress conditions (Marques *et al*., 2015). Therefore, this points out that Rsp5 may be involved in the regulation of the Ena monovalent cation transporters, which are crucial for cation homeostasis.

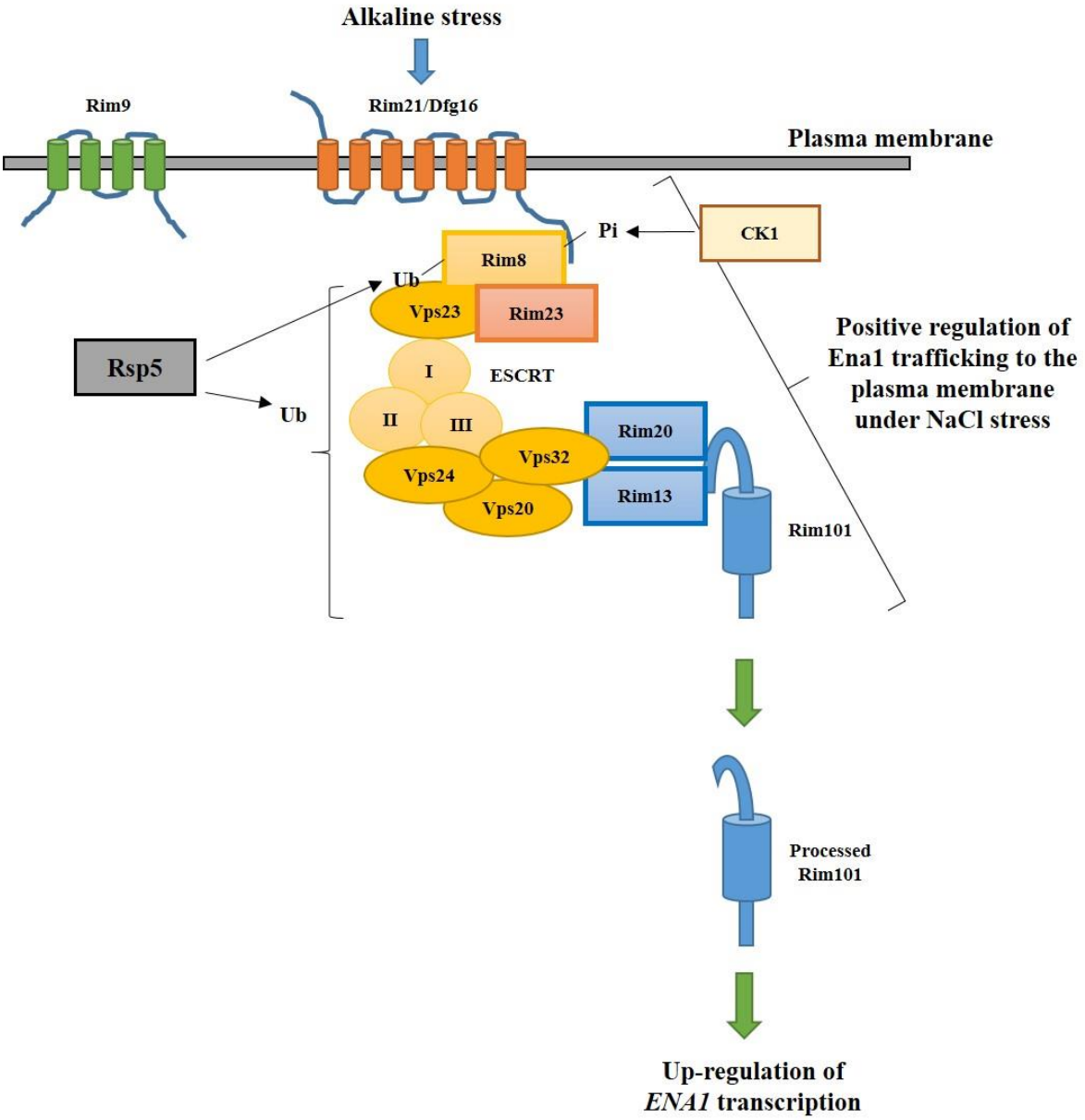

Figure 6. The Rim signaling pathway

The Rim signaling cascades in *S. cerevisiae*. External pH sensing involves the plasma membrane complex including Rim21, Dfg16, Rim9, Rim8, and Rim23. At alkaline pH, Rim8 is recruited to the plasma membrane and binds to Rim21/Dfg16 complex, leading to the recruitment of ESCRT complexes to the plasma membrane. Vps32, a key component of ESCRT-III, interacts with Rim23 and Rim20. Rim20 in and the signaling protease Rim13 recruit Rim101 to the plasma membrane complex. Rim13 mediates the cytoplasmic proteolysis of the full-length Rim101. The processed Rim101 then enters the nucleus to control the transcription of alkaline-responsive genes such as *ENA1*. It should be noted that under NaCl stress, the transcription of *ENA1* is predominantly controlled by Hog1 (Marques *et al.*, 2015). After sensing the signal, Rim21/Dfg16 complex undergoes endocytosis for its desensitization and turnover. (Modified from Cornet and Gaillardin, 2014; Obara and Kihara, 2014)

11. Summary of Rsp5 studies in my laboratory

Rsp5 research in my laboratory is particularly focused on the function of WW domains. Previously, my laboratory has discovered that several mutations in the WW domains of Rsp5 cause either resistance or sensitivity to particular stress conditions. By using Gap1 as a model substrate for plasma membrane proteins, Hoshikawa *et al*. (2003) have found that the *rsp5*^{A401E} mutant protein fails to recognize and ubiquitinate Gap1, consequently, Gap1 remains stable on the plasma membrane even in the presence of ammonium sulfate. This accounts for the hypersensitivity to a toxic L-proline analogue, L-acetidine-2-carboxylate (AZC), of *rsp5*^{A401E} mutant cells. In contrast, the *RSP5*^{T357A} mutant protein causes constitutive endocytosis and vacuolar degradation of Gap1, leading to AZC tolerance (Haitani *et al*., 2008; Sasaki and Takagi, 2013). In addition, the *rsp5*^{A401E} mutant strain is also hypersensitive to various environmental stress conditions including several toxic amino acid analogues, ethanol, heat shock, oxidative stress, high temperature in a rich medium, supporting the idea that Rsp5 is important for the quality control of stress-induced abnormal proteins including plasma membrane proteins (Hoshikawa *et al*., 2003; Shiga *et al*., 2014). It has also been shown that the *HSF1* and *MSN2/4* mRNA are restricted in the nuclei of the *rsp5*^{A401E} mutant cells under both non-stress and stress conditions including temperature upshift from 25˚C to 37˚C and exposure to 10% ethanol (Haitani and Takagi, 2008). Based on these previous studies, my laboratory hypothesizes that the WW domains of Rsp5 have a crucial role in the determination of substrate specificity. To study the contribution of each WW domain to Gap1 recognition, Watanabe *et al*. (2015) utilize the WW domain mutants (*rsp5*$^{W257F/P260A}$ in WW1, *rsp5*$^{W359F/P362A}$ in WW2, and *rsp5*$^{W415F/P418A}$ in WW3) and the putative phosphorylation site mutants of conserved threonine residues (*rsp5*^{T255A} in WW1, *RSP5*^{T357A} in WW2, and *rsp5*^{T413A} in WW3). Interestingly, all WW domains possess a cooperative role in Gap1 recognition mediated by arrestin-like Bul1/2 adaptor proteins. Notably, the *rsp5*^{T255A} and *rsp5*^{T413A} mutant proteins impair the interaction to Bul1 and possibly to Bul2; however, the *RSP5*^{T357A} mutant protein showed the strong physical interaction to Bul2. This supports the idea that the conserved Thr357 has a negative role in the Rsp5-Bul2 interaction. By using human α-synuclein as a model substrate for abnormal or unfolded proteins, Wijayanti *et al*. (2015) identify four mutations including T255A, D295G, P343S, and N427D located in the WW domains of Rsp5. These four mutants are able to alleviate α-synuclein toxicity more efficiently than did the wild-type Rsp5. Among them, *RSP5*^{P343S} improves the interaction and ubiquitination toward α-synuclein, leading to the acceleration of α-synuclein degradation rate and its resistance. In contrast,

rsp5^{T255A} confers α-synuclein resistance without affecting its degradation rate and improves cell growth under NaAc stress conditions. However, the molecular mechanism is still unknown. It is hypothesized that Rsp5 ubiquitinates an unknown target and the T255A mutant enhances this ubiquitination process that mediates the alleviation of α-synuclein toxicity and causes the NaAc tolerance (Wijayanti *et al*., 2015). It should be noted that the *rsp5*^{T255A} cells also show stress sensitivity to AZC (Watanabe *et al*., 2015) and high temperature at 39˚C in a rich medium (Wijayanti *et al*., 2015). Given that phosphorylation at the conserved Thr357 is used to regulate specific interaction of Rsp5 to the Bul2 adaptor protein (Watanabe *et al*., 2015), it is intriguing to hypothesize that the conserved Thr255, corresponding in position to Thr357, is regulated in a similar manner, but to unidentified target(s) or different Rsp5 adaptor protein(s). Therefore, in my study, I focused on the molecular mechanism of NaAc tolerance conferred by the *rsp5*^{T255A} mutant and its potential for engineering industrial yeast strains used for bioethanol production under NaAc stress conditions.

CHAPTER II
OBJECTIVES

1. To elucidate the molecular mechanism underlining the increased NaAc tolerance caused by the T255A mutation in the *RSP5* gene.

2. To examine the potential of the T255A mutant for engineering the industrial yeast strain used for bioethanol production under NaAc stress conditions.

CHAPTER III
MATERIALS AND METHODS

1. Strains and plasmids

Yeast strains used in this study were *S. cerevisiae* laboratory strains with haploid BY4741, BY4742, and diploid BY4743 (EUROSCARF) backgrounds as well as diploid *S. cerevisiae* industrial strain Ethanol Red® (Le Saffre). Ethanol Red® is the specially developed industrial yeast strain that has been particularly utilized for effective bioethanol production from molasses even at high temperature. All yeast strains are listed in Table 3. *Escherichia coli* strain DH5α (Invitrogen) was used for plasmid construction. Plasmids used in this study are listed in Table 4. Oligonucleotide primers used in this study are listed in Table 5.

The BY4741 T255A strain chromosomally expressing the *rsp5*^{T255A} mutant gene and harboring the *kanMX6* cassette was previously constructed by Dr. Indah Wijayanti (unpublished). The overlapping PCR was performed to fuse the *rsp5*^{T255A} gene with the *kanMX6* cassette. First, the *rsp5*^{T255A} gene with its native promoter and terminator was amplified from pRS415-*rsp5*^{T255A} (Wijayanti *et al*., 2015) using primers RSP5_-459bp_F and RSP5_+463bp_R. Second, the *kanMX6* cassette conferring resistance to kanamycin-derivative drug, G418, was amplified from pFA6a-3HA-kanMX6 using primers F-kanMX6 (5'- AAC TGA ATA GTG ACC TGG GTA TTA TAC TAC GAC ATG GAG GCC C-3') and KanMX6-Rev(-) (5'-GGG AAA ACG GAC ACC ATA AAT AAA AAA AAA ATT GGT GCG GAA TAA CAG TAT AGC GAC CAG C-3'). The underlined sequences indicate 30 bp of the downstream sequence of the *RSP5* gene from position 433 to 463 bp after the stop codon in F-kanMX6 and 45 bp of the downstream sequence of *RSP5* gene immediately after the stop codon in KanMX6-Rev(-), respectively. Finally, the resulting *rsp5*^{T255A} and *kanMX6* PCR products were mixed and amplified by KOD-Plus-Neo DNA polymerase using primers RSP5_-459bp_F and KanMX6-Rev(-), generating the fusion PCR product composed of *rsp5*^{T255A} gene fused with *kanMX6* cassette at position 463 bp downstream of the stop codon of *rsp5*^{T255A} gene. The *rsp5*^{T255A}*-kanMX6* cassette (4,754 bp) was introduced into the BY4741 wild-type strain. The transformants harboring the *rsp5*^{T255A}*-kanMX6* cassette were selected on YPD agar plates containing 200 µg/mL G418. The genomic integration at the *RSP5* locus of each transformant was verified by genomic PCR using primers RSP5-676F and RSP5-560R. The T255A mutation and whole *RSP5* sequence after the genomic integration were confirmed by sequencing.

To confirm the phenotype of BY4741 *rsp5*^{T255A}-*kanMX6* and check whether phosphorylation affects the function of Thr255 residue, BY4741 *rsp5*^{T255A} and BY4741 *rsp5*^{T255D} without *kanMX6* cassette were constructed by the two-step gene replacement method (Rothstein, 1991). *RSP5* PCR product with 500 bp upstream and downstream regulatory sequences was amplified from pRS416-*RSP5* by using primers RSP5-*Cla*I-Up500 and RSP5-*Xba*I-Down500, and cloned into pRS406 by *Cla*I/*Xba*I restriction digestion to generate the integrating plasmid pRS406-*RSP5*. The T255A and T255D mutations were introduced into pRS406-*RSP5* by using QuikChange II XL Site-Directed Mutagenesis Kit (Agilent) and primers RSP5_WW1_T255A_F and RSP5_WW1_T255A_R to generate pRS406-*rsp5*^{T255A} as well as primers RSP5_WW1_T255D_Fw and RSP5_WW1_T255D_Rv to generate pRS406-*rsp5*^{T255D}. The plasmid pRS406-*rsp5*^{T255A} and pRS406-*rsp5*^{T255D} were then linearized by either *Msc*I or *Pml*I restriction digestion and integrated into the genomic *RSP5* locus in the BY4741 wild-type strain. The transformants harboring pRS406-*rsp5*^{T255A} or pRS406-*rsp5*^{T255D} were selected on SC-Ura agar plates. The genomic integration was verified by PCR using primers RSP5-676F and RSP5-560R, and RSP5-676F and URA3-Rv, as well as URA3-Fw and RSP5-560R, respectively. pRS406 poping out was performed by growing the pRS406-*rsp5*^{T255A} or pRS406-*rsp5*^{T255D} integrated transformants in YPD overnight and counter-selecting them on SC+5-FOA agar plates. After counter selection, strains carrying the T255A or T255D mutation in the *RSP5* gene were isolated by sequencing. The BY4741 *rsp5*^{A401E}, BY4741 *rsp5*^{L733S}, BY4741 *rsp5*^{T357A}, BY4741 *rsp5*^{T413A} strains were previously constructed by Dr. Toshiya Sasaki by the similar method (Sasaki and Takagi, 2013).

The BY4742 T255A strain was constructed by introducing the *rsp5*^{T255A}-*kanMX6* cassette, which was amplified from the genomic DNA of the BY4741 T255A strain by primers RSP5-676F and RSP5-560R, into the genomic *RSP5* locus in the BY4742 wild-type strain. The transformants harboring the *rsp5*^{T255A}-*kanMX6* cassette were selected on YPD agar plates containing 200 μg/mL G418. The genomic integration was verified by PCR using primers RSP5-1kb-UpF and RSP5-1kb-DownR, and RSP5-1kb-UpF and KanMX6-Rev(-), respectively. The T255A mutation and whole *RSP5* sequence were confirmed by sequencing.

To construct diploid strains BY4741 X BY4742, BY4741 T255A X BY4742, BY4741 X BY4742 T255A, and BY4741 T255A X BY4742 T255A, haploid strains BY4741 wild-type, BY4742 wild-type, BY4741 T255A, and BY4742 T255A were mated in YPD overnight and selected on SD+His+Leu+Ura agar plates. The BY4743 wild-type strain was used as a positive

control. The diploid strains were verified by mating-type PCR using *MATa*, *MATα*, and *MAT* locus specific primers, and microscopic analysis.

Single disruption of the *BUL1, BUL2, ART1, RIM8, HOG1, PBS2, SSK1, STE50, STE11, BCK1, SLT2, FPS1, NHA1, JEN1,* or *ADY2* gene, and double disruption of the *BUL1* and *BUL2, ART1* and *RIM8, SSK2* and *SSK22,* or *SSK1* and *STE11* genes, as well as triple disruption of the *SSK2, SSK22,* and *STE11,* or *ENA1, ENA2,* and *ENA5* genes in strains BY4741 wild-type and BY4741 *rsp5*^{T255A}-*kanMX6* or BY4741 *rsp5*^{T255A} or BY4741 *rsp5*^{T357A} were performed using PCR-based gene disruption method (Janke *et al*., 2004). The disruption cassettes were amplified by using S1 and S2 primers specific for each gene and pFA6a-hphNT1, pFA6a-natNT2, or pFA6a-kanMX6 as a template, and then integrated into specific gene loci. Gene disruptants harboring *hphNT1*, *natNT2*, or *kanMX6* were selected on YPD agar plates containing 200 μg/mL hygromycin B, 100 μg/mL nourseothricin, or 200 μg/mL G418, respectively. Correct gene disruption was verified by genomic or colony PCR using primers bind to upstream and downstream regions of each gene as well as primers specific to the disruption cassette *hphNT1*, *natNT2*, or *kanMX6*, including hphFw1001 and hphRv21, clonNAT-317F and clonNAT-R, or kanMX4F and kanMX4R.

Ethanol Red® expressing the *rsp5*^{T255A} mutant gene from both chromosomes was constructed similarly as described above. The *rsp5*^{T255A}-*kanMX6* cassette, amplified from the genomic DNA of the BY4741 T255A strain using primers RSP5_-459bp_F and KanMX6-Rev(-), was introduced into the genomic *RSP5* locus in Ethanol Red®. After selection on YPD containing 200 μg/mL G418, the genomic integration at the *RSP5* locus and homozygosity of each transformant were verified by genomic PCR using primers RSP5-676F and RSP5-560R. Genomic DNA from transformants harboring the *rsp5*^{T255A}-*kanMX6* cassette in only one chromosome (heterozygous alleles) yielded two PCR products with the size of 3,666 bp and 5,486 bp whereas the genomic DNA from transformants harboring the same cassette in both chromosomes (homozygous alleles) yielded only the larger PCR product (5,486 bp). The correct T255A mutation and whole *RSP5* sequence after the genomic integration were confirmed by sequencing. Ethanol Red® harboring homozygous *rsp5*^{T255A} mutant alleles was selected and called ER-T255A.

To construct plasmid pDONR221-RIM8, the *RIM8* coding sequence was amplified from the genomic DNA of BY4741 using primers attB1-RIM8-F and attB2-RIM8-R. The obtaining attB1-RIM8-attB2 PCR product was purified and recombined with pDONR221 using BP reaction. *E. coli* DH5α transformation was performed using the BP reaction product and the

transformants were selected on LB agar plates containing 50 μg/mL kanamycin. The correct plasmid pDONR221-RIM8 was screened using colony PCR using primers M13 Fw and M13 Rv, and verified by sequencing. To construct plasmid pAG416-GPD-EGFP-RIM8, *RIM8* in the pDONR221-RIM8 was recombined with pAG416-GPD-EGFP-ccdB via LR reaction. *E. coli* DH5α transformation was performed using the LR reaction product and the transformants were selected on LB agar plates containing 100 μg/mL amplicilin. The correct plasmid pAG416-GPD-EGFP-RIM8 was screened by colony PCR using primers M13 Fw and M13 Rv, and M13 Fw and RIM8-520F, and verified by sequencing using primers M13 Fw, EGFP-C, and RIM8-520F.

Plasmids pRS316-RIM8-3HA (pOK476), pRS316-RIM8 (P506A Y508A)-3HA (pOK477), and pRS316-RIM8 (K521R)-3HA (pOK573) expressing *RIM8* and its mutant forms tagged with *3HA* at the C-terminus under the control of its native promoter were kindly provided by Dr. Keisuke Obara from Hokkaido University. Plasmid pRS416 was used as an empty vector for uracil auxotrophic complementation.

Table 3. Yeast strains used in this study

Strain	Genotype	Source or reference
BY4741	*MAT*a *his3Δ1 leu2Δ0 met15Δ0 ura3Δ0*	EUROSCARF
BY4742	*MAT*α *his3Δ1 leu2Δ0 lys2Δ0 ura3Δ0*	EUROSCARF
BY4743	*MAT*a/α *his3Δ1/his3Δ1 leu2Δ0/leu2Δ0 ura3Δ0/ura3Δ0 met15Δ0 lys2Δ0*	EUROSCARF
BY4741 T255A	BY4741 *rsp5*^{T255A}*-kanMX6*	Dr. Indah Wijayanti
T255A	BY4741 *rsp5*^{T255A}	This study
T255D	BY4741 *rsp5*^{T255D}	This study
T357A	BY4741 *rsp5*^{T357A}	Dr. Toshiya Sasaki
T413A	BY4741 *rsp5*^{T413A}	Dr. Toshiya Sasaki
TSY259	BY4741 *rsp5*^{A401E}	Dr. Toshiya Sasaki
Y1174	BY4741 *rsp5*^{L733S}	Dr. Toshiya Sasaki
BY4742 T255A	BY4742 *rsp5*^{T255A}*-kanMX6*	This study
BY4741 X BY4742	BY4743	This study
BY4741 T255A X BY4742	BY4743 *RSP5/ rsp5*^{T255A}*-kanMX6*	This study
BY4741 X BY4742 T255A	BY4743 *RSP5/ rsp5*^{T255A}*-kanMX6*	This study
BY4741 T255A X BY4742 T255A	BY4743 *rsp5*^{T255A}*-kanMX6/ rsp5*^{T255A}*-kanMX6*	This study
Δbul1	BY4741 *Δbul1::hphNT1*	This study
T255A *Δbul1*	BY4741 *rsp5*^{T255A}*Δbul1::hphNT1*	This study
Δbul2	BY4741 *Δbul2::natNT2*	This study
T255A *Δbul2*	BY4741 *rsp5*^{T255A} *Δbul2::natNT2*	This study
Δart1	BY4741 *Δart1::hphNT1*	This study
T255A *Δart1*	BY4741 *rsp5*^{T255A} *Δart1::hphNT1*	This study
Δrim8	BY4741 *Δrim8::natNT2*	This study
T255A *Δrim8*	BY4741 *rsp5*^{T255A} *Δrim8::natNT2*	This study
Δhog1	BY4741 *Δhog1::natNT2*	This study
T255A *Δhog1*	BY4741 *rsp5*^{T255A}*-kanMX6 Δhog1::natNT2*	This study
Δpbs2	BY4741 *Δpbs2::natNT2*	This study
T255A *Δpbs2*	BY4741 *rsp5*^{T255A}*-kanMX6 Δpbs2::natNT2*	This study
Δssk1	BY4741 *Δssk1::natNT2*	This study
T357A *Δssk1*	BY4741 *rsp5*^{T357A} *Δssk1::natNT2*	This study
T255A *Δssk1*	BY4741 *rsp5*^{T255A}*-kanMX6 Δssk1::natNT2*	This study
Δste50	BY4741 *Δste50::natNT2*	This study
T357A *Δste50*	BY4741 *rsp5*^{T357A} *Δste50::natNT2*	This study
T255A *Δste50*	BY4741 *rsp5*^{T255A}*-kanMX6 Δste50::natNT2*	This study
Δste11	BY4741 *Δste11::natNT2*	This study
T357A *Δste11*	BY4741 *rsp5*^{T357A} *Δste11::natNT2*	This study
T255A *Δste11*	BY4741 *rsp5*^{T255A}*-kanMX6 Δste11::natNT2*	This study
Δbck1	BY4741 *Δbck1::natNT2*	This study
T255A *Δbck1*	BY4741 *rsp5*^{T255A}*-kanMX6 Δbck1::natNT2*	This study

Strain	Genotype	Source or reference
Δslt2	BY4741 *Δslt2::natNT2*	This study
T255A *Δslt2*	BY4741 *rsp5*^{T255A}*-kanMX6 Δslt2::natNT2*	This study
Δfps1	BY4741 *Δfps1::natNT2*	This study
T255A *Δfps1*	BY4741 *rsp5*^{T255A}*-kanMX6 Δfps1::natNT2*	This study
Δnha1	BY4741 *Δnha1::natNT2*	This study
T255A *Δnha1*	BY4741 *rsp5*^{T255A}*-kanMX6 Δnha1::natNT2*	This study
Δjen1	BY4741 *Δjen1::natNT2*	This study
T255A *Δjen1*	BY4741 *rsp5*^{T255A}*-kanMX6 Δjen1::natNT2*	This study
Δady2	BY4741 *Δady2::natNT2*	This study
T255A *Δady2*	BY4741 *rsp5*^{T255A}*-kanMX6 Δady2::natNT2*	This study
Δbul1Δbul2	BY4741 *Δbul1::hphNT1 Δbul2::natNT2*	This study
T255A *Δbul1Δbul2*	BY4741 *rsp5*^{T255A} *Δbul1::hphNT1 Δbul2::natNT2*	This study
Δart1Δrim8	BY4741 *Δart1::hphNT1 Δrim8::natNT2*	This study
T255A *Δart1Δrim8*	BY4741 *rsp5*^{T255A} *Δart1::hphNT1 Δrim8::natNT2*	This study
Δssk2 Δssk22	BY4741 *Δssk2::natNT2 Δssk22::hphNT1*	This study
T357A *Δssk2 Δssk22*	BY4741 *rsp5*^{T357A} *Δssk2::natNT2 Δssk22::hphNT1*	This study
T255A *Δssk2 Δssk22*	BY4741 *rsp5*^{T255A}*-kanMX6 Δssk2::natNT2 Δssk22::hphNT1*	This study
Δssk1 Δste11	BY4741 *Δssk1::natNT2 Δste11::hphNT1*	This study
T357A *Δssk1 Δste11*	BY4741 *rsp5*^{T357A} *Δssk1::natNT2 Δste11::hphNT1*	This study
T255A *Δssk1 Δste11*	BY4741 *rsp5*^{T255A}*-kanMX6 Δssk1::natNT2 Δste11::hphNT1*	This study
Δssk2Δssk22Δste11	BY4741 *Δssk2::natNT2 Δssk22::hphNT1 Δste11::kanMX6*	This study
T255A *Δssk2Δssk22 Δste11*	BY4741 *rsp5*^{T255A} *Δssk2::natNT2 Δssk22::hphNT1 Δste11::kanMX6*	This study
Δena1/2/5	BY4741 *Δena1/ena2/ena5::natNT2*	This study
T255A *Δena1/2/5*	BY4741 *rsp5*^{T255A}*-kanMX6 Δena1/ena2/ena5::natNT2*	This study
Ethanol Red®	*MAT*a/α	Le Saffre
ER-T255A	Ethanol Red® *rsp5*^{T255A}*-kanMX6/ rsp5*^{T255A}*-kanMX6*	This study

Table 4. Plasmids used in this study

Plasmids	Description	Source or reference
pRS406	*URA3*	Stratagene
pRS406-*RSP5*	*URA3*, 500 bp *RSP5* promoter, *RSP5*, 500 bp *RSP5* terminator	This study
pRS406-*rsp5*^{T255A}	*URA3*, 500 bp *RSP5* promoter, *rsp5*^{T255A}, 500 bp *RSP5* terminator	This study
pRS406-*rsp5*^{T255D}	*URA3*, 500 bp *RSP5* promoter, *rsp5*^{T255D}, 500 bp *RSP5* terminator	This study
pRS416	*CEN, URA3*	Stratagene
pRS416-*RSP5*	*CEN, URA3*, 500 bp *RSP5* promoter, *RSP5*, 500 bp *RSP5* terminator	Dr. Satoshi Oshiro
pRS415-*rsp5*^{T255A}	*CEN, LEU2*, 500 bp *RSP5* promoter, *rsp5*^{T255A}, 500 bp *RSP5* terminator	Wijayanti *et al*., 2015
pFA6a-hphNT1	*hphNT1*	Janke *et al*., 2004
pFA6a-natNT2	*natNT2*	Janke *et al*., 2004
pFA6a-kanMX6	*kanMX6*	Jurg Bahler and John Pringle
pFA6a-3HA-kanMX6	*3HA-kanMX6*	Jurg Bahler and John Pringle
pDONR221	*ccdB, KanR*	Invitrogen
pDONR221-RIM8	*RIM8, KanR*	This study
pAG416-GPD-EGFP-ccdB	*CEN, URA3, GPD* promoter, *EGFP, ccdB, CYC1* terminator	Invitrogen
pAG416-GPD-EGFP-RIM8	*CEN, URA3, GPD* promoter, *EGFP, RIM8, CYC1* terminator	This study
pOK476	*CEN, URA3, RIM8* promoter, *RIM8-3HA, ADH1* terminator in pRS316	Dr. Keisuke Obara
pOK477	*CEN, URA3, RIM8* promoter, *RIM8 (P506A Y508A)-3HA, ADH1* terminator in pRS316	Dr. Keisuke Obara
pOK573	*CEN, URA3, RIM8* promoter, *RIM8 (K521R)-3HA, ADH1* terminator in pRS316	Dr. Keisuke Obara

Table 5. Oligonucleotide primers used in this study

Primer	Sequence (5' to 3')	Target gene	Source or Reference
RSP5_-459bp_F	GCATCTGCTAATTGATAAAAGGAC	*RSP5*	Dr. Indah Wijayanti
RSP5_+463bp_R	GTAGTATAATACCCAGGTCAC	*RSP5*	Dr. Indah Wijayanti
F-kanMX6	AACTGAATAGTGACCTGGGTATTATACTACGACATGGAGGCCC	*kanMX6*	Dr. Indah Wijayanti
KanMX6-Rev(-)	GGGAAAACGGACACCATAAATAAAAAAAAAATTGGTGCGGAATAACAGTATAGCGACCAGC	*kanMX6*	Dr. Indah Wijayanti
RSP5-676F	ACAGTCACGTGACAGTATACGATC	*RSP5*	Dr. Toshiya Sasaki
RSP5-560R	CAAATAACCGATACTCTCCGTGTG	*RSP5*	Dr. Toshiya Sasaki
RSP5-1kb-UpF	CCCAGCTATGTCGTCATGACTA	*RSP5*	Dr. Indah Wijayanti
RSP5-1kb-DownR	AACGTTTCGGAATTGGGGATGG	*RSP5*	Dr. Indah Wijayanti
RSP5-*Cla*I-Up500	ACCATCGATAAAAGACATACGCTTAACCA	*RSP5*	Dr. Toshiya Sasaki
RSP5-*Xba*I-Down500	AAGCTCTAGACGTTTCAAGTATGTACCTCA	*RSP5*	Dr. Toshiya Sasaki
RSP5_WW1_T255A_F	AACACAAGGACTGCCACTTGGAAAC	*RSP5*	Dr. Toshiya Sasaki
RSP5_WW1_T255A_R	GTTTCCAAGTGGCAGTCCTTGTGTTATG	*RSP5*	Dr. Toshiya Sasaki
RSP5_WW1_T255D_Fw	CATAACACAAGGACTGACACTTGGAAACGTC	*RSP5*	Hiroki Murai
RSP5_WW1_T255D_Rv	GACGTTTCCAAGTGTCAGTCCTTGTGTTATG	*RSP5*	Hiroki Murai
URA3-Fw	ATGTCGAAAGCTACATATAAGGAACG	*URA3*	Dr. Yu Sasano
URA3-Rv	TTAGTTTTGCTGGCCGCATCTTCTC	*URA3*	Dr. Yu Sasano
MATa	ACTCCACTTCAAGTAAGAGTTTG	*MATa*	Keisuke Hashida
MATα	GCACGGAATATGGGACTACTTCG	*MATα*	Keisuke Hashida
MAT locus	AGTCACATCAAGATCGTTTATGG	*MATa* and *MATα*	Keisuke Hashida
BUL1-S1	GGGCGAAAAGAGACTGTTCGTGTGTGTCAACAGGTATATCGTACGCTAAATGCGTACGCTGCAGGTCGAC	*BUL1*	Dr. Toshiya Sasaki
BUL1-S2	TCTATATCTATAAGAAAAGTAACGAGAATTTTTTCTAATGTTTTTTTAGC ATAGGCCACTAGTGGATCTG	*BUL1*	Dr. Toshiya Sasaki
BUL2-S1	ACTGAAGCAGCAGATTTGAGATATATTCTGGGGAACAAAAGAAGTATTAA TGCGTACGCTGCAGGTCGAC	*BUL2*	Dr. Toshiya Sasaki
BUL2-S2	TCAATTATTTGTAAAACTGCGAGATTACTGTTAGTGTTGTATGGTCTAGC ATAGGCCACTAGTGGATCTG	*BUL2*	Dr. Toshiya Sasaki
ART1-S1	TGATTTTTACTCCTACTTAGTATACATTTCACTAAACAATACGTTTTACCCGGATCCCCGGGTTAATTAA	*ART1*	This study
ART1-S2	TATCTAAGATAAAAATATATGGTAAATACCTTTAACGAATATTATAAAATATCGATGAATTCGAGCTCG	*ART1*	This study

Primer	Sequence (5’ to 3’)	Target gene	Source or Reference
RIM8-S1	TAGTATAGTATCATCAGCATCACCCTCACTATCGGTAGCATTGACCAAACCGGATCCCCGGGTTAATTAA	*RIM8*	This study
RIM8-S2	AGTTCCAACACGGCGCAAGCTGCGAGTATATGACTTGTTACCTGCACTTTATCGATGAATTCGAGCTCG	*RIM8*	This study
HOG1-S1	AAAAAGGAACAAAGGGAAAACAGGGAAAACTACAACTATCGTATATAATACGGATCCCCGGGTTAATTAA	*HOG1*	This study
HOG1-S2	ACATCAAAAAGAAGTAAGAATGAGTGGTTAGGGACATTAAAAAAACACGTATCGATGAATTCGAGCTCG	*HOG1*	This study
PBS2-S1	CTATAGATACATTATTATATTAAGCAGATCGAGACGTTAATTTCTCAAAGCGGATCCCCGGGTTAATTAA	*PBS2*	This study
PBS2-S2	TTTTTGTTGTTATATTCACGTGCCTGTTTGCTTTTATTTGGATATTAACGATCGATGAATTCGAGCTCG	*PBS2*	This study
SSK1-S1	AAAGGCTGCTGTAAATCAAAAACGAATCGATTTTGGGGAGACAAGTAAAACGGATCCCCGGGTTAATTAA	*SSK1*	This study
SSK1-S2	TAAATATCGTTACATTCTATCATAATGTCCTCTACACGGTACAACCAAACATCGATGAATTCGAGCTCG	*SSK1*	This study
SSK2-S1	TACTAAAAAGAAGAGAAGCCTTTGCGTAAACTATTTGACAGGCACAAATACGGATCCCCGGGTTAATTAA	*SSK2*	This study
SSK2-S2	TACATTATATTTTGATTTTACATATAATACAACAAACCTTCTCAACTTAAATCGATGAATTCGAGCTCG	*SSK2*	This study
SSK22-S1	ATGTTGTTTTACTTAGGGTGGCTATAAAAGGTAGTTCCTTGTAGGTGAAACGGATCCCCGGGTTAATTAA	*SSK22*	This study
SSK22-S2	TACATTACATTATATATCGTAGTATATCATATTTTTAGACGTTGACCACTATCGATGAATTCGAGCTCG	*SSK22*	This study
STE50-S1	TCGAAGGACTCGAAAAGACAGAGGTCGTACTAGCAGAGATAGCAAATCAGCGGATCCCCGGGTTAATTAA	*STE50*	This study
STE50-S2	TTATCCTATTCGTGTAAGTTTAGTATGATGATGTGCATGACAACTGCACAATCGATGAATTCGAGCTCG	*STE50*	This study
STE11-S1	GACCACTTAATAAAGCTAGTATGATAAGATCACCGGTAGACGAAATATACCGGATCCCCGGGTTAATTAA	*STE11*	This study
STE11-S2	TCGGCCAGAGCACTTTAGTGCCATAAAAAGAATTAATAAGTAGCCCTTTTATCGATGAATTCGAGCTCG	*STE11*	This study
BCK1-S1	TAGTACGAAACACTAAATATAGTATTAAAATAGTTCAACTCCACCTCCAACGGATCCCCGGGTTAATTAA	*BCK1*	This study
BCK1-S2	TATATTATTACGTATGCATAAATATCTTAAGTATAGATCGATCCTAATAGATCGATGAATTCGAGCTCG	*BCK1*	This study
SLT2-S1	CTATCAAAATAGTAGAAATAATTGAAGGGCGTGTATAACAATTCTGGGAGCGGATCCCCGGGTTAATTAA	*SLT2*	This study
SLT2-S2	TTACATCTATGGTGATTCTATACTTCCCCGGTTACTTATAGTTTTTTGTCATCGATGAATTCGAGCTCG	*SLT2*	This study
FPS1-S1	TATTATTTTACCAAGTACGCTCGAGGGTACATTCTAATGCATTAAAAGACCGGATCCCCGGGTTAATTAA	*FPS1*	This study
FPS1-S2	ATTTTTTTCTATCAGTCTATATTATTTGTTTCTTTTTCTTGTCTGTTTTCATCGATGAATTCGAGCTCG	*FPS1*	This study
JEN1-S1	ACAGTTTCAAAAGTTTTTCCTCAAAGAGATTAAATACTGCTACTGAAAATCGGATCCCCGGGTTAATTAA	*JEN1*	This study
JEN1-S2	ATGCAGTTACATAGAGAAGCGAACACGCCCTAGAGAGCAATGAAAAGTGAATCGATGAATTCGAGCTCG	*JEN1*	This study
ADY2-S1	CACAGATATAACTAAACAACCACAAAACAACTCATATACAAACAAATAATCGGATCCCCGGGTTAATTAA	*ADY2*	This study
ADY2-S2	AAACTACTCTTTTTTATTTCAATAGTTCTCGTTATTAGTAGGTCGTGCTCATCGATGAATTCGAGCTCG	*ADY2*	This study
NHA1-S1	CGTGTTTTTTTGTACATTATAAAAAAAAATCCTGAACTTAGCTAGATATTCGGATCCCCGGGTTAATTAA	*NHA1*	This study

Primer	Sequence (5’ to 3’)	Target gene	Source or Reference
NHA1-S2	CATTTCGTTTATATATATACTAAAATAATATATCTTTGTGTATTAATAAAATCGATGAATTCGAGCTCG	*NHA1*	This study
ENA-S1	TTAATTCACATTTATTTGAGGCAACAATACGTATATTTACTAATTAAAGATGCGTACGCTGCAGGTCGAC	*ENA1*	This study
ENA-S2	TAAAAAAATCTAAACTATTACGTAAGGGGGAGAAGGGATAAGGGATGCTTAATCGATGAATTCGAGCTCG	*ENA5*	This study
BUL1-Fw-501	TGCGCCAGCGGCACT	*BUL1*	Yuko Shimizu
BUL1-Rv+620	TGCCAAGGGTTTGGCAATGC	*BUL1*	Yuko Shimizu
BUL2-Fw-498	CGCGGGGAATTTGTCTAGTTACA	*BUL2*	Yuko Shimizu
BUL2-Rv+510	ACCTGTAATGGGCTCGATGA	*BUL2*	Yuko Shimizu
Upart1-266F	AGACGGAAAAGCACGACTCA	*ART1*	This study
Downart1-570R	CCACTATCTGCCCACCCTTT	*ART1*	This study
Uprim8-323F	GGACTTTTCCGCTCCAATCC	*RIM8*	This study
Downrim8-709R	GAGCTGTGTCCACAGTTGAG	*RIM8*	This study
Uphog1-748F	GCTGGCTCCAGATACATCCT	*HOG1*	This study
Downhog1-553R	TTTCTGCCACAGTCCGTGAA	*HOG1*	This study
Uppbs2-884F	TCTGTTCCCCTTGAGCATAG	*PBS2*	This study
Downpbs2-823R	GGGCACTCTACTCATCGTTC	*PBS2*	This study
Upssk1-540F	CCCTGTTACAGGTGCAGAGA	*SSK1*	This study
Downssk1-674R	GGCGGATACTTCTGTCCCAA	*SSK1*	This study
Upssk2-115F	TTGTGTGAGCTCCGTCTGTC	*SSK2*	This study
Downssk2-348R	CGACAAGACCCCTACCGTTT	*SSK2*	This study
Upssk22-948F	AGTTTGACGGAATCTCTACC	*SSK22*	This study
Downssk22-845R	CCGTAGCAATTACTTCTCCA	*SSK22*	This study
Upste50-453F	ATCCACAACGAGCGTCGAAC	*STE50*	This study
Downste50-509R	GCGTGAAGCTCAAGCACAAG	*STE50*	This study
Upste11-272F	TTCTCGCCCAACTTTTCCTC	*STE11*	This study
Downste11-282R	CCTGTTTCTTCGTGCTTCCA	*STE11*	This study
Upbck1-831F	GTCGACCTTCACAGCCTACT	*BCK1*	This study
Downbck1-187R	TGAAGGGTCGAATCGTCGTT	*BCK1*	This study

Primer	Sequence (5’ to 3’)	Target gene	Source or Reference
Upslt2-176F	AGGGAAATCAGATCCTACAC	*SLT2*	This study
Downslt2-662R	CAGCGCCTATTTTACATTCC	*SLT2*	This study
Upfps1-807F	CCCAATTTTGACGGCAGTTC	*FPS1*	This study
Downfps1-977R	GTCCATCATAGGCGACAAGG	*FPS1*	This study
Upjen1-592F	CTAATAGCCGACAAACGGAC	*JEN1*	This study
Downjen1-715R	CAAGGTTAGGGAATGACCTC	*JEN1*	This study
Upady2-221F	TGTACTCCAACCTGTCAGAG	*ADY2*	This study
Downady2-658R	TTCTCTCACGTCTGCCTGTT	*ADY2*	This study
Upnha1-431F	CACTGTTCTTGGAGAAAGCC	*NHA1*	This study
Downnha1-340R	TGTTTTGACCCATCGTGTCT	*NHA1*	This study
ENA1-F	TCCTCTTATTCCGTTCTTTC	*ENA1*	Dr. Satoshi Oshiro
ENA5-R	GGAAGTCAAAAAGGAAGAAG	*ENA5*	Dr. Satoshi Oshiro
clonNAT-317F	CTGACCGTCGAGGACATCG	*natNT2*	Dr. Toshiya Sasaki
clonNAT-R	CGATGTCCTCGACGGTCAG	*natNT2*	Dr. Toshiya Sasaki
hphFw1001	CCAGCACTCGTCCGAG	*hphNT1*	Yuko Shimizu
hphRv21	GACAGACGTCGCGGTG	*hphNT1*	Yuko Shimizu
kanMX4F	CATGGCAAAGGTAGCGTTG	*kanMX4* or *kanMX6*	Dr. Susumu Morigasaki
kanMX4R	CCGACTCGTCCAACATCAATAC	*kanMX4* or *kanMX6*	Dr. Susumu Morigasaki
attB1-RIM8-F	GGGGACAAGTTTGTACAAAAAAGCAGGCTTTTCGTTACTGAGACTGTGGAA	*RIM8*	This study
attB2-RIM8-R	GGGGACCACTTTGTACAAGAAAGCTGGGTCTTAATAGTCATCACAAGGGG	*RIM8*	This study
M13 Fw	GTAAAACGACGGCCAG	*M13*	Prof. Hiroshi Takagi
M13 Rv	CAGGAAACAGCTATGAC	*M13*	Prof. Hiroshi Takagi
RIM8-520F	CCCTCAACAACATCAACG	*RIM8*	This study
EGFP-C	CATGGTCCTGCTGGAGTTCGTG	*EGFP*	This study

2. Culture media

Media used for cultivation of *S. cerevisiae* strains were a nutrient rich yeast extract-peptone-dextrose medium (YPD) (1% yeast extract, 2% peptone, and 2% glucose) adjusted to pH 4.5 or 6 using 1 M HCl when indicated and a synthetic complete medium (SC) (0.17% yeast nitrogen base without amino acids and ammonium sulfate, 0.5% ammonium sulfate, 2% glucose, and 0.2% amino acid powder) adjusted to pH 6 using 1 M KOH. For selection of *URA3*-harboring yeast strains, SC lacking uracil (SC-Ura) was used. For counter selection of *URA3*-harboring yeast strains, SC containing 1 mg/mL 5-fluorootic acid (5-FOA) (SC+5-FOA) was used. For mating between BY4741 and BY4742 strains, minimal medium synthetic dextrose (SD) (0.17% yeast nitrogen base without amino acids and ammonium sulfate, 0.5% ammonium sulfate, and 2% glucose) containing 0.005% histidine, 0.01% leucine, and 0.01% uracil (SD+His+Leu+Ura) was used for auxotrophic selection of diploid cells. For selection of yeast strains harboring *hphNT1*, *natNT2*, or *kanMX6*, YPD containing 200 μg/mL hygromycin B, 100 μg/mL nourseothricin, or 200 μg/mL G418 was used respectively. For NaAc stress treatment, yeast strains were cultured in YPD containing 0.33 M NaAc, pH 6, prepared by adding 99.5% acetic acid (Wako) to the sterilized YPD to the final concentration of 0.33 M and adjusting pH of the medium to 6.2-6.8 using 5 M NaOH. *E. coli* cells were grown in Luria-Bertani (LB) medium (Sambrook and Russell, 2001). LB medium containing 100 μg/mL ampicillin or 50 μg/mL kanamycin was used for cultivation of *E. coli* recombinant strains. If necessary, 2% agar was added to solidify the medium. To examine stress responses, yeast strains were cultured on YPD agar plates containing 0.33 M NaAc, 0.33 M KAc, 1 M KCl, 0.1 M LiCl, 1 M NaCl at pH 6, and that containing 0.042 M or 0.050 M acetic acid at pH 4.4 or 4.5, respectively. For fermentation tests at high glucose concentrations, YPD containing 10% glucose (YPD10) or 20% glucose (YPD20) was used.

3. Spot test for phenotypic analysis

Yeast strains were pre-cultured in 2 mL YPD at 30˚C with shaking at 300 rpm overnight and then inoculated in 2 mL YPD with the initial OD_{600} of 0.25. The main cultures were incubated at 30˚C with shaking at 300 rpm for approximately 4 hours. The log-phase cells (OD_{600}~1) were 10 fold-serially diluted to 10^{-4}. All dilutions were spotted onto control and stress agar plates as indicated. Then, the plates were incubated at 30˚C or 39˚C (high temperature) for 1-2 days.

4. Growth curve analysis in liquid medium

Yeast cells were pre-cultured in 3 mL YPD, pH 6 at 30˚C with shaking at 300 rpm overnight and then inoculated in 30-50 mL YPD, pH 6 (control) and YPD containing 0.33 M NaAc, pH 6 (stress) with the initial OD_{600} of 0.1. The main cultures were incubated at 30˚C with shaking at 114 rpm. OD_{600} was measured approximately every 4 hours until reaching stationary phase or when indicated.

5. Detection of Hog1 phosphorylation under NaAc stress

BY4741 wild-type and BY4741 T255A mutant cells were pre-cultured in 3 mL YPD, pH 6 overnight and then inoculated in 10 mL YPD, pH 6 with the initial OD_{600} of 0.2. The main cultures were incubated at 30˚C with shaking at 114 rpm for approximately 4 hours until reaching the log phase (OD_{600}~1). For non-stress condition, 1.1 mL 100% w/v trichloroacetic acid (TCA) was added to the culture. Approximately, 10 OD_{600} cells were collected by centrifugation at 3,000 rpm, room temperature for 3 min and washed twice with 1 mL 10% w/v TCA. The collected cells were re-suspended in 200 µl 10% w/v TCA. For stress conditions, approximately, 10 OD_{600} cells were collected by centrifugation at 3,000 rpm, room temperature for 3 min. Supernatants were discarded completely. Then, the collected cells were re-suspended in 10 mL YPD containing 0.33 M NaAc, pH 6 for tests and 10 mL YPD containing 0.8 M NaCl, pH 6 for a positive control. The cultures under NaAc stress were incubated for 10, 20 and 30 min, whereas those under NaCl stress were incubated for 10 min at 30˚C with shaking at 114 rpm. To stop Hog1 phosphorylation, 1.1 mL 100% w/v TCA was immediately added to the cultures after stress treatment. Approximately, 10 OD_{600} cells were collected at room temperature, washed twice with 1 mL 10% w/v TCA, and re-suspended in 200 µl 10% w/v TCA. To extract total proteins by the TCA method, the TCA re-suspended cells from non-stress and stress conditions were transferred to 2-mL tubes containing 0.5 mm glass beads. The cells in suspension were crushed by the glass beads using the Multi-beads shocker® (Yasui Kikai) at 2,500 rpm, 30 sec ON/30 sec OFF, 9 times. Another 200 µl 10% w/v TCA was added to each tube. The sample tubes with pores at the bottom were put into 5-mL falcon tube and centrifuged at 3,000 rpm, 4˚C for 10 min. The supernatants were removed completely. The precipitates were re-suspended in 100 µl 1X sample buffer (50 mM Tris-HCl (pH 6.8), 2% SDS, 2.25% glycerol, 5% 2-mercaptoethanol, and 0.0125% bromophenol blue), transferred to 1.5-mL tubes, incubated at 65˚C for 15 min, and centrifuged at 10,000 rpm, 25˚C for 10 min. The whole cell extracts (WCE) in the supernatants were transferred to new 1.5-mL tubes. The protein concentration was quantified by Bradford assay (Bio-Rad). 5 ug WCE were run on 10% SDS-

PAGE, blotted onto the PVDF membranes, and then blocked in 5% w/v BSA in 1X TBS-T buffer (20 mM Tris-base, 150 mM NaCl, concentrated HCl to neutralize the solution to pH 7.6 and 0.1% Tween-20). All washing steps were carried out using 1X TBS-T buffer. The Thr174 and Tyr176 dually-phosphorylated Hog1, Hog1, and glyceraldehyde 3-phosphate dehydrogenase (GAPDH) proteins were detected by the polyclonal anti-phospho p38 rabbit antibody (Cell Signaling Technology) at 1:1,000 dilution, the polyclonal anti-Hog1 (yC-20) goat antibody (Santa Cruz Biotechnology) at 1:1,000 dilution, and the polyclonal anti-GAPDH rabbit antibody (Nordic Immunological Laboratories) at 1:10,000 dilution, respectively. HRP-conjugated polyclonal anti-rabbit or anti-goat IgG (Promega) was used at 1:2,000 dilution for secondary probing. Signals were produced by Amersham ECL prime reagents (GE healthcare) and captured by using ImageQuant^{TM} LAS4000 (GE healthcare).

6. Intracellular Na^+ analysis by inductively coupled plasma mass spectrometry

Approximately, 5 OD_{600} cells from different yeast strains under indicated conditions were collected by centrifugation at 3,000 rpm, 4˚C, washed twice with ice-cold washing solution (20 mM $MgCl_2$ and 180 mM Sorbitol) (Marqués *et al.*, 2015), and re-suspended in 1 mL MilliQ water. Intracellular ions were extracted by heating cell suspension at 95˚C for 15 min. Cell debris was pelleted by centrifugation at 15,000 rpm at room temperature. Supernatant containing intracellular ions was taken up and filtrated through 2 μM filter (Advantech). For standard curve, 1,000 ppm sodium (Na^+) standard (AAS grade, Sigma-Aldrich) was diluted to 0, 25, 50, 75, and 100 ppb. The samples and Na^+ standards were mixed with nitric acid (HNO_3) (Ultratrace analysis grade, Wako) to the final concentration of 0.5% and indium (In) standard solution (AAS grade, Fluka) to the final concentration of 10 ppb. The Na^+ content was analyzed by inductively coupled plasma mass spectrometry (ICP-MS) using ICPM-8500 (Shimadzu). Intracellular Na^+ concentration was calculated by using the standard curve.

7. Rim8 ubiquitination assay

For non-stress condition, Δ*rim8* and T255A Δ*rim8* cells harboring pRS416, pRS316-RIM8-3HA (pOK476), pRS316-RIM8 (P506A Y508A)-3HA (pOK477), or pRS316-RIM8 (K521R)-3HA (pOK573) were pre-cultured in 3 mL SC-Ura, pH 6 at 30˚C with shaking at 300 rpm overnight and then inoculated in 10 mL SC-Ura, pH 6 with the initial OD_{600} of 0.2. The main cultures were incubated at 30°C with shaking at 133 rpm for approximately 4.5 hours until

reaching the log phase (OD_{600}~ 1). Approximately, 3 OD_{600} cells were collected by centrifugation at 13,000 rpm, 4˚C for 1 min and washed once with 1 mL sterilized DW.

For NaAc stress conditions, Δ*rim8* and T255A Δ*rim8* cells harboring pRS416 and pRS316-RIM8-3HA (pOK476) were pre-cultured in 3 mL SC-Ura, pH 6 at 30˚C with shaking at 300 rpm overnight and then inoculated in 30 mL of SC-Ura, pH 6 with the initial OD_{600} of 0.2. The main cultures were incubated at 30°C with shaking at 133 rpm for approximately 4.5 hours until reaching the log phase (OD_{600}~ 1). Approximately, 30 OD_{600} cells were collected by centrifugation at 3,000 rpm, 25˚C for 3 min, washed once with 1 mL sterilized DW, and re-suspended in 30 mL YPD containing 0.33 M NaAc, pH 6. The NaAc-treated cultures were incubated at 30˚C with shaking at 133 rpm. Approximately, 3 OD_{600} cells were collected at 0, 30, 60, and 90 min after incubation by centrifugation at 3,000 rpm, 4˚C for 3 min and washed once with 1 mL sterilized DW.

To extract total proteins by the alkaline-TCA method, the collected cells were re-suspended in 1 mL ice-cold N/β solution (0.25 N NaOH and 1% 2-mercaptoethanol) and put on ice for 10 min. After that, 70 µl 100% w/v TCA was added to the samples and mixed. The samples were put on ice for 10 min and centrifuged at 15,000 rpm, 4˚C for 20 min. The supernatants were removed completely. 500 µl 1 M Tris without adjusting pH was added to the precipitates. The samples were centrifuged at 15,000 rpm, 4˚C for 20 min and the supernatants were discarded completely. The precipitates were re-suspended in 100 µl 1X sample buffer (50 mM Tris-HCl (pH 6.8), 2% SDS, 2.25% glycerol, 5% 2-mercaptoethanol, and 0.0125% bromophenol blue) and incubated with sonication for 1.5 hours. The samples were incubated at 37°C for 10 min and centrifuged at 15,000 rpm, 25˚C for 3 min. The supernatants were collected as whole cell extracts (WCE). Approximately, 0.45 OD_{600} WCE were run on 7.5% SDS-PAGE, blotted on to the PVDF membranes, and then blocked in 5% w/v BSA in 1X TBS-T buffer (20 mM Tris-base, 150 mM NaCl, concentrated HCl to neutralize the solution to pH 7.6 and 0.1% Tween-20). All washing steps were carried out using 1X TBS-T buffer. The Ub-Rim8-3HA or Rim8-3HA, and Pgk1 proteins were detected by the monoclonal anti-HA (12CA5) mouse antibody (Santa Cruz Biotechnology) at 1:1,000 dilution, the monoclonal anti-Pgk1 mouse antibody (Novex) at 1:20,000 dilution, respectively. HRP-conjugated polyclonal anti-mouse IgG (Promega) was used at 1:2,000 dilution for secondary probing. Signals were produced by Amersham ECL prime reagents (GE healthcare) and captured by using ImageQuant™ LAS4000 (GE healthcare).

8. Co-immunoprecipitation between Rsp5 and Rim8

Δ*rim8* and T255A Δ*rim8* cells harboring pAG416-GPD-EGFP-ccdB or pAG416-GPD-EGFP-RIM8 were pre-cultured in 3 mL SC-Ura, pH 6 at 30˚C with shaking at 300 rpm, overnight and then inoculated in 30 mL SC-Ura, pH 6 with the initial OD_{600} of 0.2. The main cultures were incubated at 30˚C with shaking at 133 rpm for approximately 4.5 hours until reaching the log phase (OD_{600}~ 1). Approximately, 30 OD_{600} cells were collected by centrifugation at 3,000 rpm, 4˚C for 3 min and washed once with 2 mL sterilized DW. Supernatants were discarded completely. The collected cells were re-suspended in 700 µl ice-cold lysis buffer (20 mM Tris-HCl (pH 8.0), 150 mM sodium chloride, 10% glycerol, 0.5% NP-40, and protease inhibitors) (Sasaki and Takagi, 2013) and transferred to 2 mL tubes containing 0.5 mm glass beads. The cells in suspension were crushed by the glass beads using the Multi-beads shocker® (Yasui Kikai) at 2,700 rpm, 30 sec ON/30 sec OFF, 15 times. The sample tubes with pores at the bottom were put into 5-mL falcon tube and centrifuged at 3,000 rpm, 4˚C for 3 min. The supernatants were retrieved and transferred to 1.5-mL tubes, and centrifuged at 15,000 rpm, 4˚C for 10 min. The supernatants were collected to 1.5-mL tubes. The protein concentration was measured by Bradford assay (Bio-Rad) and adjusted to be equally the same among each sample using lysis buffer. After normalization, 80 µl of each sample was kept for whole cell extract (WCE) and the remaining was proceeded for co-immunoprecipitation (Co-IP). The ice-cold lysis buffer-equilibrated anti-GFP magnetic beads (Medical & Biological Laboratories) were added to the Co-IP samples (10 µl/sample). Immunoprecipitation was performed at 4˚C for 1.5 hours using rotating wheel with tapping. During Co-IP, 80 µl WCE was mixed with 20 µl 5X sample buffer (250 mM Tris-HCl (pH 6.8), 10% SDS, 11.25% glycerol, 25% 2-mercaptoethanol, and 0.0625% bromophenol blue) and incubated at 65˚C for 15 min. After Co-IP, the anti-GFP magnetic beads were washed 3 times with the wash buffer (50 mM Tris-HCl (pH 8.0), 150 mM sodium chloride, 10% glycerol, and 0.1% NP-40) (Sasaki and Takagi, 2013) and incubated with 80 µl 1X sample buffer (50 mM Tris-HCl (pH 6.8), 2% SDS, 2.25% glycerol, 5% 2-mercaptoethanol, and 0.0125% bromophenol blue) at 65˚C for 15 min. The anti-GFP magnetic beads were removed by putting the sample tubes onto the magnetic stand and transferring the Co-IP supernatants to new tubes. 10 µl IP, 5 ug WCE (for anti-GFP), and 10 ug WCE (for anti-Rsp5) were run on 7.5% SDS-PAGE, blotted onto the PVDF membranes, and then blocked in 5% w/v BSA in 1X TBS-T buffer (20 mM Tris-base, 150 mM NaCl, concentrated HCl to neutralize the solution to pH 7.6 and 0.1% Tween-20). All washing steps were carried out using 1X TBS-T buffer. The Rsp5, GFP-Rim8, and 3-phosphoglycerate

kinase (Pgk1) proteins were detected by the polyclonal anti-Rsp5 rabbit antibody (provided by Jon Huibregste) at 1:2,000 dilution, the monoclonal anti-GFP mouse antibody (Roche) at 1:2,000 dilution, and the monoclonal anti-Pgk1 mouse antibody (Novex) at 1:20,000 dilution, respectively. HRP-conjugated polyclonal anti-rabbit or anti-mouse IgG (Promega) was used at 1:2,000 dilution for secondary probing. Signals were produced by Amersham ECL prime reagents (GE healthcare) and captured by using ImageQuant™ LAS4000 (GE healthcare).

9. Fermentation analysis using Fermograph

To examine the fermentation properties under NaAc stress conditions, Ethanol Red® and ER T255A mutant cells were grown in 3 mL YPD overnight and then inoculated in 50 mL YPD or YPD containing 0.33 M NaAc, pH 6.8 in 250 mL bottles with the initial OD_{600} of 0.1. The culture bottles were connected to the Fermograph®II-W (Atto) and incubated at 30˚C with shaking at 120 rpm. Total CO_2 gas was real-time measured and the CO_2 gas emission rate was automatically calculated.

To examine the fermentation properties under NaAc stress conditions at high glucose concentrations, YPD containing 10% glucose (YPD10) and 20% glucose (YPD20) were used. Ethanol Red® and ER T255A mutant cells were grown in 3 mL YPD10 and YPD20 overnight and then inoculated in 50 mL YPD10 or YPD10 containing 0.33 M NaAc, pH 6.8 and YPD20 or YPD20 containing 0.33 M NaAc, pH 7.0, respectively, in the 250 mL bottles with the initial OD_{600} of 0.1. The culture bottles were connected to the Fermograph®II-W (Atto) and incubated at 30˚C with shaking at 120 rpm. Total CO_2 gas was real-time measured and the CO_2 gas emission rate was automatically calculated.

CHAPTER IV
RESULTS

Section 1.
Elucidation of the molecular mechanism underlining the increased NaAc tolerance caused by the T255A mutation in the *RSP5* gene

1. Growth phenotype of the T255A mutant

Recently, my laboratory discovered that the T255A mutation in the WW1 domain of Rsp5 confers tolerance to NaAc stress on *S. cerevisiae* cells (Wijayanti *et al.*, 2015). However, the molecular mechanisms in which Rsp5 involves in NaAc stress remains unknown. First, an involvement of Rsp5 in NaAc stress was examined by phenotypic analysis using Leu733Ser (*rsp5*^{L733S} or *rsp5-1*) mutant. The *rsp5-1* mutant is known as the thermo-sensitive allele of *RSP5* (Wang *et al.*, 1999). This mutant harbors the substitution of Leu733 with Ser in the catalytic HECT domain of Rsp5 which causes the defect in ubiquitin-thioester bond formation. Thus, the function of Rsp5 is impaired at the permissive temperature of 25˚C to 30˚C and inactive at the restrictive temperature of more than 35˚C. As shown in Figure 6, the wild-type and *rsp5-1* mutant cells grew at the similar level under the non-stress condition, whereas the *rsp5-1* mutant cells were more highly sensitive to NaAc stress condition than did the wild-type cells. This result suggests that the impaired function of Rsp5 in the *rsp5-1* mutant cells is responsible for the NaAc sensitive phenotype. Thus, Rsp5 ubiquitination activity is required for NaAc stress responses.

To determine whether the T255A mutation is gain- or loss-of-function, the NaAc tolerant phenotype of the T255A mutant was compared with that of the Ala401Glu (*rsp5*^{A401E}) and the *rsp5-1* mutants. The A401E mutant has been previously reported as the hypersensitive mutant form of Rsp5, which renders yeast cells sensitivity to various stresses including oxidative stress caused by 0.5 mM H_2O_2 treatment, toxic amino acid analogues (0.1 mM L-azetidine-2-carboxylate (AZC), 0.5 μg/mL L-canavanine and 10 μg/mL *o*-fluoro-DL-phenylalanine), high temperature in rich medium (YPD) at 37˚C and 39˚C, and heat shock treatment at 50˚C for 6 hours (Hoshikawa *et al.*, 2003). In addition, the endocytosis of Gap1 is also impaired in the A401E mutant cells exposed to 15% ethanol (Shiga *et al.*, 2014). Thus, both of them are classified as loss-of-function *rsp5* mutants. As shown in Figure 7, while the

T255A mutant increased the NaAc tolerance, the A401E and *rsp5-1* mutants were more sensitive to NaAc stress. Therefore, the T255A mutation is regarded as gain-of-function.

To determine whether the T255A mutation is dominant or recessive, phenotypic analysis of diploid cells was performed. First, the T255A mutation was introduced into the BY4742 cells with the different mating type. As shown in Figure 8, BY4742 T255A mutant cells increased the NaAc tolerance. This result indicates that the T255A mutation in *RSP5* gene confers NaAc tolerance independent of mating type. Next, mating between BY4741 wild-type and BY4742 T255A, BY4741 T255A and BY4742 wild-type, BY4741 T255A and BY4742 T255A, and BY4741 wild-type and BY4742 wild-type (control) strains were performed. As shown in Figure 9, in the diploid cells, the heterozygous T255A mutant grew similar to the wild-type strain under NaAc stress conditions, whereas the homozygous T255A mutant exhibited higher NaAc tolerance, indicating that the T255A mutation is recessive. In addition, it was noticed that the diploid cells were more resistant to NaAc stress than did the haploid cells as their growth was apparent until 0.5 M NaAc, pH 6 where the growth of haploid cells was strongly inhibited. Based on these results, it is suggested that the recessive allele of *rsp5*^{T255A} enhances the NaAc tolerance by unknown mechanism(s) and it appears that the dosage of the *RSP5* gene is involved in the NaAc tolerance.

To understand the NaAc stress responses and stress specificity of the T255A mutant, its growth phenotype was tested under salt stress conditions at pH 6 including 0.33 M KAc, 1 M KCl, 0.1 M LiCl and 1 M NaCl and acetic acid stress conditions including 0.042 M and 0.050 M acetic acid at pH 4.5 and pH 4.4, respectively. As shown in Figure 10, the T255A mutant specifically increased tolerance to NaAc, but not to other salt stress conditions particularly NaCl or acetic acid stress conditions. Thus, the result suggests that NaAc stress responses are unique and different from that of NaCl or acetic acid.

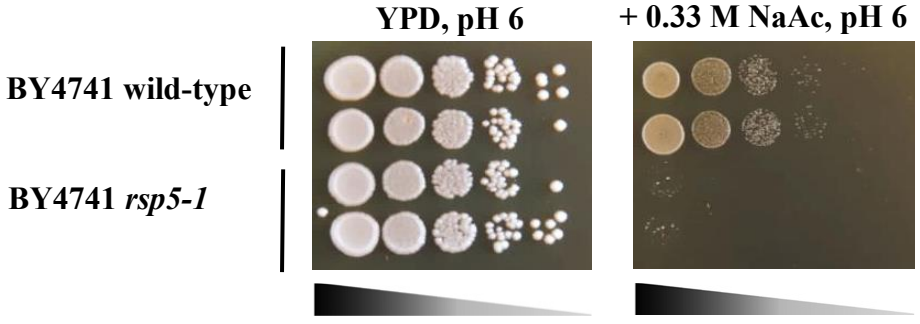

Figure 6. Rsp5 played a positive role in NaAc stress responses.
Spot test of *S. cerevisiae* strains BY4741 wild-type and *rsp5*^{L733S} (*rsp5-1*) on NaAc stress. Approximately, 1 OD_{600} cells were 10-fold serially diluted to 10^{-4} (from left to right), spotted on YPD at pH 6 (control) and YPD containing 0.33 M NaAc at pH 6 (NaAc stress), and incubated at 30˚C for approximately 2 days.

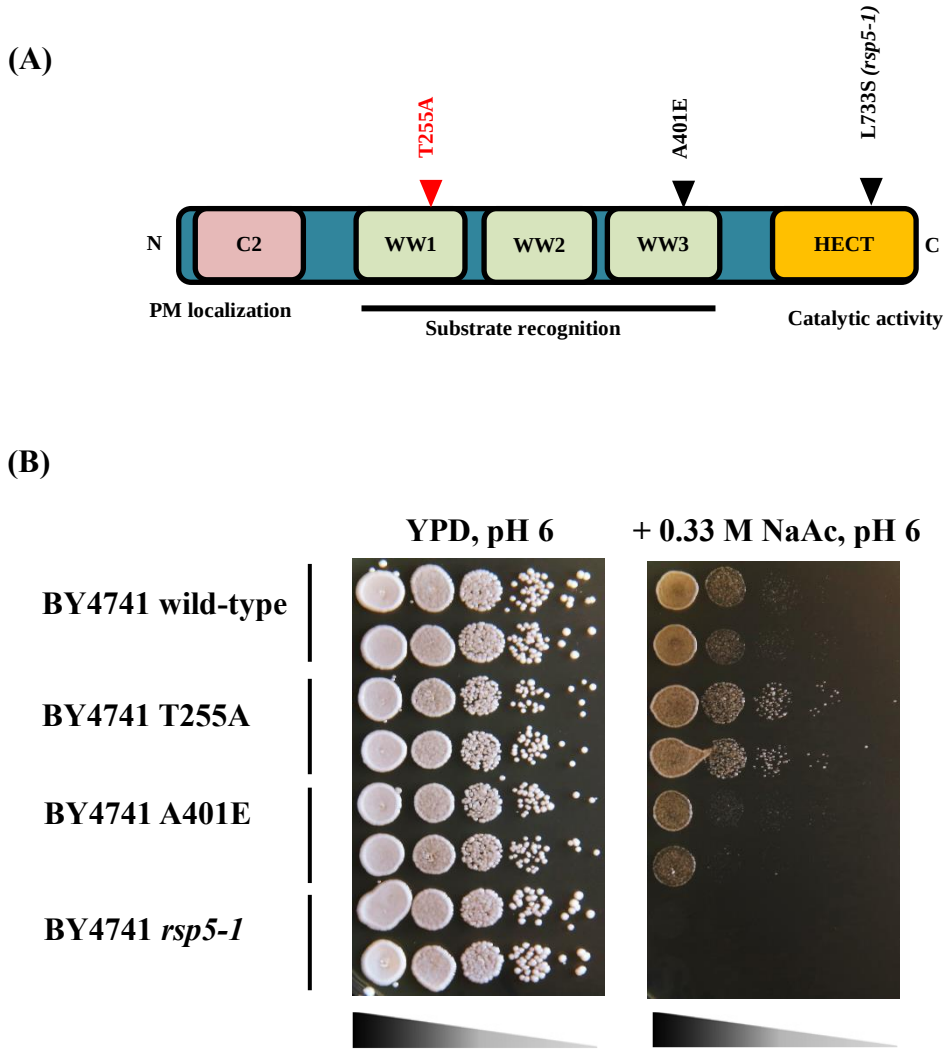

Figure 7. The T255A mutation in the *RSP5* gene was considered as a gain-of-function mutation.

(A) Schematic diagram represents corresponding mutations in *RSP5* gene including T255A in the WW1 domain *(*Wijayanti *et al*., 2015*)*, partially loss-of-function A401E in the WW3 domain *(*Hoshikawa *et al.*, 2003*)*, and L733S *(rsp5-1)* in the HECT domain *(*Wang *et al*., 1999*)*.

(B) Spot test of *S. cerevisiae* strains BY4741 wild-type, *rsp5*^{T255A}*-kanMX6* (T255A), *rsp5*^{A401E} (A401E), and *rsp5*^{L733S} *(rsp5-1)* on NaAc stress. Approximately, 1 OD_{600} cells were 10-fold serially diluted to 10^{-4} (from left to right), spotted on YPD at pH 6 (control) and YPD containing 0.33 M NaAc at pH 6 (NaAc stress), and incubated at 30˚C for approximately 2 days.

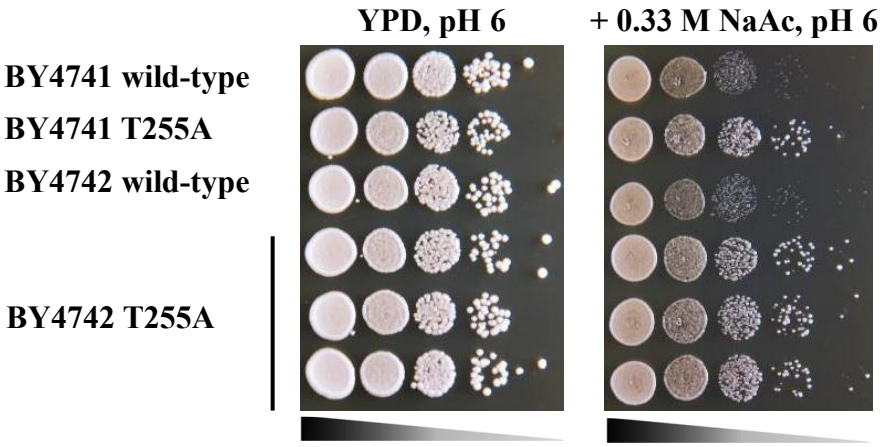

Figure 8. BY4742 T255A increased NaAc tolerance
Spot test of *S. cerevisiae* strains BY4741 wild-type, BY4741 *rsp5*^{T255A}*-kanMX6* (T255A), BY4742 wild-type, and BY4742 *rsp5*^{T255A}*-kanMX6* (T255A) cells on NaAc stress. Approximately, 1 OD_{600} cells were 10-fold serially diluted to 10^{-4} (from left to right), spotted on YPD at pH 6 (control) and YPD containing 0.33 M NaAc at pH 6 (NaAc stress), and incubated at 30˚C for approximately 2 days.

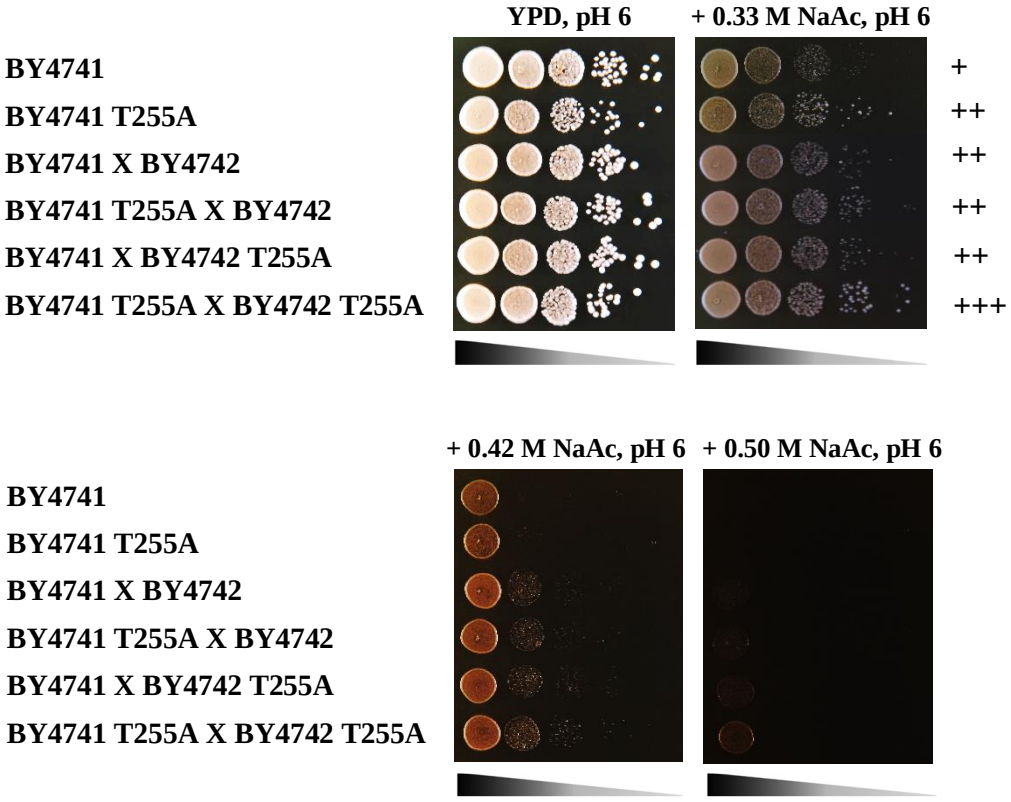

Figure 9. The T255A mutation in the *RSP5* gene was regarded as a recessive mutation.
Spot test of *S. cerevisiae* haploid strains BY4741 wild-type and *rsp5*^{T255A} *-kanMX6* (T255A) cells as well as diploid strains BY4741 wild-type X BY4742 wild-type, BY4741 T255A X BY4742 wild-type, BY4741 wild-type X BY4742 T255A, and BY4741 T255A X BY4742 T255A cells on NaAc stress. Approximately, 1 OD_{600} cells were 10-fold serially diluted to 10^{-4} (from left to right), spotted on YPD at pH 6 (control) and YPD containing 0.33 M, 0.42 M, and 0.50 M NaAc at pH 6 (NaAc stress), and incubated at 30˚C for approximately 2 days.

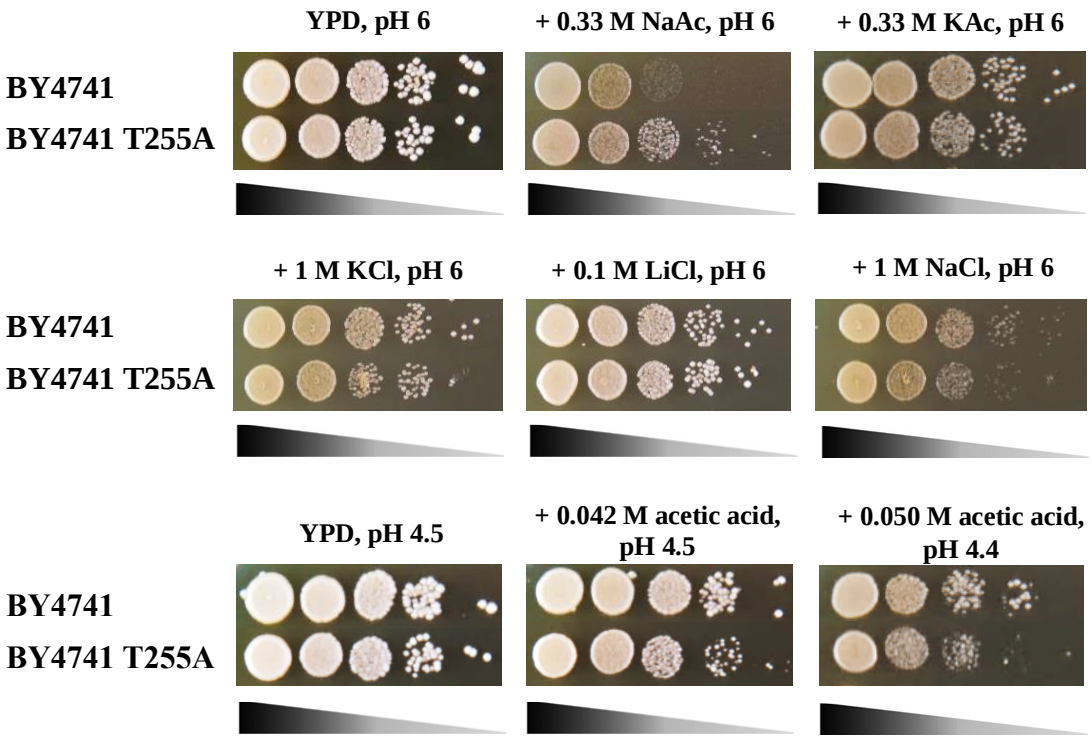

Figure 10. The T255A mutant was specifically tolerant to NaAc stress.
Spot test of *S. cerevisiae* strains BY4741 wild-type and *rsp5*^{T255A} or *rsp5*^{T255A}-*kanMX6* (T255A) cells on NaAc, KAc, KCl, LiCl, NaCl, and acetic acid stress conditions. Approximately, 1 OD_{600} cells were 10-fold serially diluted to 10^{-4} (from left to right), spotted on YPD at pH 6 or at pH 4.5 (control), YPD containing 0.33 M NaAc, 0.33 M KAc, 1 M KCl, 0.1 M LiCl, and 1 M NaCl at pH 6 and YPD containing 0.042 M and 0.050 M acetic acid at pH 4.5 and 4.4, respectively, and then incubated at 30˚C for approximately 2 days.

2. NaAc tolerance of the T255A mutant and the HOG signaling

To find a clue to molecular mechanisms by which the T255A mutation confers NaAc tolerance, genetic interaction with the high osmolarity glycerol (HOG) signaling pathway was examined. Activation of the Hog1 MAPK is the key to hyperosmotic stress responses, as well as to NaAc stress responses, through intracellular glycerol accumulation that counteracts with loss of cytoplasmic water (Mollapour and Piper, 2006). For each component of HOG signaling, please refer to Figure 4 in Chapter I: Introduction. Here, in my study, genetic analysis revealed that the NaAc tolerance increased by the T255A mutation was fully abrogated by disruption of the *HOG1* gene or the *PBS2* gene, which encodes a MAPKK upstream of Hog1 as shown in Figure 11. In addition, Δ*hog1* and Δ*pbs2* strains were sensitive to NaCl as previously reported, confirming their defects in salt stress responses (Figure 15B). Notably, it was confirmed that the T255A mutant did not increase NaCl tolerance (Figure 15B). Thus, these results indicate that the NaAc tolerance of the T255A mutant is dependent on the Hog1 MAPK signaling.

To determine whether the T255A mutation enhances activation of Hog1, western blot analysis was performed to detect the phosphorylated form of Hog1 under NaAc stress conditions. NaCl stress was used as a positive control for Hog1 phosphorylation. As shown in Figure 12, the T255A mutation in the *RSP5* gene did not affect the timing and the intensity of Hog1 phosphorylation triggered by NaAc stress. This result suggests that the T255A mutant form of Rsp5 functions at the downstream level of Hog1 to enhance NaAc tolerance.

To determine which branch of the HOG signaling pathway is responsible for the NaAc tolerance of the T255A mutant, genetic analysis on the upstream regulators of Hog1 was performed. As shown in Figures 13 and 14, either blocking of the Sln1 branch by single disruption of the *SSK1* gene encoding response regulator or double disruption of the *SSK2* and *SSK22* genes encoding two redundant MAPKKKs or blocking of the Sho1 branch by single disruption of the *STE50* gene encoding the adaptor protein or the *STE11* gene encoding MAPKKK did not abrogate the NaAc tolerance of the T255A mutant. These results suggest that both Sln1 and Sho1 branches perform redundant functions and compensate each other for the NaAc tolerant phenotype of the T255A mutant. To block both Sln1 and Sho1 branches, double disruption of the *SSK1* and *STE11* genes, and triple disruption of the *SSK2*, *SSK22*, and *STE11* genes were performed. As shown in Figure 15, the blocking of both branches did not abolish the NaAc tolerance of the T255A mutant, indicating that the NaAc tolerance of the T255A mutant is independent of the known MAPKKKs of the HOG signaling pathway. In addition, the result also indicates that the filamentous/invasive growth and the pheromone response pathways are not involved in the NaAc tolerance of the T255A mutant since Ste11 MAPKKK is shared by these two pathways. It should be noted that the *Δssk2Δssk22Δste11* mutant strains were less sensitive to 0.33 M NaCl, pH 6 than did the *Δpbs2* and *Δhog1* mutant strains (Figure 15B), supporting the alternative Pbs2-Hog1 activation mechanism (Wuytswinkel *et al*., 2000). Moreover, the T357A mutant, which constitutively down-regulated Gap1 and possessed AZC tolerance (Sasaki and Takagi, 2013), was highly sensitive to NaAc stress (Figures 13-15), confirming the important role of Rsp5 in NaAc stress responses.

There are only four known MAPKKKs including Ssk2, Ssk22, Ste11, and Bck1 in *S. cerevisiae* (Saito and Tatebayashi, 2004). Thus, it was asked whether the Bck1 MAPKKK of the cell wall integrity (CWI) pathway could be used as an alternative MAPKKK for Hog1 activation in the T255A mutant (O'Rourke and Herskowitz, 2004). To examine this possibility, disruption of the *BCK1* gene or the *SLT2* gene encoding MAPK of the CWI pathway (Levin, 2011) was performed and the NaAc tolerant phenotype was tested. As shown in Figure 16, neither the disruption of *BCK1* nor *SLT2* conferred NaAc sensitivity to the T255A mutant,

eliminating the possibility that Pbs2 MAPKK of the HOG signaling pathway is crossly activated by the Bck1 MAPKKK. This result also indicates that the CWI pathway is not involved in the NaAc tolerance of the T255A mutant cells. Taken together, these results underline the important relevance of the HOG signaling in the NaAc tolerance of the T255A mutant and suggest that the Pbs2-Hog1 activation is alternative and independent of the four known MAPKKKs.

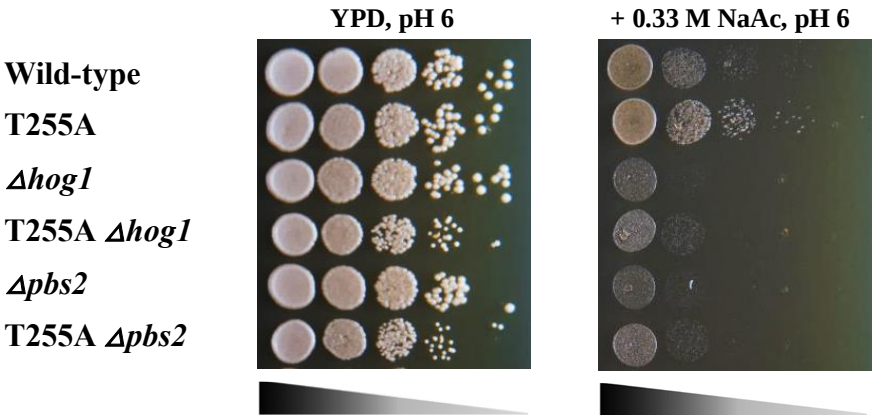

Figure 11. NaAc tolerance of the T255A mutant was dependent on the HOG signaling pathway.
Spot test of *S. cerevisiae* strains BY4741 wild-type, *rsp5*^{T255A}*-kanMX6* (T255A), *Δhog1*, T255A *Δhog1*, *Δpbs2*, and T255A *Δpbs2* cells on NaAc stress. Approximately, 1 OD_{600} cells were 10-fold serially diluted to 10^{-4} (from left to right), spotted on YPD at pH 6 (control) and YPD containing 0.33 M NaAc at pH 6 (NaAc stress) and incubated at 30˚C for approximately 2 days.

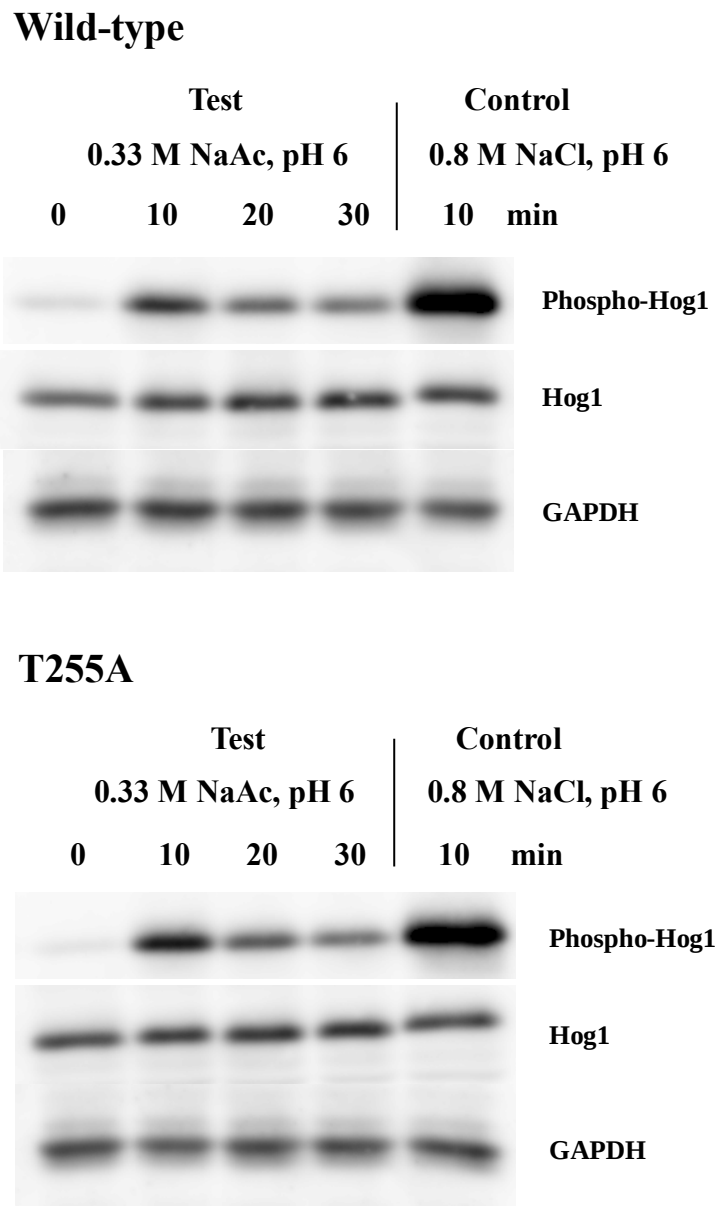

Figure 12. Hog1 phosphorylation was not enhanced in the T255A mutant.
Hog1 dual phosphorylation at Thr174 and Tyr176 of *S. cerevisiae* strains BY4741 wild-type and *rsp5*^{T255A}-*kanMX6* (T255A) cells under NaAc stress condition.

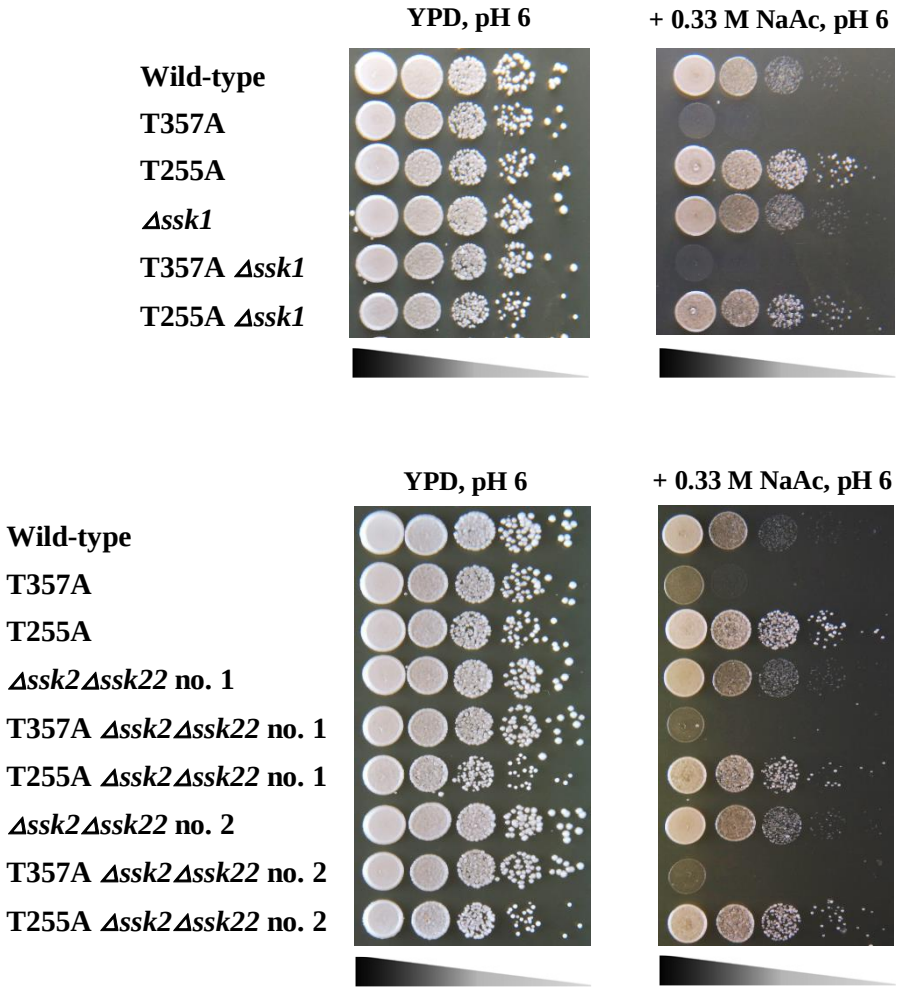

Figure 13. Blocking of Sln1 branch of the HOG signaling pathway did not abolish the NaAc tolerance of the T255A mutant.

Spot test of *S. cerevisiae* strains BY4741 wild-type, *rsp5*^{T357A} (T357A), *rsp5*^{T255A}-*kanMX6* (T255A), *Δssk1*, T357A *Δssk1*, T255A *Δssk1*, *Δssk2Δssk22*, T357A *Δssk2Δssk22*, and T255A *Δssk2Δssk22* cells on NaAc stress. Approximately, 1 OD_{600} cells were 10-fold serially diluted to 10^{-4} (from left to right), spotted on YPD at pH 6 (control) and YPD containing 0.33 M NaAc at pH 6 (NaAc stress), and incubated at 30˚C for approximately 2 days.

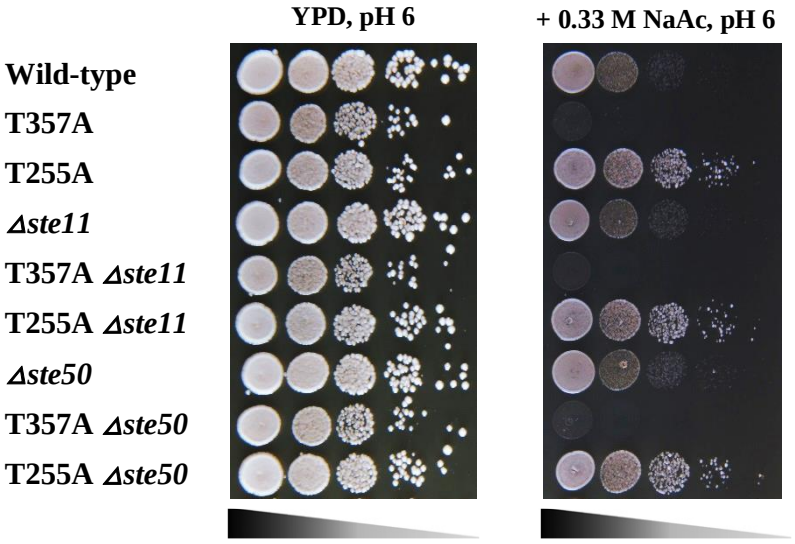

Figure 14. Blocking of Sho1 branch of the HOG signaling pathway did not abrogate the NaAc tolerance of the T255A mutant.

Spot test of *S. cerevisiae* strains BY4741 wild-type, *rsp5*^{T357A} (T357A), *rsp5*^{T255A}-*kanMX6* (T255A), *Δste11*, T357A *Δste11*, T255A *Δste11*, *Δste50*, T357A *Δste50*, and T255A *Δste50* cells on NaAc stress. Approximately, 1 OD_{600} cells were 10-fold serially diluted to 10^{-4} (from left to right), spotted on YPD at pH 6 (control) and YPD containing 0.33 M NaAc at pH 6 (NaAc stress), and incubated at 30˚C for approximately 2 days.

(A)

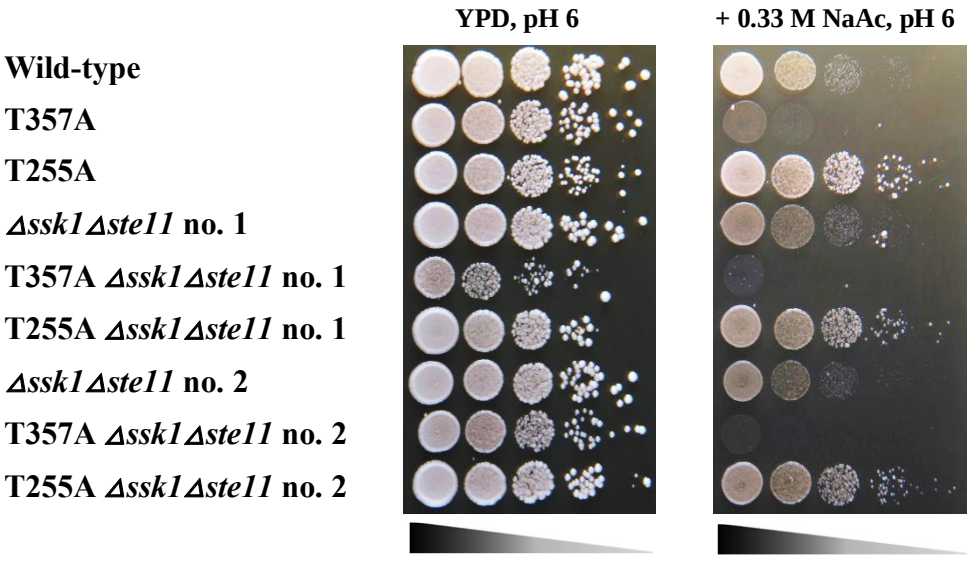

(B)

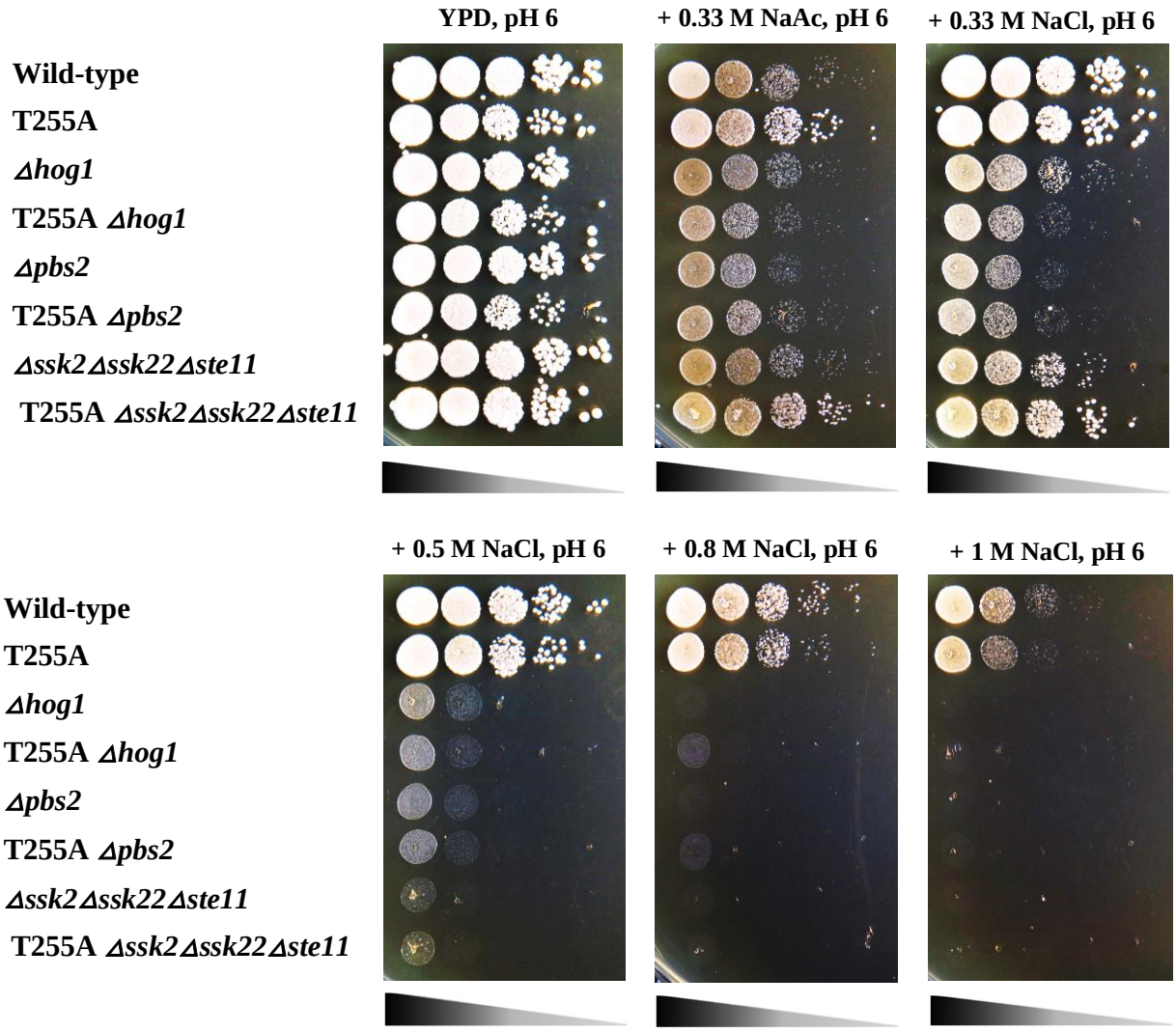

Figure 15. Blocking of both Sln1 and Sho1 branches of the HOG signaling pathway did not abrogate the NaAc tolerance of the T255A mutant.

(A) Spot test of *S. cerevisiae* strains BY4741 wild-type, *rsp5*^{T357A} (T357A), *rsp5*^{T255A}*-kanMX6* (T255A), *Δssk1Δste11*, T357A *Δssk1Δste11*, T255A *Δssk1Δste11* cells on NaAc stress.

(B) Spot test of *S. cerevisiae* strains BY4741 wild-type, *rsp5*^{T255A}*-kanMX6* (T255A), *Δhog1*, T255A *Δhog1*, *Δpbs2*, T255A *Δpbs2*, *Δssk2Δssk22Δste11*, and T255A *Δssk2Δssk22Δste11* cells on NaAc and NaCl stress conditions. Approximately, 1 OD_{600} cells were 10-fold serially diluted to 10^{-4} (from left to right), spotted on YPD at pH 6 (control) and YPD containing 0.33 M NaAc at pH 6 (NaAc stress) as well as YPD containing 0.33, 0.5, 0.8, and 1 M NaCl at pH 6 (NaCl stress), and incubated at 30˚C for approximately 2 days.

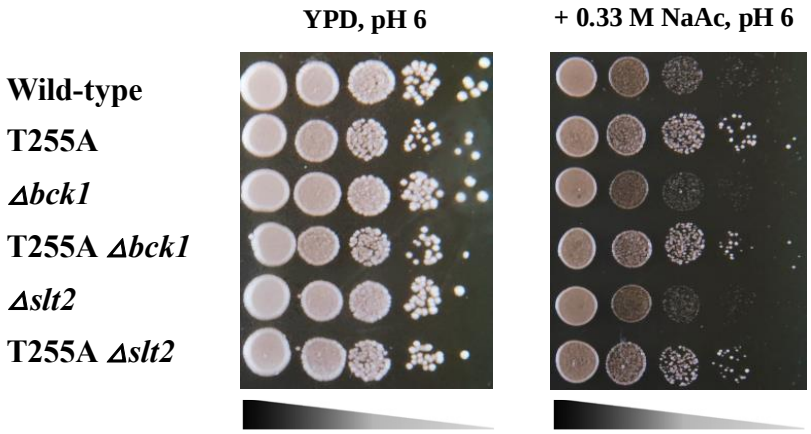

Figure 16. Blocking of the cell wall integrity (CWI) pathway did not affect the NaAc tolerance of the T255A mutant.
Spot test of *S. cerevisiae* strains BY4741 wild-type, *rsp5*^{T255A}*-kanMX6* (T255A), *Δbck1*, T255A *Δbck1*, *Δslt2*, and T255A *Δslt2* cells on NaAc stress. Approximately, 1 OD_{600} cells were 10-fold serially diluted to 10^{-4} (from left to right), spotted on YPD at pH 6 (control) and YPD containing 0.33 M NaAc at pH 6 (NaAc stress), and incubated at 30˚C for approximately 2 days.

3. NaAc tolerance of the T255A mutant and the P-type ATPases Ena1/2/5

Based on my results, it is hypothesized that the T255A mutant form of Rsp5 functions at the downstream level of Hog1. To identify the downstream target of Hog1 responsible for the NaAc tolerance of the T255A mutant, genetic analysis was performed. For the following transporters, please refer to Figures 2 and 3 in Chapter I: Introduction. Three putative ones were tested: (i) *FPS1*, encoding an aquaglyceroporin channel involved in the uptake of undissociated acetic acids; (ii) *NHA1*, encoding a Na^+/H^+ antiporter required for Na^+ extrusion under acidic conditions; (iii) *ENA1*, *ENA2*, and *ENA5* (*ENA1/2/5*), encoding the P-type ATPase Na^+ extrusion pumps crucial for long-term maintenance of monovalent cation homeostasis.

As shown in Figure 17, triple disruption of the *ENA1/2/5* genes strongly suppressed the NaAc tolerance of the T255A mutant, although disruption of the *FPS1* or *NHA1* gene did not affect the phenotype of wild-type and T255A mutant cells. This result indicates that the NaAc tolerance of the T255A mutant is dependent on the Ena1/2/5 Na^+ extrusion system.

To confirm that the Na^+ ions play an important inhibitory role in NaAc stress, the phenotypic test of the wild-type and T255A mutant cells lacking the *ENA1/2/5* genes under NaCl stress was performed. As shown in Figure 18, Δ*ena1/2/5* and T255A Δ*ena1/2/5* cells were highly sensitive to NaCl stress in a dose-dependent manner, suggesting that the tolerance to NaAc is mainly relied on the response to Na^+ stress. However, the level of growth inhibition of 0.33 M NaAc, pH 6 on the Δ*ena1/2/5* and T255A Δ*ena1/2/5* cells was comparable to that of 0.5 M NaCl, pH 6. Notably, 1 M NaCl, pH 6 also caused the similar growth inhibition to 0.33

M NaAc, pH 6 on the wild-type cells. Based on these results, it is suggested that the growth inhibition by Na^+ is aggravated by acetate under NaAc stress condition.

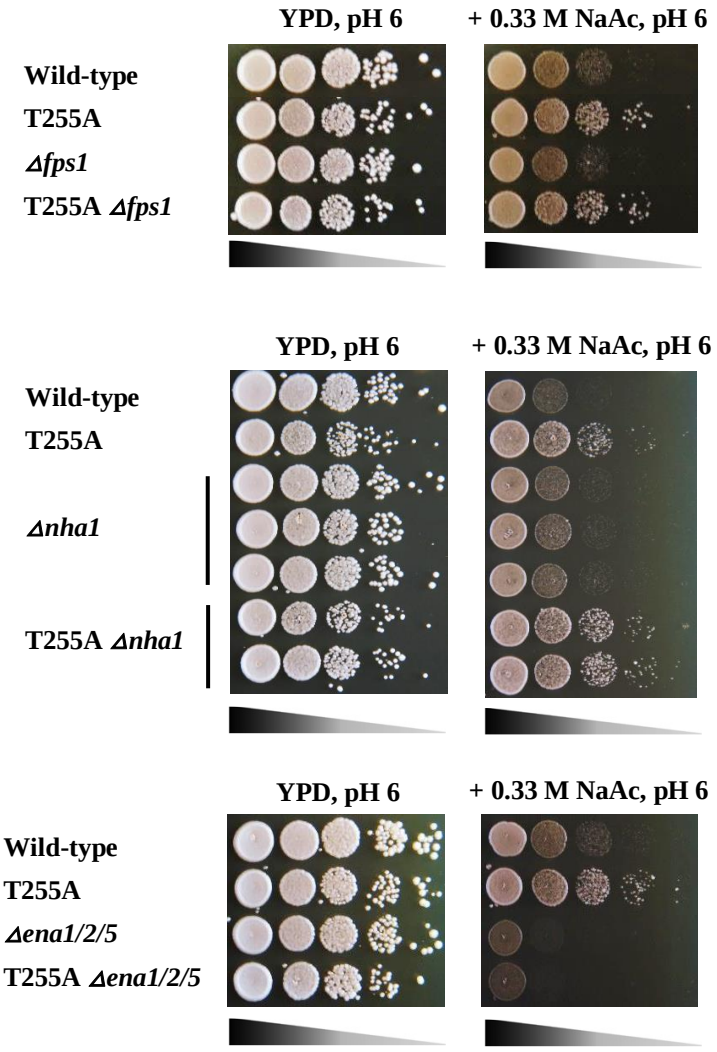

Figure 17. *ENA1/2/5* genes encoding P-type ATPase Na^+ pumps were required for the NaAc tolerance of the T255A mutant.

Spot test of *S. cerevisiae* strains BY4741 wild-type, *rsp5*^{T255A}-*kanMX6* (T255A), *Δfps1*, T255A *Δfps1*, *Δnha1*, T255A *Δnha1*, *Δena1/2/5*, and T255A *Δena1/2/5* cells on NaAc stress. Approximately, 1 OD_{600} cells were 10-fold serially diluted to 10^{-4} (from left to right), spotted on YPD at pH 6 (control) and YPD containing 0.33 M NaAc at pH 6 (NaAc stress), and incubated at 30˚C for approximately 2 days.

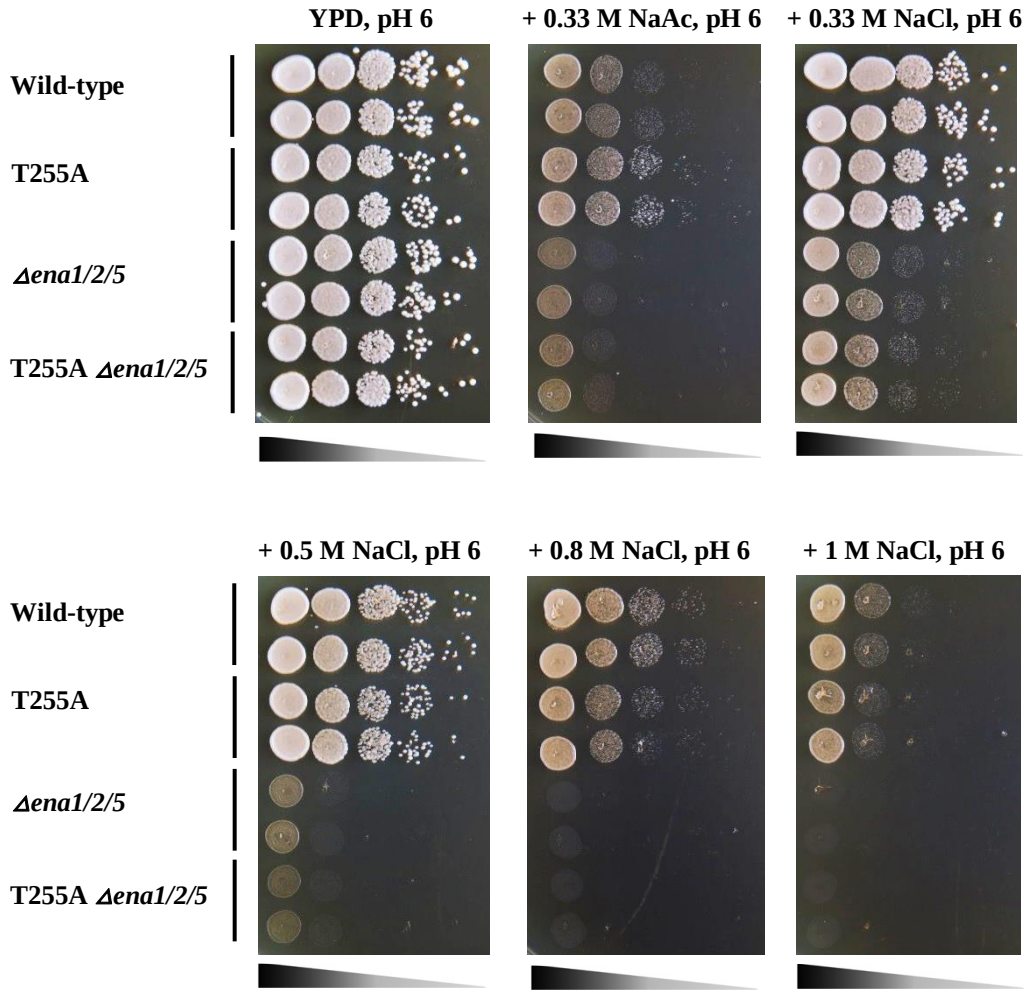

Figure 18. The NaAc tolerance of the T255A mutant was mainly involved in the Na^+ tolerance in the presence of acetate.

Spot test of *S. cerevisiae* strains BY4741 wild-type, *rsp5*^{T255A}*-kanMX6* (T255A), *Δena1/2/5*, and T255A *Δena1/2/5* cells on NaAc stress. Approximately, 1 OD_{600} cells were 10-fold serially diluted to 10^{-4} (from left to right), spotted on YPD at pH 6 (control) and YPD containing 0.33 M NaAc at pH 6 (NaAc stress) as well as YPD containing 0.33 M, 0.5 M, 0.8 M, and 1 M NaCl at pH 6 (NaCl stress), and incubated at 30˚C for approximately 2 days.

4. NaAc tolerance of the T255A mutant and acetate toxicity

Based on the calculation by Henderson-Hasselbalch equation, the fraction of acetate anions accounts for approximately 95% at pH 6. Thus, it is hypothesized that the amount of undissociated acetic acids enters the cells under 0.33 M NaAc at pH 6 is not significant to cause weak acid stress on yeast cells. Indeed, that the disruption of *FPS1* did not affect the phenotype of wild-type and T255A mutant cells under NaAc stress condition supports this hypothesis.

To examine whether extracellular acetate is uptaken and then cause the toxicity intracellularly, the possible acetate uptake system operated by Ady2 and Jen1, the two carboxylic acid transporters (Casal *et al.*, 2008), was examined. However, as shown in Figure

19, disruption of the *ADY2* or *JEN1* did not affect the growth phenotype of the wild-type and T255A mutant cells under NaAc stress condition. Therefore, it is unlikely that the extracellular acetate is uptaken into the cells via Ady2 or Jen1 under NaAc stress conditions tested in my study. Taken together, these results suggest that the acetate anions play an inhibitory role extracellularly under NaAc stress condition.

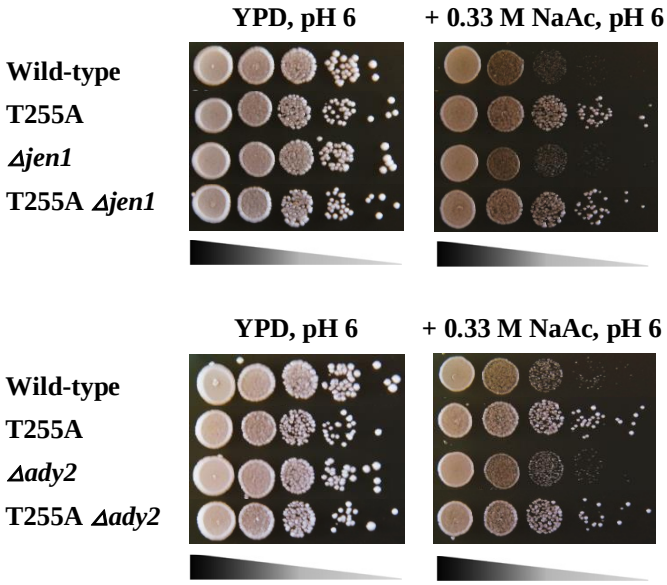

Figure 19. The carboxylic acid transporters Ady2 and Jen1 were not involved in the NaAc tolerance of the T255A mutant.
Spot test of *S. cerevisiae* strains BY4741 wild-type, *rsp5*^{T255A}*-kanMX6* (T255A), *Δady2*, T255A *Δady2*, *Δjen1*, and T255A *Δjen1* cells on NaAc stress. Approximately, 1 OD_{600} cells were 10-fold serially diluted to 10^{-4} (from left to right), spotted on YPD at pH 6 (control) and YPD containing 0.33 M NaAc at pH 6 (NaAc stress), and incubated at 30˚C for 2 days.

5. NaAc tolerance of the T255A mutant and intracellular Na^+ accumulation

To examine whether the NaAc tolerance of the T255A mutant was due to the lower accumulation of intracellular Na^+ ions, the wild-type and T255A mutant cells were grown in YPD containing 0.33 M NaAc, pH 6 and the cells were collected at different time points. As shown in Figure 20, the T255A mutant cells grew better than did the wild-type cells under NaAc stress condition, although it grew slower than did the wild-type cells under non-stress condition (Figure 20A). The intracellular Na^+ content was analyzed by using the inductively coupled plasma mass spectrometry (ICP-MS). As expected, the intracellular Na^+ content of the T255A mutant cells was significantly lower than that of the wild-type cells after 4-hour incubation (Figure 20B). This result indicates that the NaAc tolerance of the T255A mutant is due to the

lower steady-state level of intracellular Na^+ content accumulated during NaAc stress. Thus, it is suggested that the T255A mutant positively regulates the Na^+ extrusion that may be mediated by the P-type ATPase Na^+ pumps Ena1/2/5.

To examine a possible inhibitory role of the extracellular acetate under NaAc stress conditions, I focused on intracellular Na^+ accumulation. The intracellular Na^+ contents of the wild-type and T255A mutant cells under NaAc and NaCl stress conditions were analyzed by using ICP-MS. The log-phase wild-type and T255A mutant cells were treated by NaAc or NaCl stress condition in YPD containing 0.33 M NaAc, pH 6 or 0.5 M NaCl, pH 6, respectively, for 3 hours. As shown in Figure 21, the intracellular Na^+ contents of the wild-type and T255A mutant cells treated with 0.33 M NaAc, pH 6 were higher than those treated with 0.5 M NaCl, pH 6, even though the concentration of NaCl was higher than that of NaAc. Notably, it was confirmed that the intracellular Na^+ content of the T255A mutant cells under NaAc stress condition was lower than that of the wild-type cells. As expected, the intracellular Na^+ content of the T255A mutant cells under NaCl stress condition was likely to be higher than that of the wild-type cells. This result corresponded to the growth phenotype of the T255A mutant which included the increased NaAc tolerance and the slightly decreased NaCl tolerance. These results indicate that the extracellular acetate causes an increased intracellular Na^+ accumulation. This may account for the inhibitory role of extracellular acetate under NaAc stress condition.

(A) YPD, pH6

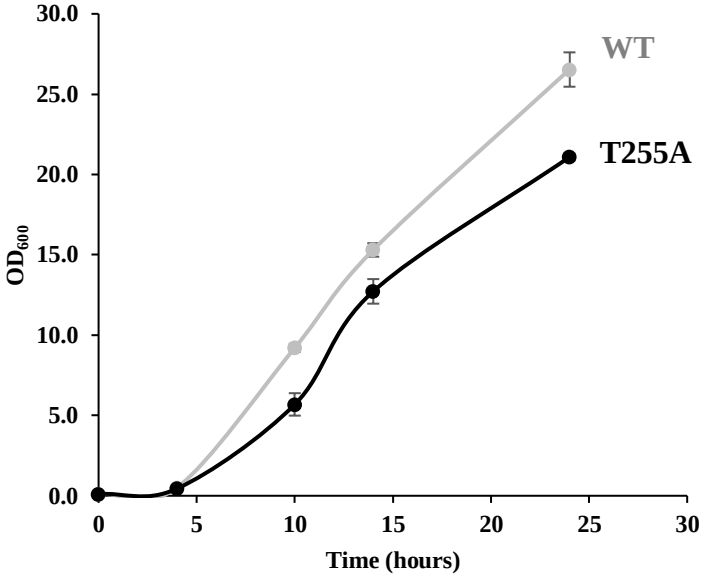

(B) YPD + 0.33 M NaAc, pH 6

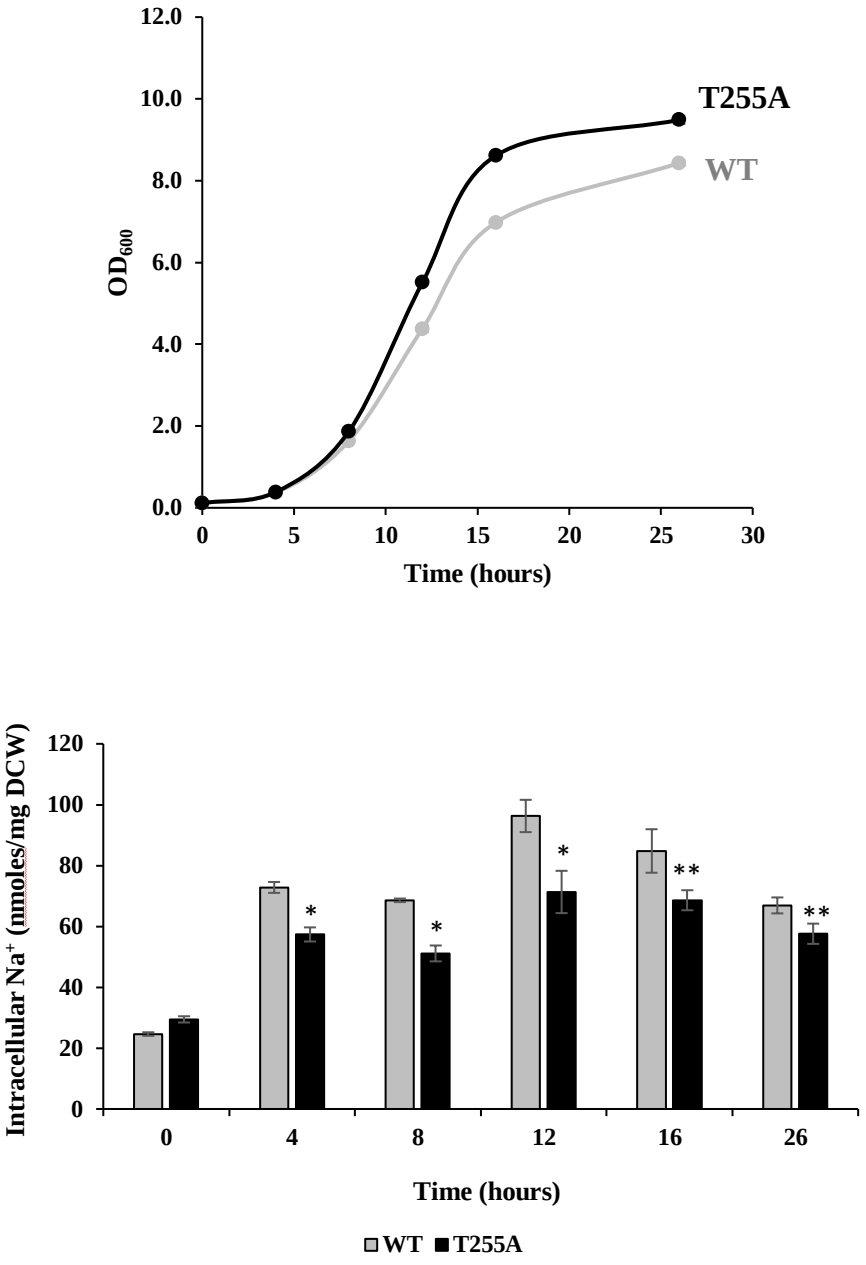

Figure 20. The T255A mutant possessed lower steady-state level of intracellular Na^+ content under NaAc stress than did the wild-type cells.

(A) Growth curve of the wild-type and T255A mutant cells under non-stress condition. *S. cerevisiae* strains BY4741 wild-type (WT) and *rsp5*^{T255A}-*kanMX6* (T255A) cells were pre-cultured in YPD at pH 6 overnight and then inoculated in YPD at pH 6 with the initial OD_{600} of 0.1. The cultures were incubated at 30˚C with shaking at 114 rpm. OD_{600} was measured at 0, 4, 10, 14, and 24 hours after incubation.

(B) Growth curve and intracellular Na^+ content of the wild-type and T255A mutant cells under NaAc stress condition. *S. cerevisiae* strains BY4741 wild-type (WT) and *rsp5*^{T255A}-*kanMX6* (T255A) cells were pre-cultured in YPD at pH 6 overnight and then inoculated in YPD containing 0.33 M NaAc at pH 6 with the initial OD_{600} of 0.1. The cultures were incubated at 30˚C with shaking at 114 rpm. OD_{600} was measured and approximately, 5 OD_{600} cells were collected at 0, 4, 8, 12, 16, and 26 hours after incubation for the analysis of intracellular Na^+ content using ICP-MS. * and ** indicate the significant difference at $p<0.01$ and $p<0.05$, respectively.

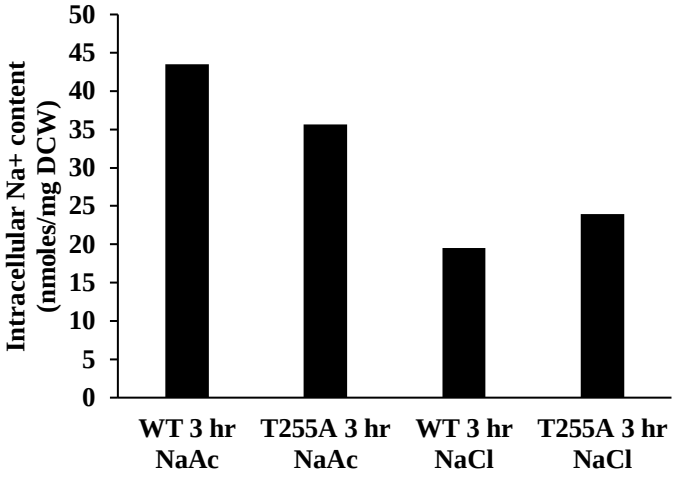

Figure 21. Intracellular Na^+ accumulation was increased in the presence of acetate under NaAc stress condition.

Intracellular Na^+ content under NaAc and NaCl stress conditions. *S. cerevisiae* strains BY4741 wild-type (WT) and *rsp5*^{T255A}-*kanMX6* (T255A) cells were grown until log phase and treated with NaAc or NaCl in YPD containing 0.33 M NaAc at pH 6 and YPD containing 0.5 M NaCl at pH 6, respectively, for 3 hours at 30˚C with shaking at 114 rpm. Approximately, 5 OD_{600} cells were collected for the analysis of intracellular Na^+ content using ICP-MS.

6. NaAc tolerance of the T255A mutant and the Rsp5 adaptor proteins

Although the target of Rsp5 is still unknown, in many cellular processes, adaptor proteins mediate the function of Rsp5. To identify the adaptor proteins required for the NaAc tolerance of the T255A mutant, genetic screening was performed. For the information about each adaptor protein, please refer to Tables 1 and 2 in Chapter I: Introduction. Among the known adaptor proteins for Rsp5: Bul1, Bul2, Bul3, and Art1 to Art10, the homologous proteins Bul1 and Bul2 (Bul1/2), Bul3, Art1, and Art9 (Rim8) were shown to cause NaAc sensitivity on the wild-type cells when deleted (Figure 22). It is noteworthy that Art2, Art4, Art5, Art6, and Art7 were found to confer NaAc tolerance on the wild-type cells when disrupted. This result may suggest the role of ART family protein in NaAc stress responses. Bul3 has been identified as a third member of the Bul family proteins (Novoselova *et al*., 2012). However, the disruption of *BUL3* did not cause any defects in endocytosis of Gap1, Smf1, and Can1 which are the known targets of Bul1/2-medaited endocytosis even though Bul3 has been shown to interact with Rsp5 (Novoselova *et al*., 2012). In addition, the disruption of *BUL3* also enhanced the Gap1 endocytosis in the Δ*bul1/2* cells (Shiga *et al.*, 2014). Thus, the role of Bul3 as an Rsp5 adaptor is still unclear and will not be focused. From the first screen (Figure 22), Bul1/2, Art1, and Rim8 were selected as candidate adaptor proteins involved in the NaAc tolerance.

To confirm this, single and double disruption of the *BUL1* and *BUL2* genes as well as single and double disruption of the *ART1* and *RIM8* genes were performed in the wild-type and T255A mutant cells and their NaAc tolerant phenotype was tested. As shown in Figure 23,

double disruption of the *BUL1* and *BUL2* genes abrogated the NaAc tolerance of the T255A mutant. However, single disruption of either *BUL1* or *BUL2* did not affect the NaAc tolerance of the T255A mutant, indicating the redundant functions of Bul1 and Bul2 for the NaAc tolerance of the T255A mutant. It should be noted that single disruption of the *BUL1* or *BUL2* gene, but not the double disruption, slightly increased the NaAc tolerance of the wild-type cells although their single and double disruption rendered the NaAc sensitivity on the wild-type cells in the first screening (Figure 22). As a control, the high temperature sensitivity at 39˚C was tested. It is known that cells lacking *BUL1* show sensitivity to high temperature (Yashiroda *et al*., 1996). However, Bul2 does not have the phenotype at high temperature. As shown in Figure 23, Δ*bul1* and Δ*bul1*Δ*bul2* mutant strains showed sensitivity to high temperature at 39˚C, whereas Δ*bul2* strains were not affected. Thus, these results confirmed that the disruption of *BUL1* or *BUL2* gene in this study was correct. Furthermore, the independent colonies of these Δ*bul1*, Δ*bul2*, and Δ*bul1*Δ*bul2* mutant strains constructed in this study were tested on NaAc stress and basically the same results (Figure 23) were obtained from four independent experiments, confirming their reproducibility. The Δ*bul1*, Δ*bul2*, and Δ*bul1*Δ*bul2* mutant strains used in the first screening (Figure 22) was constructed by Miss Yuko Shimizu and had been used repeatedly for long time. Thus, it is plausible that some unknown mutations which caused stress sensitivity might be accumulated. Notably, the high-temperature sensitivity at 39˚C of the T255A mutant (Wijayanti *et al*., 2015) was reproducible and the T255A mutation seemed to have synergistic effect to the disruption of *BUL1* (Figure 23). In addition, single disruption of the *ART1* or *RIM8* gene negatively affect the NaAc tolerance of the wild-type and T255A mutant cells although the NaAc-sensitive phenotype of the Δ*art1* strain in the second screening (Figure 23) was milder than that in the first screening (Figure 22). It should be noted that the Δ*art1* strain used in the first screening was derived from the knockout collection created by kanMX4 disruption cassette whereas the Δ*art1* strain used in the second screening was constructed in this study by using hphNT1 disruption cassette. Thus, this might account for a slight phenotypic difference. Most notably, disruption of the *RIM8* gene severely abolished the NaAc tolerance of both wild-type and T255A mutant as shown by the NaAc tolerant phenotype of *Δrim8*, T255A *Δrim8*, *Δart1Δrim8*, and T255A *Δart1Δrim8* cells (Figure 23). Thus, these results indicate that Rim8 is predominantly involved in the NaAc tolerance of the T255A mutant, and Bul1/2 and Art1 also have a redundant role.

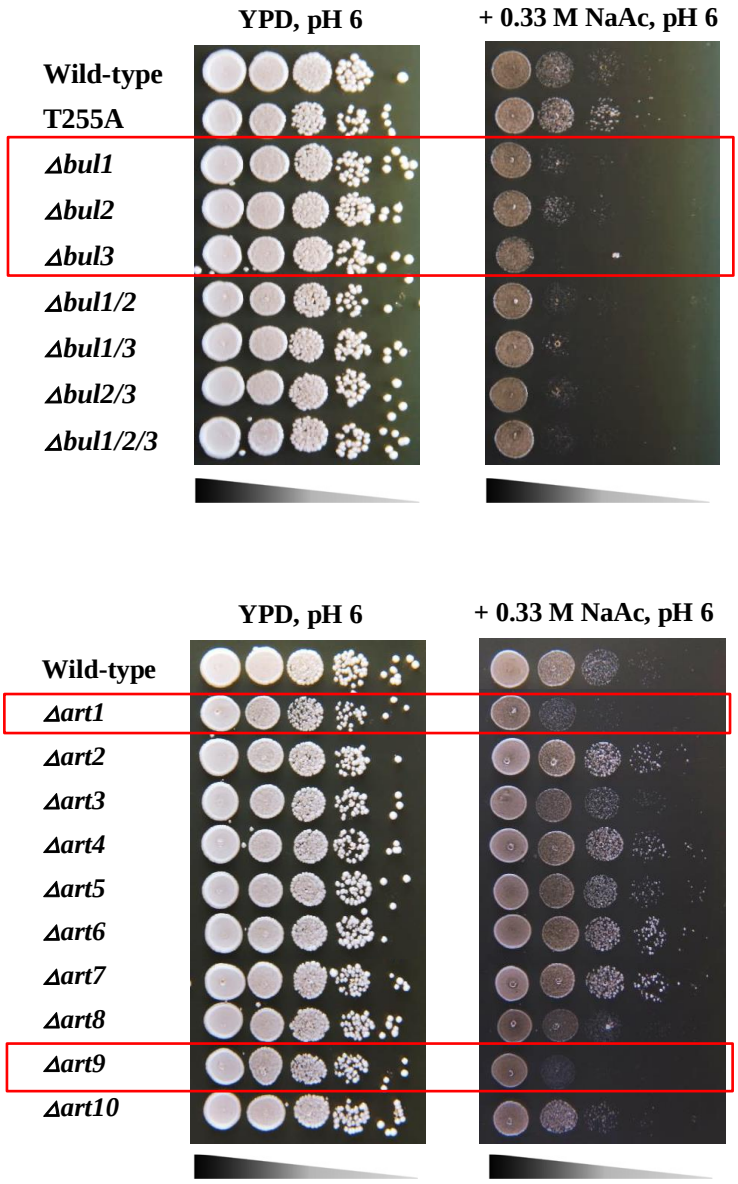

Figure 22. Genetic screening for Rsp5 adaptor proteins required for NaAc tolerance.
Spot test of *S. cerevisiae* BY4741 wild-type, *rsp5*^{T255A}*-kanMX6* (T255A), *Δbul1*, *Δbul2*, *Δbul3*, *Δbul1/2*, *Δbul1/3*, *Δbul2/3*, *Δbul1/2/3* (constructed by Yuko Shimizu) and *Δart1* to *Δart10* (derived from knockout collection) cells on NaAc stress. Approximately, 1 OD_{600} cells were 10-fold serially diluted to 10^{-4} (from left to right), spotted on YPD at pH 6 (control) and YPD containing 0.33 M NaAc at pH 6 (NaAc stress), and incubated at 30˚C for approximately 2 days.

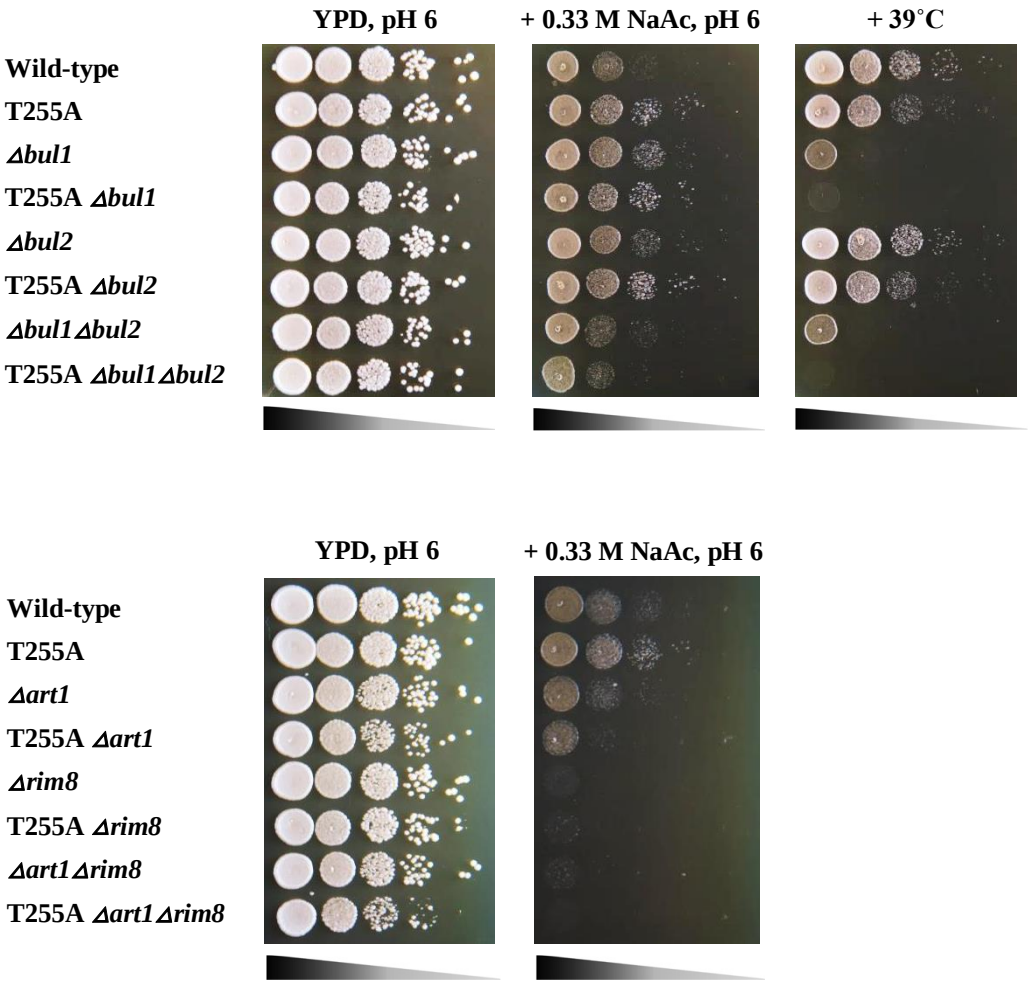

Figure 23. Rsp5 adaptor proteins Bul1, Bul2, Art1 and Rim8 were involved in the NaAc tolerance of the T255A mutant.

Spot test of *S. cerevisiae* strains BY4741 wild-type, *rsp5*^{T255A} (T255A), *Δbul1*, T255A *Δbul1*, *Δbul2*, T255A *Δbul2*, *Δbul1Δbul2*, T255A *Δbul1Δbul2*, *Δart1*, T255A *Δart1*, *Δrim8*, T255A *Δrim8*, *Δart1Δrim8* and T255A *Δart1Δrim8* cells on NaAc and high temperature stress conditions. Approximately, 1 OD_{600} cells were 10-fold serially diluted to 10^{-4} (from left to right), spotted on YPD at pH 6 (control) and YPD containing 0.33 M NaAc at pH 6 (NaAc stress), and incubated at 30˚C or 39˚C (high temperature stress) for approximately 2 days.

7. NaAc tolerance of the T255A mutant and the Hog1-Rim8-Ena1/2/5 system

To examine the role of Hog1, Rim8, and Ena1/2/5 in the homeostasis of intracellular Na^+ ions in the T255A mutant, the analysis of intracellular Na^+ content was performed in the wild-type and T255A mutant cells lacking either *HOG1*, *RIM8*, or *ENA1/2/5* treated with NaAc stress in YPD containing 0.33 M NaAc, pH 6 for 4 hours. As shown in Figure 24, the T255A mutant accumulated significantly lower intracellular Na^+ content than did the wild-type cells. When the *ENA1/2/5* genes were deleted, the intracellular Na^+ content was increased in both wild-type and T255A mutant cells and the difference was cancelled, indicating that the P-type ATPases Ena1/2/5 are mainly required for maintaining the lower intracellular Na^+ content in

the T255A mutant. In addition, disruption of the *HOG1* or the *RIM8* gene also increased the intracellular Na^+ content in the T255A mutant under NaAc stress condition, but to lesser extent than did the disruption of *ENA1/2/5*. Based on these data, it is suggested that the T255A mutation alleviates NaAc stress via positively regulating Na^+ extrusion possibly through the P-type ATPases Ena1/2/5, which requires cooperative functions of Hog1 and Rim8. Interestingly, the *Δrim8* mutant still showed higher intracellular Na^+ level than did the T255A *Δrim8* mutant cells under NaAc stress. However, this trend was abrogated in the *Δena1/2/5* and T255A *Δena1/2/5* mutant cells, suggesting that the T255A mutant form of Rsp5 might be able to exhibit its function via Rim8-independent Ena1/2/5 system possibly by using other adaptor proteins including Bul1/2 and Art1.

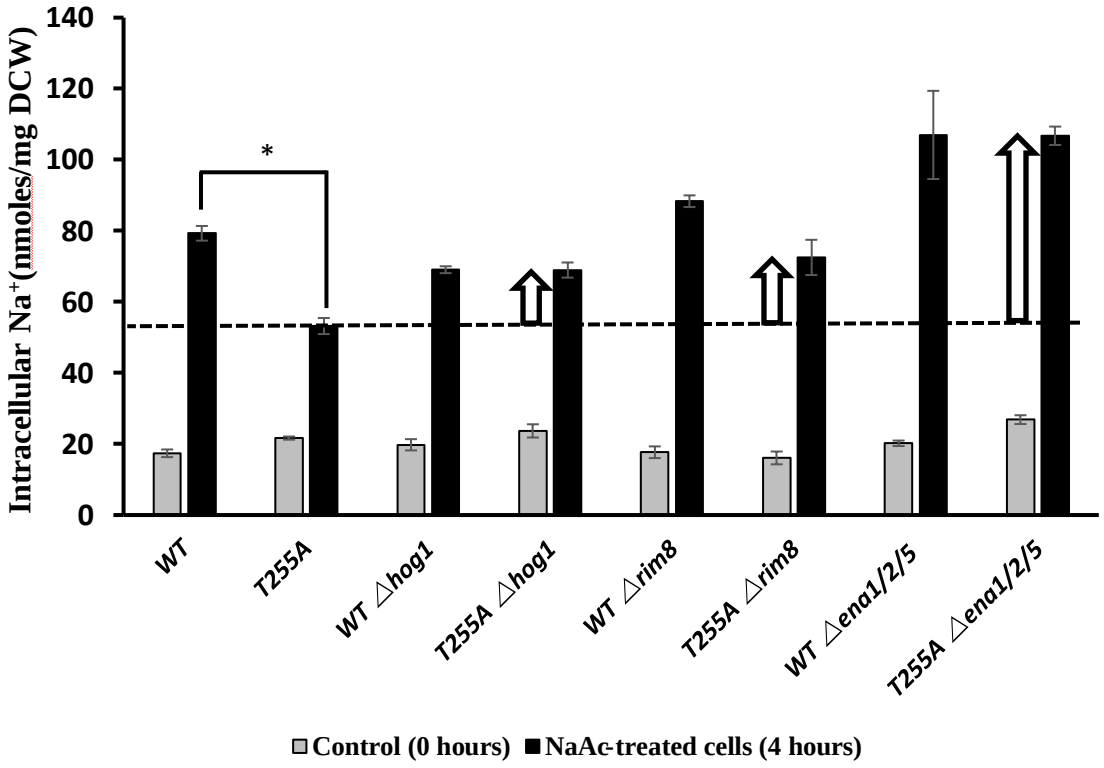

Figure 24. The T255A mutant positively regulated Na^+ extrusion through Hog1-Rim8-Ena1/2/5 system.

Steady-state intracellular Na^+ content in the wild-type, T255A, *Δhog1, Δrim8,* and *Δena1/2/5* strains under NaAc stress. *S. cerevisiae* strains BY4741 wild-type (WT), *rsp5*^{T255A}*-kanMX6* (T255A), *Δhog1*, T255A *Δhog1, Δrim8,* T255A *Δrim8, Δena1/2/5,* and T255A *Δena1/2/5* cells were pre-cultured in YPD, pH 6 overnight and then inoculated in YPD containing 0.33 M NaAc, pH 6 with the initial OD_{600} of 0.1. The cultures were incubated at 30˚C with shaking at 114 rpm. Approximately, 5 OD_{600} cells were collected at 4 hours after incubation for the analysis of intracellular Na^+ content using ICP-MS. * and arrows indicate the significant difference at $p<0.01$.

8. Rim8 ubiquitination and Rsp5-Rim8 interaction

Rim8 has been previously reported to play a role in proper Ena1 accumulation at the plasma membrane under NaCl stress condition (Marques *et al*., 2015). Since Rsp5 is known to physically interact and mono-ubiquitinate Rim8 (Herrador *et al*., 2010; 2013), it is intriguing to hypothesize that if the T255A mutation in the WW1 domain of Rsp5 positively affects either its interaction or ubiquitination toward Rim8, which may lead to enhanced Ena1/2/5 trafficking to the plasma membrane. To test this hypothesis, Rim8 ubiquitination in the wild-type and T255A mutant cells was examined. As shown in Figure 25A, under non-stress condition, mono-ubiquitinated form of Rim8 was detected in the *Δrim8* and T255A *Δrim8* cells harboring plasmid pRS316-RIM8-3HA (pOK476) which expresses *RIM8-3HA*. The mutations at the PXY motif (P506A, Y508A) and ubiquitinated lysine residue (K521R) impaired the Rim8 ubiquitination as previously reported (Obara and Kihara, 2014). However, the level of Rim8 mono-ubiquitination by Rsp5 was unaffected by the T255A mutation. It should be noted that in the other experiment, the expression of P506A Y508A and K521R mutant forms of Rim8 in the T255A mutant were not lower than that in the wild-type cells (Figure 25B).

To test whether Rim8 ubiquitination is enhanced by the T255A mutation under NaAc stress conditions, the *Δrim8* and T255A *Δrim8* cells harboring pRS416 (empty vector) or pRS316-RIM8-3HA (pOK476) were treated with NaAc in YPD containing 0.33 M NaAc, pH 6 for 0, 30, 60, and 90 min. As shown in Figure 26, the level of mono-ubiquitinated form of Rim8 was unchanged in the T255A *Δrim8* cells expressing *RIM8-3HA* under NaAc stress conditions when compared with that of the *Δrim8* cells expressing *RIM8-3HA*. This result indicates that the T255A mutation in *RSP5* gene does not affect the ubiquitination of Rim8 under non-stress and NaAc stress conditions.

To test whether Rsp5-Rim8 interaction is increased by the T255A mutation, *in vivo* interaction between Rsp5 and N-terminal GFP-tagged Rim8 under non-stress condition was examined by co-immunoprecipitation. As shown in Figure 27, the *in vivo* physical interaction between GFP-Rim8 and Rsp5 was detected. However, the T255A mutation did not enhance the interaction between GFP-Rim8 and Rsp5. Notably, without the overexpression of GFP-Rim8, the detected Rsp5 protein level was much lower than that with the overexpression of GFP-Rim8. Since Rim8 is a cytosolic protein, it is possible that the overexpression of Rim8 recruits Rsp5 to the cytosol where it is extracted in the soluble fraction. It has been previously reported that the overexpression of Ear1, an endosomal Rsp5 adaptor protein, recruits Rsp5 to the endosome (Leon *et al*., 2008).

To test whether the interaction or ubiquitination is required for the NaAc tolerance of the T255A mutant, phenotypic test was performed. As shown in Figure 28, *⊿rim8* and T255A *⊿rim8* cells harboring pRS316-RIM8-3HA (pOK476) exhibited the NaAc tolerance similar to the wild-type and T255A mutant cells harboring pRS416 (empty vector), confirming the expression of Rim8-3HA from the plasmid in YPD containing 0.33 M NaAc, pH 6 since the *⊿rim8* and T255A *⊿rim8* cells were more sensitive to NaAc stress. However, neither the P506A Y508A or the K521R mutant form of Rim8 abolished the NaAc tolerance of the T255A mutant. The P506A mutation has been shown to completely abrogate the *in vitro* interaction between GST-Rsp5 WW domains and Rim8 (Herrador *et al.*, 2010). This result indicates that the Rsp5-Rim8 interaction and the Rim8 ubiquitination are not necessary for the NaAc tolerance of the T255A mutant. Thus, it is suggested that Rim8 is not the target of Rsp5 for the NaAc tolerance of the T255A mutant and that the T255A mutant form of Rsp5 functions at the downstream level of Rim8.

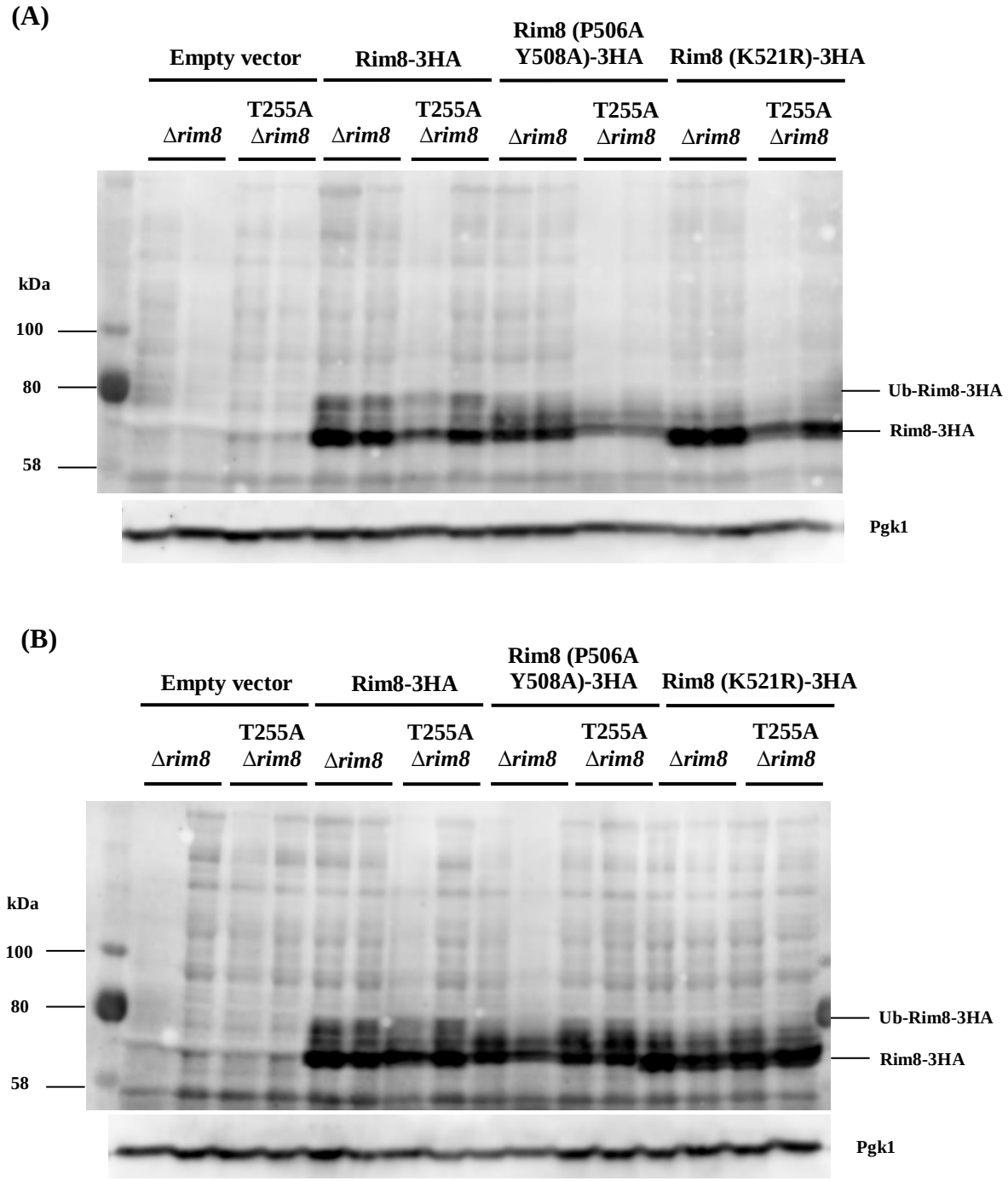

Figure 25. Rim8 ubiquitination was not enhanced by the T255A mutant under non-stress condition

S. cerevisiae strains BY4741 *Δrim8* and T255A *Δrim8* harboring plasmid pRS416 (empty vector), pRS316-RIM8-3HA (pOK476), pRS316-RIM8 (P506A Y508A)-3HA (pOK477), or pRS316-RIM8 (K521R)-3HA (pOK573) cells were pre-cultured in 3 mL SC-Ura, pH 6 overnight and then inoculated in 10 mL SC-Ura, pH 6 with the initial OD_{600} of 0.2. The cultures were incubated at 30˚C with shaking at 133 rpm. Approximately, 3 OD_{600} cells were collected at 4.5 hours (OD_{600} ~1.0) after incubation for the detection of Rim8 and its mono-ubiquitinated form. The results from 2 independent experiments are shown as (A) and (B).

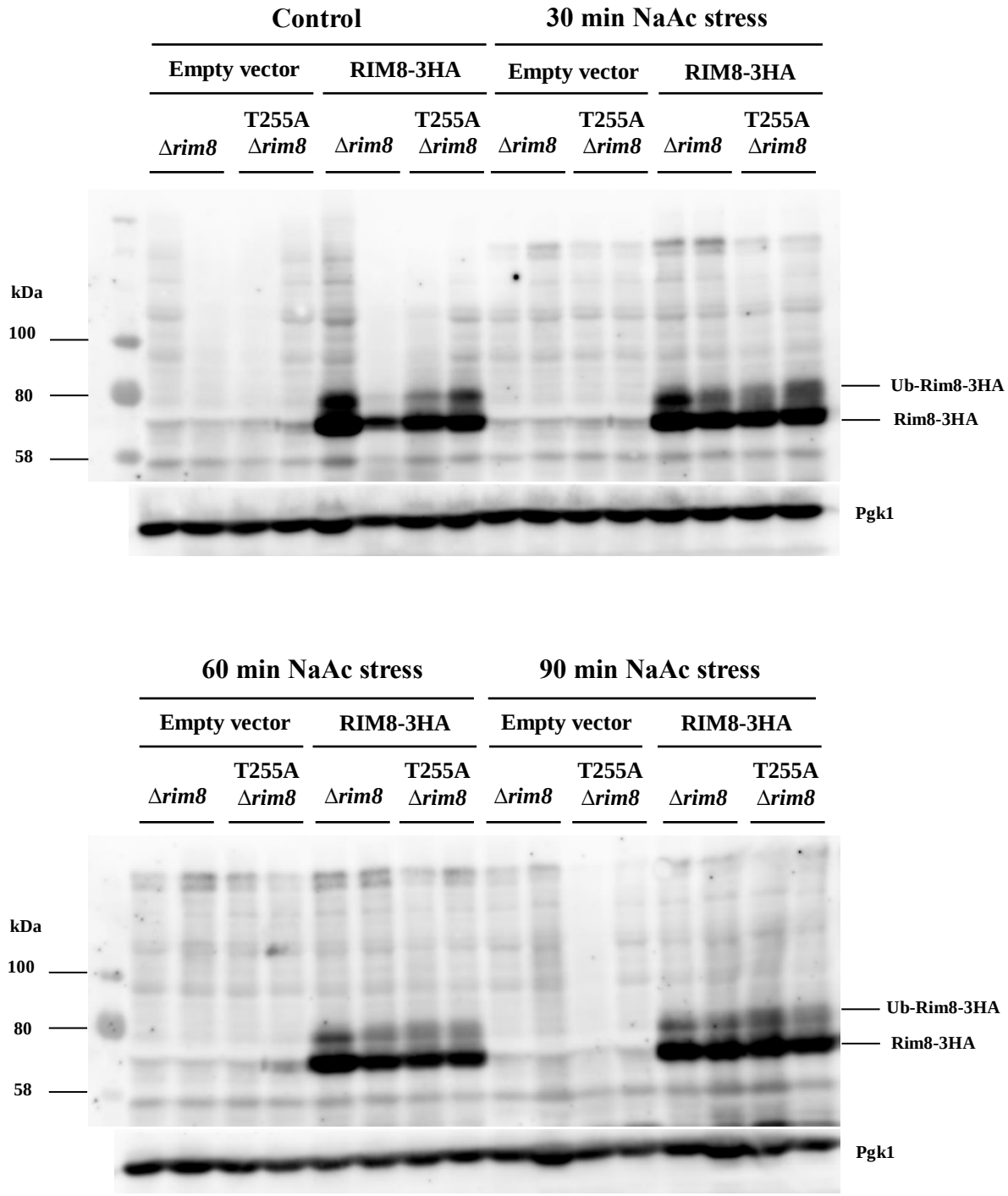

Figure 26. Rim8 ubiquitination was not enhanced by the T255A mutant under NaAc stress conditions

S. cerevisiae strains BY4741 *Δrim8* and T255A *Δrim8* harboring plasmid pRS416 (empty vector) or pRS316-RIM8-3HA (pOK476) cells were grown in 30 mL SC-Ura, pH 6 with the initial OD_{600} of 0.2. Approximately, 30 OD_{600} cells were collected at 4.5 hours (OD_{600} ~1.0) after incubation and inoculated in 30 mL YPD containing 0.33 M NaAc, pH 6. Approximately, 3 OD_{600} cells were collected at 0, 30, 60, and 90 min after incubation for the detection of Rim8 and its mono-ubiquitinated form.

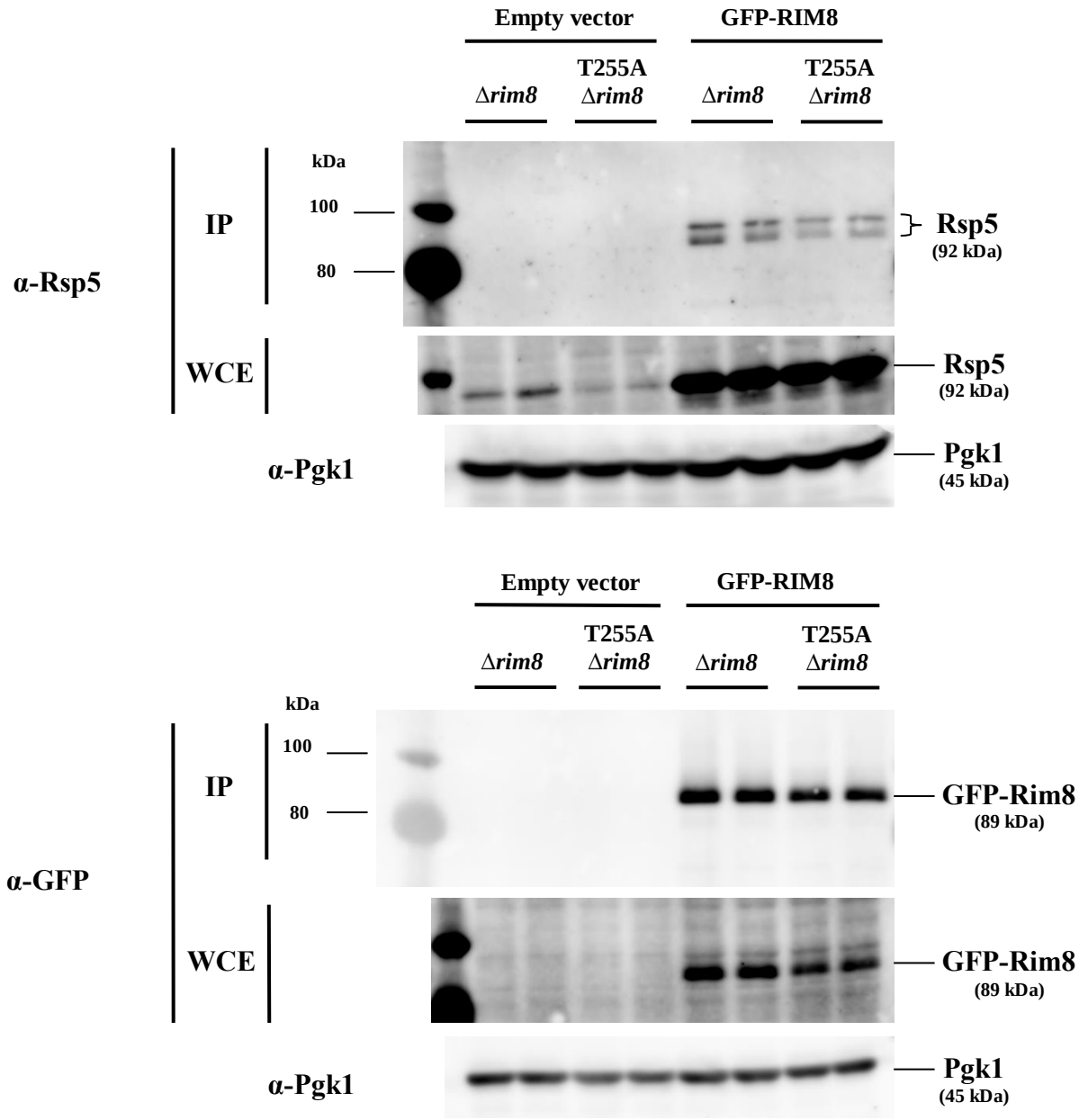

Figure 27. The Rsp5-Rim8 interaction was not increased by the T255A mutant under non-stress condition.

S. cerevisiae strains BY4741 *Δrim8* and T255A *Δrim8* harboring plasmid pAG416-GPD-EGFP-ccdB or pAG416-GPD-EGFP-RIM8 cells were pre-cultured in 3 mL SC-Ura, pH 6 overnight and then inoculated in 30 mL SC-Ura, pH 6 with the initial OD_{600} of 0.2. The cultures were incubated at 30˚C with shaking at 133 rpm. Approximately, 30 OD_{600} cells were collected at 4.5 hours (OD_{600} ~1.0) after incubation for the co-immunoprecipitation of Rsp5 and Rim8.

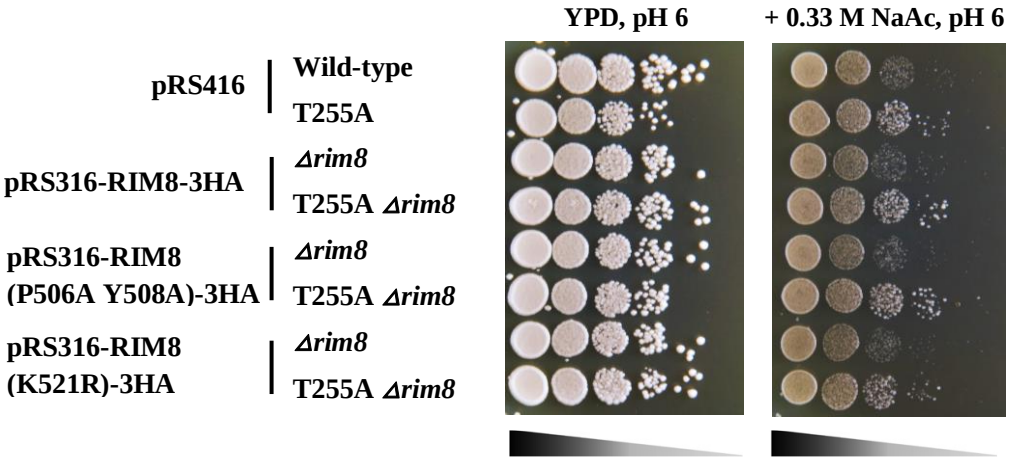

Figure 28. Rim8 ubiquitination and Rsp5-Rim8 interaction were not required for the NaAc tolerance of the T255A mutant.

Spot test of *S. cerevisiae* strains BY4741 wild-type and *rsp5*^{T255A} *–kanMX6* (T255A) harboring plasmid pRS416 (empty vector), and BY4741*Δrim8* and T255A *Δrim8* harboring plasmids pRS316-RIM8-3HA (pOK476), pRS316-RIM8 (P506A Y508A)-3HA (pOK477), or pRS316-RIM8 (K521R)-3HA (pOK573) cells on NaAc stress. Approximately, 1 OD_{600} cells were 10-fold serially diluted to 10^{-4} (from left to right), spotted on YPD at pH 6 (control) and YPD containing 0.33 M NaAc at pH 6 (NaAc stress), and incubated at 30˚C for approximately 2 days.

Section 2.

Examination of the potential of T255A mutant allele of *RSP5* for engineering the industrial yeast strain used for bioethanol production under NaAc stress conditions

1. NaAc tolerance of the ER-T255A mutant

To improve the NaAc tolerance of the industrial bioethanol yeast *S. cerevisiae* diploid strain Ethanol Red® (ER), the engineered strain was constructed by introducing *rsp5*^{T255A} fused with the *kanMX6* cassette into the genomic *RSP5* locus via homologous recombination. Due to the recessive property of *rsp5*^{T255A} allele, the homozygous T255A mutant allele is required. The diploid strain harboring the homozygous T255A mutant allele (ER-T255A) was successfully constructed.

To test the NaAc tolerance of the ER-T255A mutant, phenotypic test was performed. As shown in Figure 29, the ER-T255A mutant cells exhibited higher NaAc tolerance than did the wild-type cells on YPD containing 0.21, 0.25, 0.29, and 0.33 M NaAc (12.5, 15, 17.5, and 20 g/L acetate), pH 6. Similar to the laboratory T255A mutant cells, the ER-T255A mutant cells were more sensitive to acetic acid stress than did the wild-type cells as shown by the growth phenotype on YPD containing 0.125 M (7.5 g/L) acetate, pH 5. Therefore, these results indicate that the T255A mutant allele of *RSP5* can be used for engineering the industrial yeast strain to improve the NaAc tolerance.

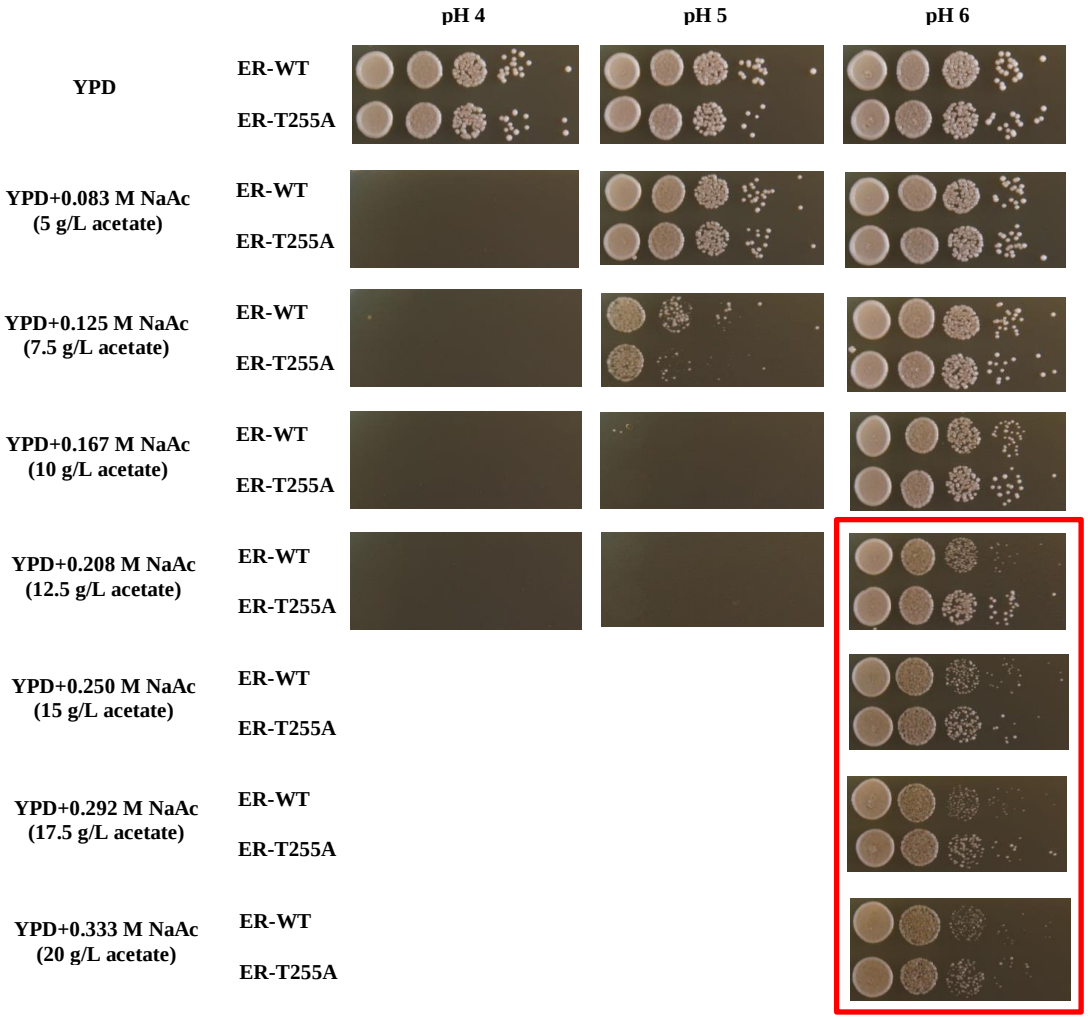

Figure 29. ER-T255A mutant was more tolerant to NaAc stress than did the wild-type strain.

Spot test of *S. cerevisiae* diploid strains Ethanol Red® wild-type (ER-WT), and *rsp5*^{T255A}-*kanMX6/ rsp5*^{T255A}-*kanMX6* (ER-T255A) cells on NaAc stress conditions. Approximately, 1 OD_{600} cells were 10-fold serially diluted to 10^{-4} (from left to right), spotted on YPD at pH 4, 5, and 6 (control) and YPD containing 0.083, 0.125, 0.167, and 0.208 M NaAc at pH 4, 5, and 6 as well as that containing 0.250, 0.292, and 0.333 M NaAc at pH 6, and incubated at 30˚C for 1 day.

2. Fermentation analysis of the ER-T255A mutant under NaAc stress condition

To examine the fermentation property of the ER-T255A mutant strain under NaAc stress, the wild-type and ER-T255A mutant cells were pre-cultured overnight in YPD medium, and then fermentation was performed in YPD or YPD containing 0.33 M NaAc, pH 6.8. Total CO_2 gas was real-time measured by Fermograph® II-W system. The CO_2 gas emission rate was automatically calculated. As shown in Figures 30 and 31, the initial fermentation rate of the ER-T255A mutant cells was slightly lower than that of the wild-type cells in YPD medium. Notably, the ER-T255A mutant cells significantly improved the initial fermentation rate under NaAc stress condition at approximately 3 hours earlier than did the wild-type cells.

To examine whether the increased initial fermentation rate of the ER-T255A mutant strain is due to the increased biomass or the increased CO_2 producing ability per cell during fermentation under NaAc stress condition, the growth curve of the wild-type and ER-T255A mutant cells under NaAc stress condition were determined. As shown in Figures 30, the increased initial fermentation rate of the ER-T255A mutant cells was correlated well with the increased OD_{600} under NaAc stress condition. This result suggested that the improved fermentation ability under NaAc stress condition of the ER-T255A mutant was at least partly due to its increased biomass.

To examine the fermentation property of the ER-T255A mutant strain under NaAc stress condition at higher glucose concentrations which are suitable for the industrial application. The wild-type and ER-T255A mutant cells were pre-cultured overnight in either YPD medium containing 10% glucose (YPD10) or 20% glucose (YPD20), and then fermentation was performed in YPD10 or YPD10 containing 0.33 M NaAc, pH 6.8, and YPD20 or YPD20 containing 0.33 M NaAc, pH 7.0. As shown in Figure 32, 33, 34, and 35, the ER-T255A mutant cells showed lower initial fermentation rate than did the wild-type cells under non-stress conditions (YPD10 and YPD 20 without NaAc stress). Importantly, the ER-T255A mutant cells exhibited significantly higher initial fermentation rate under NaAc stress condition with 10% glucose concentration at approximately 2 hours earlier than did the wild-type cells (Figures 32 and 33). Similarly, higher initial fermentation rate at approximately 3 hours earlier was observed in the ER-T255A mutant cells under NaAc stress condition with 20% glucose concentration (Figures 34 and 35). It should be noted that the addition of NaAc decreased the maximum CO_2 gas emission rate and the total CO_2 gas emission, confirming that the NaAc stress is inhibitory to the fermentation. Based on these results, it was concluded that the ER-

T255A mutant strain had higher fermentation ability than did the wild-type strain under NaAc stress condition.

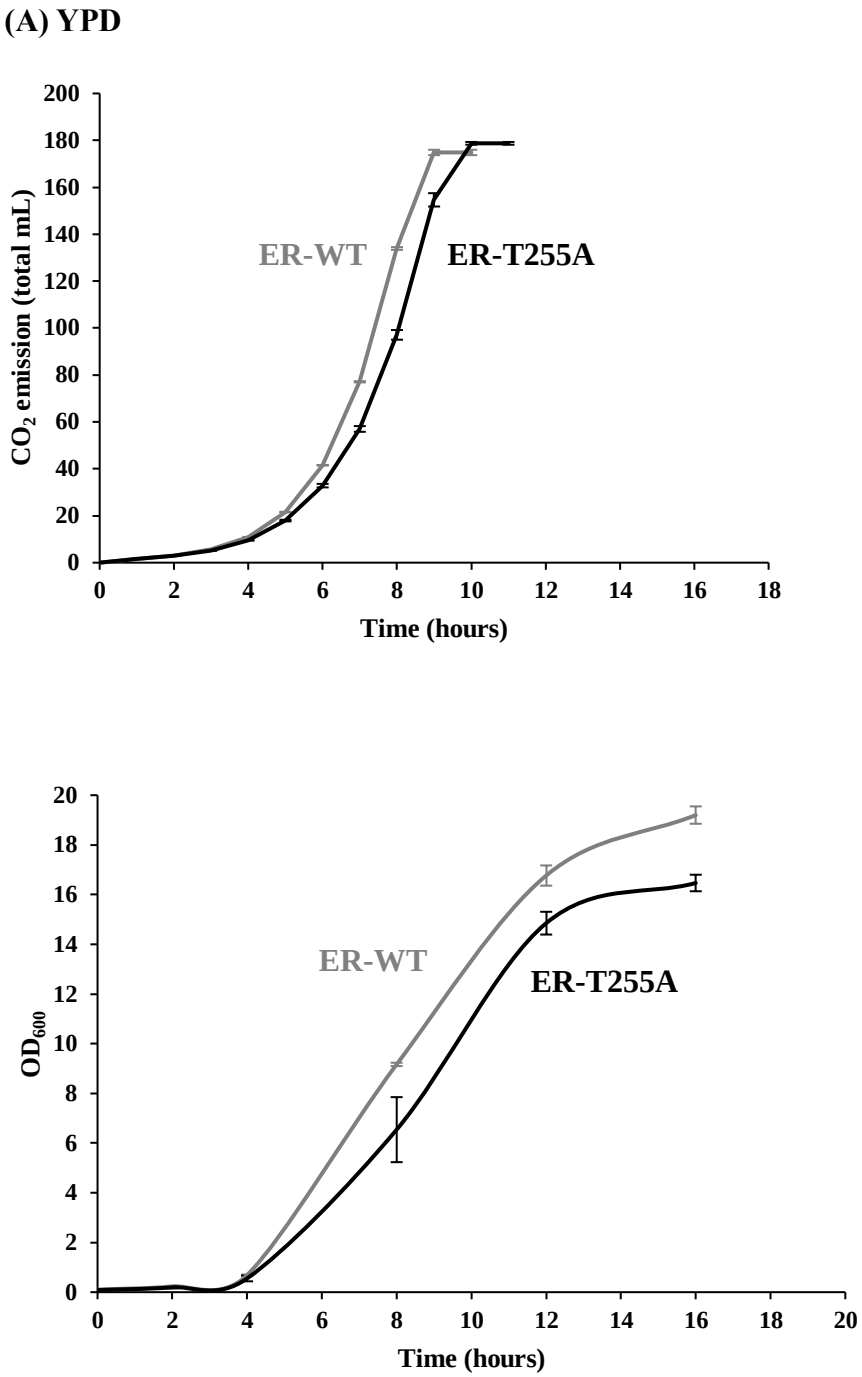

(B) YPD + 0.33 M NaAc, pH 6.8

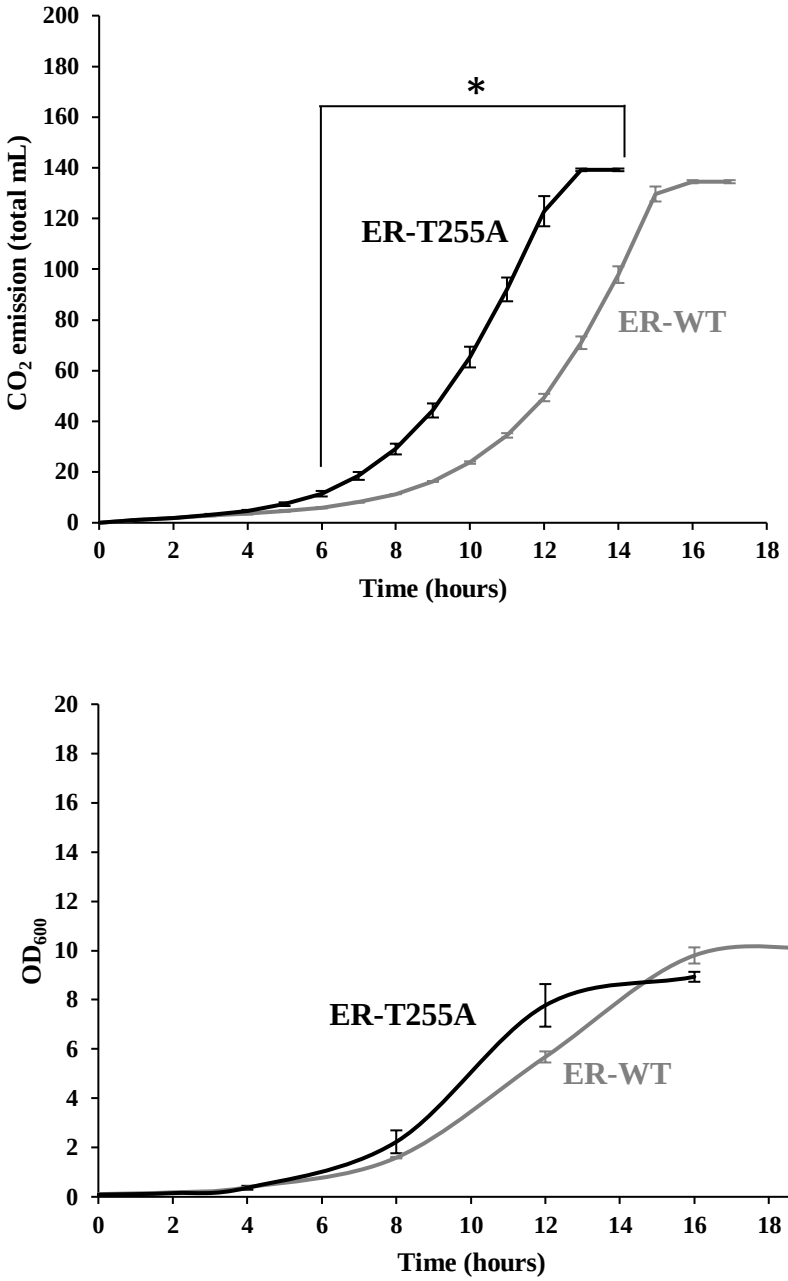

Figure 30. Total CO_2 gas emission of ER-WT and ER-T255A under NaAc stress condition with 2% glucose and their growth curves

S. cerevisiae diploid strains Ethanol Red® wild-type (ER-WT) and *rsp5*^{T255A}*-kanMX6/ rsp5*^{T255A}*-kanMX6* (ER-T255A) were pre-cultured in 3 mL YPD (2% glucose) overnight and then inoculated in 50 mL YPD (A) or YPD containing 0.33 M NaAc at pH 6.8 (B) with the initial OD_{600} of 0.1. The cultures were incubated at 30˚C with shaking at 120 rpm. Total CO_2 gas was measured by Fermograph® II-W.* indicates the significant difference at $p<0.01$. Separately, their growth curves were determined by measuring OD_{600} under similar growth conditions with shaking at 133 rpm.

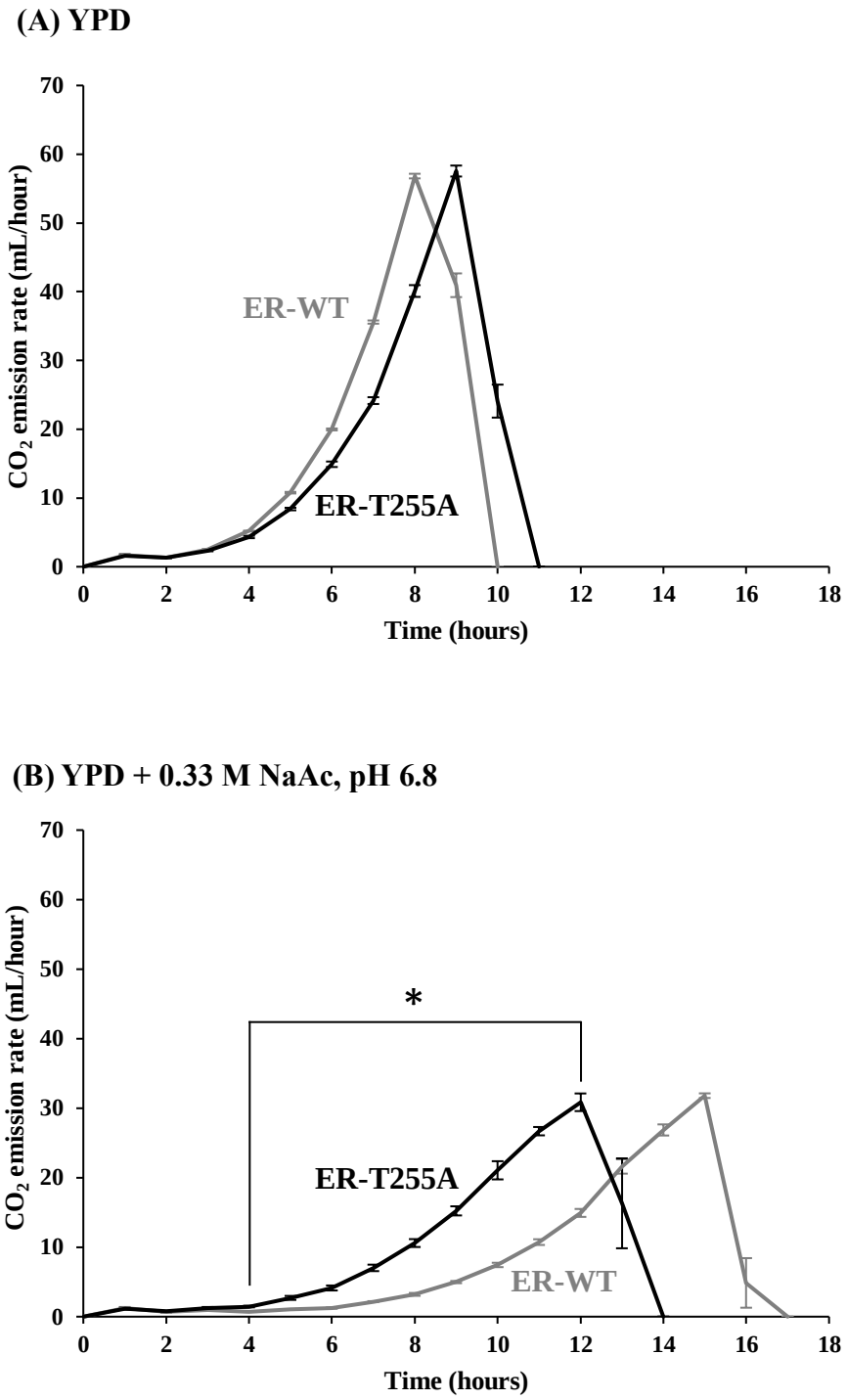

Figure 31. CO_2 gas emission rate of ER-WT and ER-T255A under NaAc stress with 2% glucose

S. cerevisiae diploid strains Ethanol Red® wild-type (ER-WT) and *rsp5*^{T255A}*-kanMX6/ rsp5*^{T255A}*-kanMX6* (ER-T255A) were pre-cultured in 3 mL YPD (2% glucose) overnight and then inoculated in 50 mL YPD (A) or YPD containing 0.33 M NaAc at pH 6.8 (B) with the initial OD_{600} of 0.1. The cultures were incubated at 30˚C with shaking at 120 rpm. Total CO_2 gas was measured by Fermograph® II-W. The CO_2 gas emission rate was automatically calculated. * indicates the significant difference at $p<0.01$.

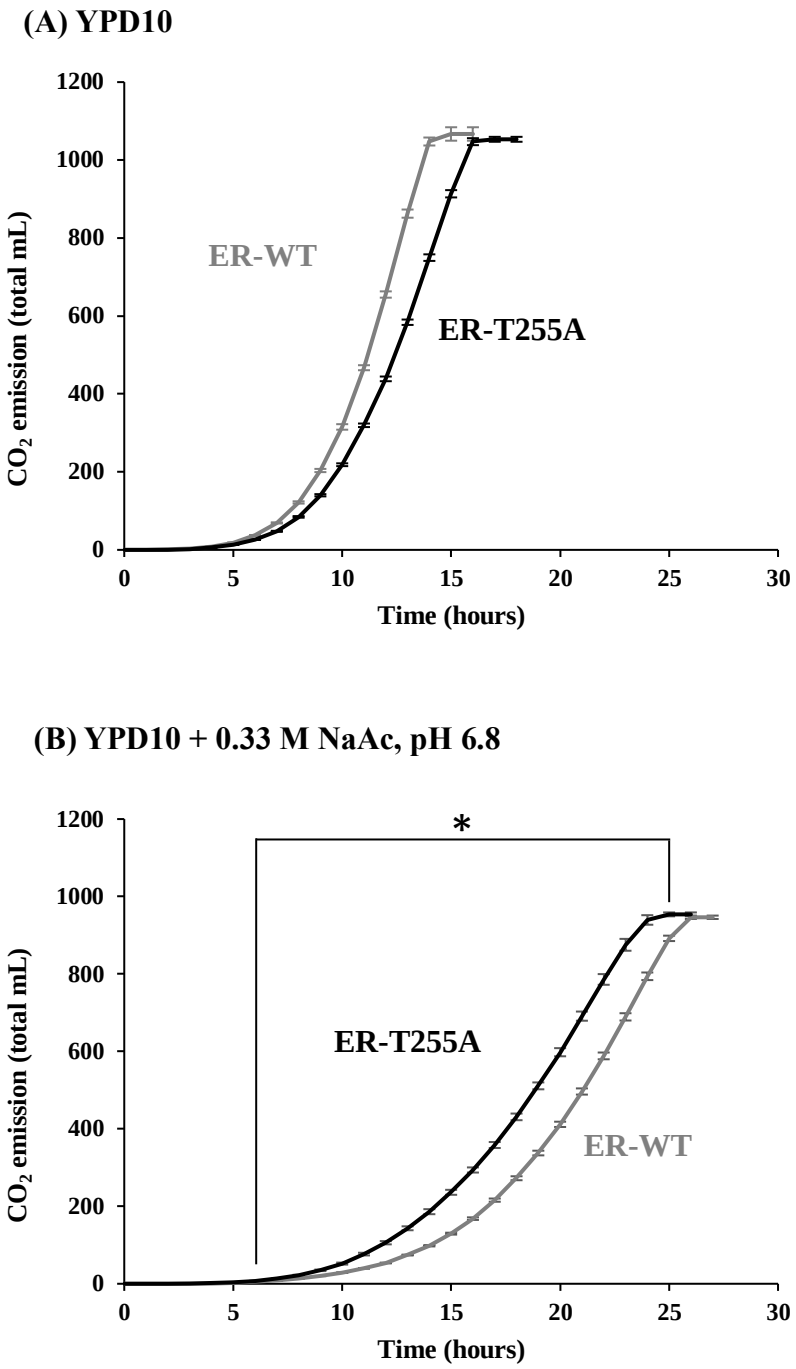

Figure 32. Total CO_2 gas emission of ER-WT and ER-T255A under NaAc stress with 10% glucose

S. cerevisiae diploid strains Ethanol Red® wild-type (ER-WT) and *rsp5*^{T255A}*-kanMX6/ rsp5*^{T255A}*-kanMX6* (ER-T255A) were pre-cultured in 3 mL YPD10 (10% glucose, pH 6.356) overnight and then inoculated in 50 mL YPD10 (A) or YPD10 containing 0.33 M NaAc, pH 6.8 (B) with the initial OD_{600} of 0.1. The cultures were incubated at 30˚C with shaking at 120 rpm. Total CO_2 gas was measured by Fermograph® II-W. * indicates the significant difference at $p<0.01$.

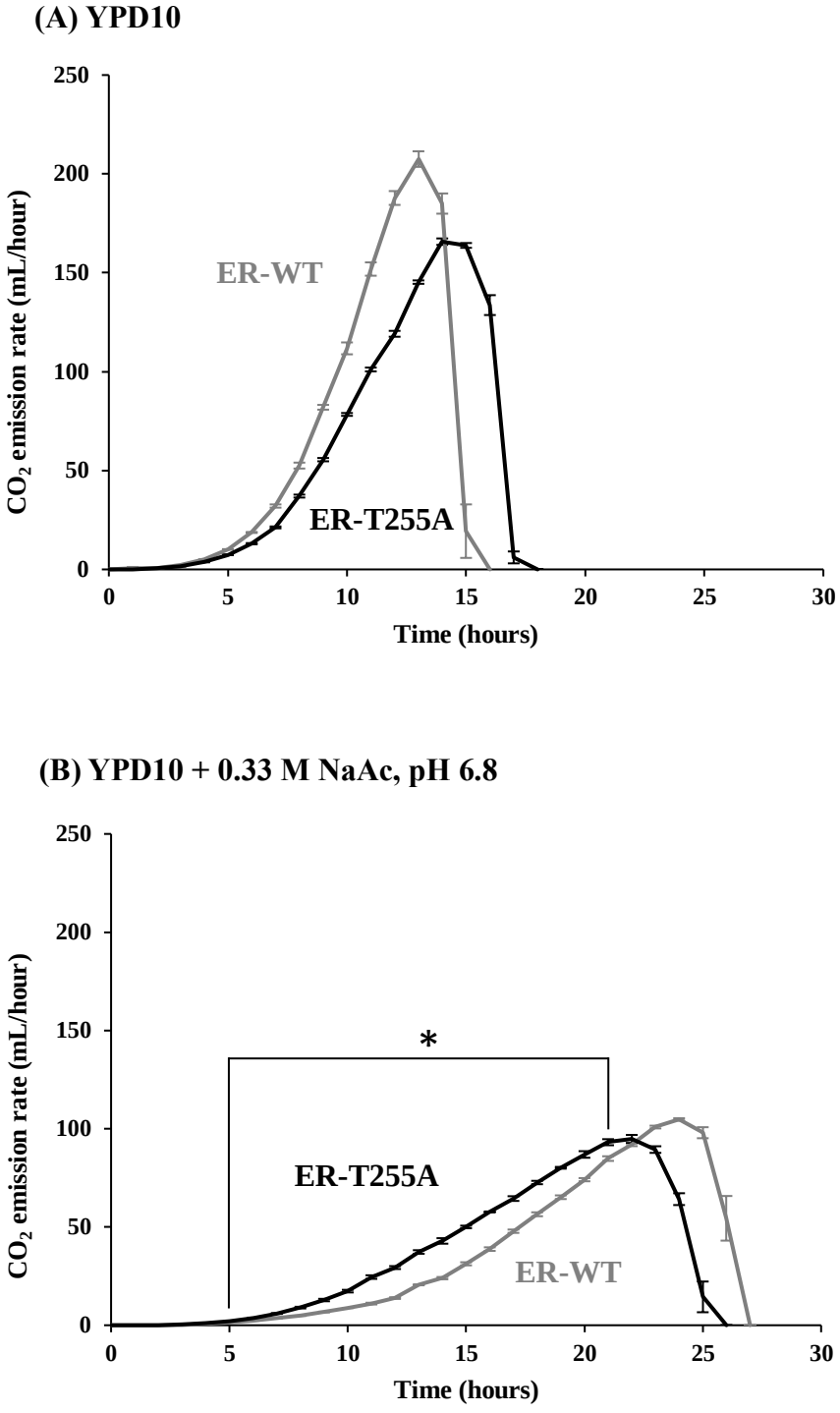

Figure 33. CO_2 gas emission rate of ER-WT and ER-T255A under NaAc stress with 10% glucose

S. cerevisiae diploid strains Ethanol Red® wild-type (ER-WT) and *rsp5*^{T255A}*-kanMX6/ rsp5*^{T255A}*-kanMX6* (ER-T255A) were pre-cultured in 3 mL YPD10 (10% glucose, pH 6.356) overnight and then inoculated in 50 mL YPD10 (A) or YPD10 containing 0.33 M NaAc, pH 6.8 (B) with the initial OD_{600} of 0.1. The cultures were incubated at 30˚C with shaking at 120 rpm. Total CO_2 gas was measured by Fermograph® II-W. The CO_2 gas emission rate was automatically calculated. * indicates the significant difference at $p<0.01$.

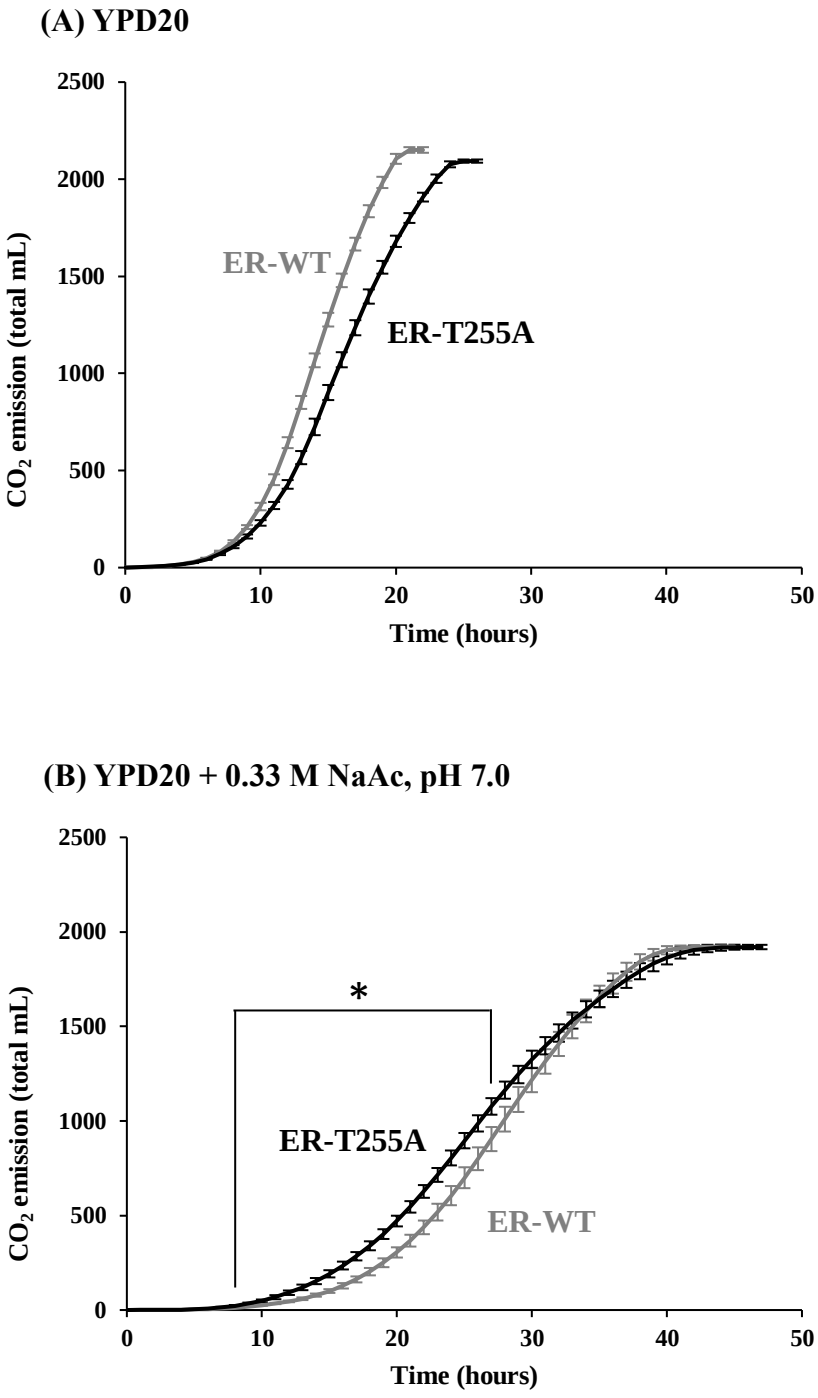

Figure 34. Total CO_2 gas emission of ER-WT and ER-T255A under NaAc stress with 20% glucose

S. cerevisiae diploid strains Ethanol Red® wild-type (ER-WT) and *rsp5*^{T255A}*-kanMX6/ rsp5*^{T255A}*-kanMX6* (ER-T255A) were pre-cultured in 3 mL YPD20 (20% glucose, pH 6.1) overnight and then inoculated in 50 mL YPD20 (A) or YPD20 containing 0.33 M NaAc, pH 7.0 (B) with the initial OD_{600} of 0.1. The cultures were incubated at 30˚C with shaking at 120 rpm. Total CO_2 gas was measured by Fermograph® II-W. * indicates the significant difference at $p<0.01$.

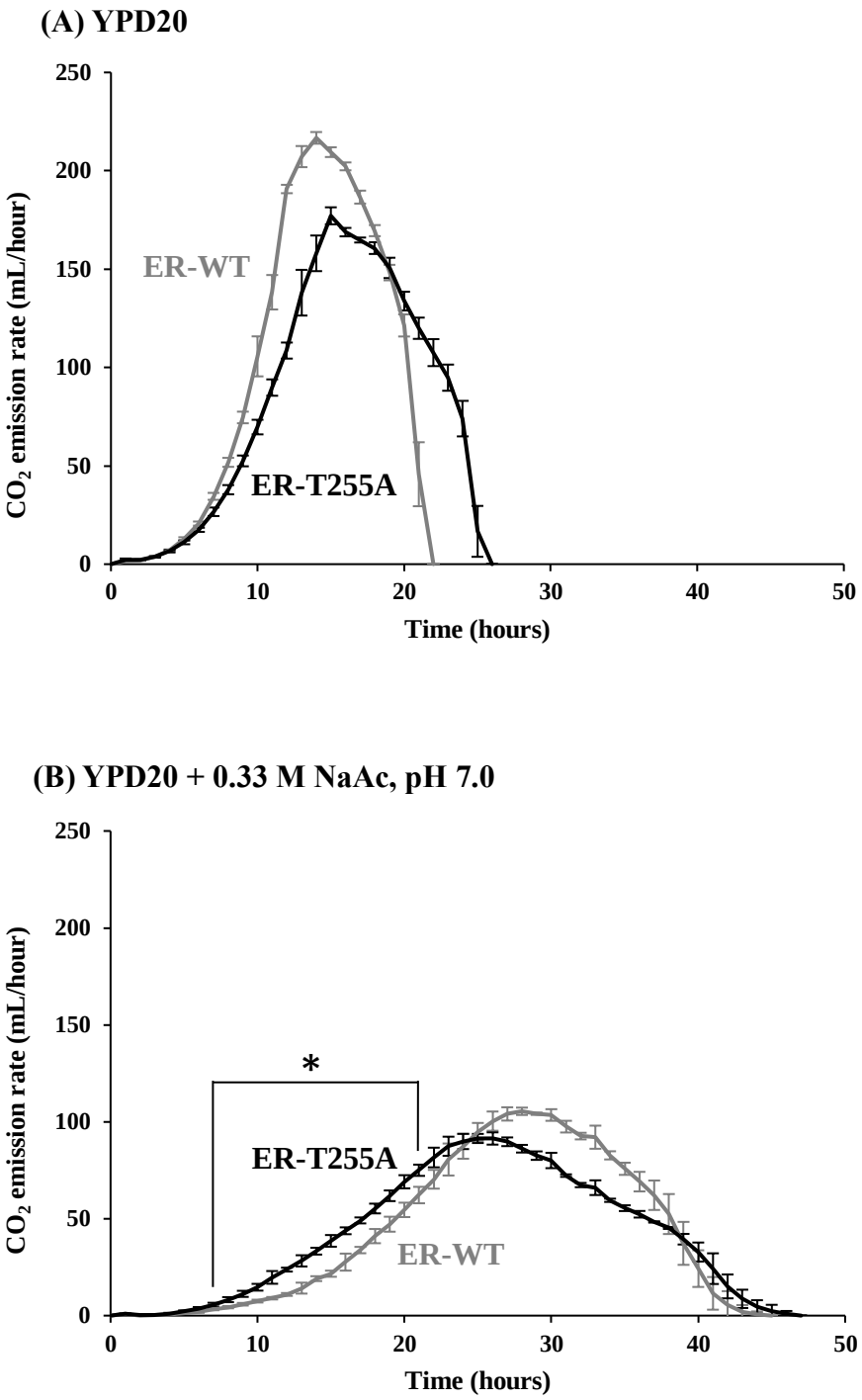

Figure 35. CO_2 gas emission rate of ER-WT and ER-T255A under NaAc stress with 20% glucose

S. cerevisiae diploid strains Ethanol Red® wild-type (ER-WT) and *rsp5*^{T255A}*-kanMX6/ rsp5*^{T255A}*-kanMX6* (ER-T255A) were pre-cultured in 3 mL YPD20 (20% glucose, pH 6.1) overnight and then inoculated in 50 mL YPD20 (A) or YPD20 containing 0.33 M NaAc, pH 7.0 (B) with the initial OD_{600} of 0.1. The cultures were incubated at 30˚C with shaking at 120 rpm. Total CO_2 gas was measured by Fermograph® II-W. The CO_2 gas emission rate was automatically calculated. * indicates the significant difference at $p<0.01$.

CHAPTER V
DISCUSSION

Protein ubiquitination is the fundamental process for regulating various cellular responses. As the essential protein, the sole Nedd4-family ubiquitin ligase Rsp5 in *S. cerevisiae* is known to regulate the intracellular trafficking of several plasma membrane proteins such as the general amino acid permease Gap1 (Springael *et al*., 1999b), the high affinity uracil transporter Fur4 (Galan et al., 1996; Hein and Andre, 1997), and the divalent cation transporter Smf1 (Sullivan *et al*., 2007). However, the knowledge regarding the role of Rsp5 in regulating the monovalent cation transporters Ena1/2/5 is still limited. Nedd4-2, the human orthologue of Rsp5, is involved in the regulation of the epithelial monovalent cation transporter EnaC. The defect in its regulation causes the hypertension disease known as Liddle's syndrome (Rotin and Staub, 2012). In this study, by using NaAc- and α-synuclein-tolerant *rsp5*^{T255A} mutant isolated by Wijayanti *et al*. (2015), I first obtained the evidence suggesting that the ubiquitin ligase Rsp5 regulated intracellular Na^+ level possibly by affecting Ena1/2/5 under NaAc stress condition (Figures 20 and 24). Acetate stress (up to 0.33 M) in the presence of Na^+ is one of the potential fermentation inhibitors in the bioethanol production from lignocellulosic biomass (Gilbert *et al*., 2009; Yang et al., 2010; Pena *et al*., 2013). In this study, I showed that the engineered industrial yeast strain Ethanol Red® harboring the homozygous *rsp5*^{T255A} mutant allele improved the NaAc tolerance and increased the initial fermentation rate under NaAc stress condition (Figures 29-35). In this chapter, the following points will be discussed.

1. What is NaAc stress?

Acetate stress in the presence of Na^+ has been described to generally inhibit cell growth by two main mechanisms including: 1) an increase in extracellular osmolarity that induces the loss of cytoplasmic water (Mollapour and Piper, 2006); 2) a possible increase in intracellular Na^+ or acetate accumulation that negatively affects cellular enzymatic functions (Yang *et al*., 2010; Gilbert *et al*., 2009; Peña *et al*., 2013). Recent study initially showed that acetate stress in the presence of Na^+ was more toxic than did NaCl based on the level of growth rate inhibition and proposed the synergistic intracellular inhibitory effect between Na^+ and acetic acid/acetate (Pena *et al*., 2013). In the present study, I propose that extracellular acetate exhibited an inhibitory role under my experimental conditions, and preliminarily showed that NaAc induced higher intracellular Na^+ accumulation than did NaCl (Figures 19 and 21), supporting the

synergistic inhibition caused by Na^+ and extracellular acetate. It is possible that the extracellular acetate interferes Trk1/Trk2, the high affinity K^+ uptake system (Mendoza *et al*., 1994; Haro and Rodríguez-Navarro, 2002), resulting in the decrease in ion specificity and/or selectivity of the channels, leading to an increased Na^+ influx. To test this hypothesis, it is interesting to measure intracellular Na^+ level in the Δ*trk1*/Δ*trk2* cells under NaAc stress condition in the future. Importantly, my study also showed that the T255A mutant form of Rsp5 specifically enhanced the tolerance to NaAc, but not to NaCl (Figure 18). This finding suggests that Rsp5 involves in the specific responses to NaAc, which is different from the responses to NaCl. This specificity can be partially explained by the increased intracellular Na^+ accumulation in the presence of acetate and that the lower intracellular Na^+ accumulation in the T255A mutant was acetate-specific (Figure 21). However, it is possible that Rsp5 mediates the responses to extracellular acetate, which may be positively affected by the T255A mutant. Taken together, this study proposes that NaAc stress is different from Na^+ and acetate stress because both Na^+ and extracellular acetate play a role in the toxicity of NaAc.

2. Plasma membrane transporters are involved in NaAc stress responses.

The Na^+ extrusion system in *S. cerevisiae* strain BY4741 is composed of two types of transporters including the Na^+/H^+ antiporter Nha1 and the P-type ATPase Na^+ pumps Ena1/2/5 (Figure 3) (Ariño *et al*., 2010). Yang *et al*. (2010) reported that the overexpression or the disruption of *NHA1* can enhance or reduce the NaAc tolerance, respectively. Gilbert *et al*. (2009) and Peña *et al*. (2013) demonstrated that the amplification of the copy number of *ENA1/2/5* gene cluster in the genome and the overexpression of *ENA2* can improve the NaAc tolerance. Here, I showed that disruption of the *ENA1/2/5* gene rendered NaAc sensitivity to yeast cells (Figures 17 and 18). Indeed, the determination of intracellular Na^+ level revealed that yeast cells lacking Ena1/2/5 accumulated high intracellular Na^+ level under NaAc stress condition (Figure 24), supporting the hypothesis that maintaining Na^+ cation homeostasis by export of Na^+ through Ena1/2/5 is one of the important responses to NaAc stress. To reveal which Ena is specifically responsible for this Na^+ extrusion under NaAc stress condition, chromosomal replacement of the *ENA* gene cluster with single *ENA1, ENA2* or *ENA5* and the growth phenotype analysis are ongoing.

3. The HOG signaling as an upstream process of NaAc stress responses

The HOG signaling pathway is the fundamental MAPK cascade responsible for hyperosmotic stress responses (Hohmann, 2009). Hog1 MAPK has been shown to play a role

in the responses to acetate stress at pH 6.8 in the presence of Na^+ by inducing intracellular glycerol accumulation for counteracting the loss of cytoplasmic water (Mollapour and Piper, 2006; Mollapour *et al.*, 2009). Consistently, in the present study, I showed that disruption of the *HOG1* MAPK gene or the *PBS2* MAPKK gene negatively affected the NaAc tolerance (Figure 11), emphasizing an important role of the HOG signaling for NaAc stress responses. However, the upstream branches used for sensing NaAc stress has not been elucidated. In this study, I showed that known MAKKKs including Ssk2, Ssk22, and Ste11 of the HOG signaling (Figure 4) and Bck1 MAPKKK of the CWI pathway were not involved in the NaAc tolerance (Figures 13-16), suggesting the alternative input of Pbs2-Hog1 activation. This alternative input has been described in the previous studies using 0.5 M KCl (O'Rourke and Herskowitz, 2004) and 1.4 M KCl or NaCl or 2.5 M sorbitol (Wuytswinkel *et al.*, 2000). To confirm whether an unidentified MAPKKK is involved in this process, the NaAc tolerance of the quadruple mutant lacking *SSK2, SSK22, STE11,* and *BCK1* should be examined.

4. Rim8 and its involvement in NaAc stress responses

Rim8 is systematically known as Art9 (Tables 1 and 2) identified as an arrestin-type Rsp5 adaptor protein in the ART family (Lin *et al.*, 2008) and shown to function as an Rsp5 adaptor protein for mediating the Pma1 endocytosis in response to the loss of V-ATPase activity (Smardon and Kane, 2014). Rim8 also has a well-stablished role in the Rim signaling (Figure 6) responsible for adaptation to alkaline stress (Cornet and Gaillardin, 2014). A recent study showed that the *rim8* mutant is salt-sensitive and has an increased accumulation of intracellular Na^+ level due to its defect in the trafficking of Ena1 to the plasma membrane under NaCl stress condition (Marques *et al.*, 2015). In this study, I showed that disruption of the *RIM8* gene caused NaAc sensitivity on yeast cells and increased intracellular Na^+ accumulation under NaAc stress condition likely due to the effect on Ena protein(s).

5. How is Rsp5 involved in NaAc stress responses?

Rsp5 is the essential E3 ubiquitin ligase known to regulate various cellular responses through recognition and ubiquitination of diverse target proteins (Kaliszewski and Żołądek, 2008). Rsp5 is known to interact and mono-ubiquitinate Rim8 (Herrador *et al.*, 2010; 2013). However, the ubiquitination of Rim8 by Rsp5 is dispensable for alkaline stress responses through the Rim signaling (Herrador *et al.*, 2010; Obara and Kihara, 2014). In fact, Rsp5 itself is essential for the Rim signaling by catalyzing the ubiquitination of unidentified target(s)

possibly downstream of Rim8 and upstream of Rim20 (Obara and Kihara, 2014). Besides Rim8, Rim101 and other Rim and ESCRT components in the Rim signaling have been shown to be important for proper accumulation of Ena1 at the plasma membrane under NaCl stress condition (Marques *et al.*, 2015). In this study, I showed that the Rsp5-Rim8 interaction and Rim8 ubiquitination by Rsp5 were dispensable for the NaAc tolerance, suggesting that Rsp5 functions at the downstream level of Rim8 (Figures 6 and 40). To test this hypothesis, the NaAc tolerant phenotype of cells lacking the *RIM101* or *RIM20* gene will be tested.

6. How does the T255A mutation in the *RSP5* gene confer an increased NaAc tolerance?

Thr255 is a conserved residue in the WW1 domain of the Nedd4 family ubiquitin ligase (Figure 36) and is corresponding in position to Thr357 in the WW2 domain and Thr413 in the WW3 domain of Rsp5 (Figure 37). These three Thr residues have been shown to be phosphorylated and the T357A mutation causes constitutive endocytosis of Gap1 (Sasaki and Takagi, 2013), possibly due to an increased interaction to Bul2 (Watanabe *et al.*, 2015). Based on the tertiary structure consisting of Rsp5 WW3/HECT domains, the adaptor protein Sna3, and a ubiquitin molecule (Kamadurai *et al.*, 2013), Thr413 lies on the β-sheet with the hydroxyl group pointing toward carboxyl group of Pro107 in the PPXY motif of Sna3 (Figure 38), likely forming hydrogen bonding. This suggests an importance of Thr413 for the interaction between Sna3 and the WW3 domain of Rsp5. Thus, I hypothesized that alteration of the amino acid property in these conserved Thr residues may affect the substrate recognition by Rsp5 under NaAc stress condition. To test this hypothesis, the NaAc tolerant phenotype of the T255A, T255D, T357A, and T413A mutants was examined. As shown in Figure 39, the T255A and T255D mutants increased tolerance to NaAc stress, whereas the T357A and T413A mutants gained NaAc sensitivity, supporting my hypothesis.

To find a clue to molecular mechanism of the NaAc tolerance of the T255A mutant, I used genetic interaction approach and analysis of intracellular Na^+ accumulation. Indeed, the T255A mutant was shown to possess significantly lower intracellular Na^+ accumulation under NaAc stress condition than did the wild-type cells (Figure 20). This lower intracellular Na^+ level may at least partly account for the NaAc tolerance of the T255A mutant (Figure 40). It is noteworthy that this required cooperative functions of Hog1, Rim8, and Ena1/2/5 (Figure 24). Thus, I hypothesized that the T255A mutant (may) positively regulate the Na^+ efflux through Ena1/2/5 by affecting an interaction or ubiquitination toward an unidentified target which may lie in Rim and ESCRT components of the Rim signaling (Figures 6 and 40). To test this hypothesis, analysis of Ena protein localization to the plasma membrane in the T255A mutant

will be in progress. It should be noted that the T255A mutant may possess a positive role in the responses to extracellular acetate in addition to the positive regulation of Na^+ efflux (Figure 18).

Elucidation of this molecular mechanism will contribute to better understanding how the Nedd4 family ubiquitin ligases recognize their substrate proteins in response to different stimuli.

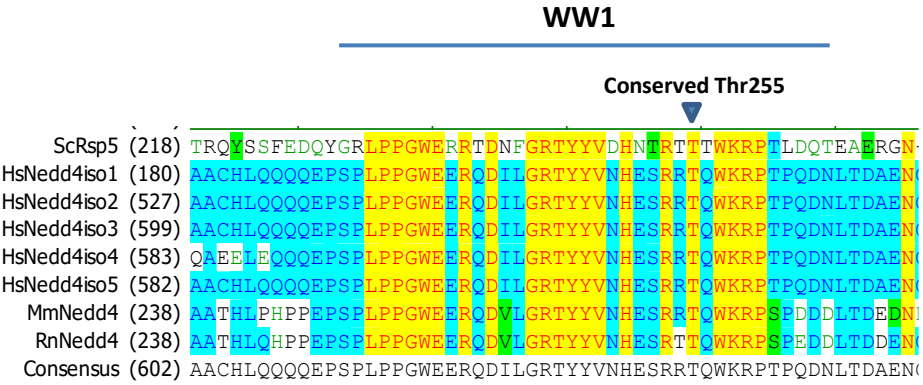

Figure 36. Thr255 is a conserved residue among HECT-type E3 ubiquitin ligases in the Nedd4 family.
ScRsp5 is from *S. cerevisiae*, accession no. P39940. HsNedd4iso1 to 5 are Nedd4 isoform 1 to 5 from *Homo sapiens* (human), accession no. NM_006154.3, NM_198400.3, NM_001284338.1, NM_001284339.1 and NM_001284340.1, respectively. MmNedd4 is from *Mus musculus* (mouse), accession no. NM_010890.3. RnNedd4 is from *Rattus norvegicus* (Rat), accession no. NM_012986.1.

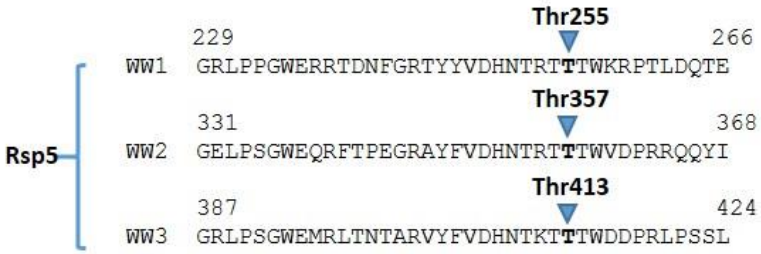

Figure 37. Thr255 in the WW1 domain of Rsp5 is corresponding to Thr at positions 357 and 413.

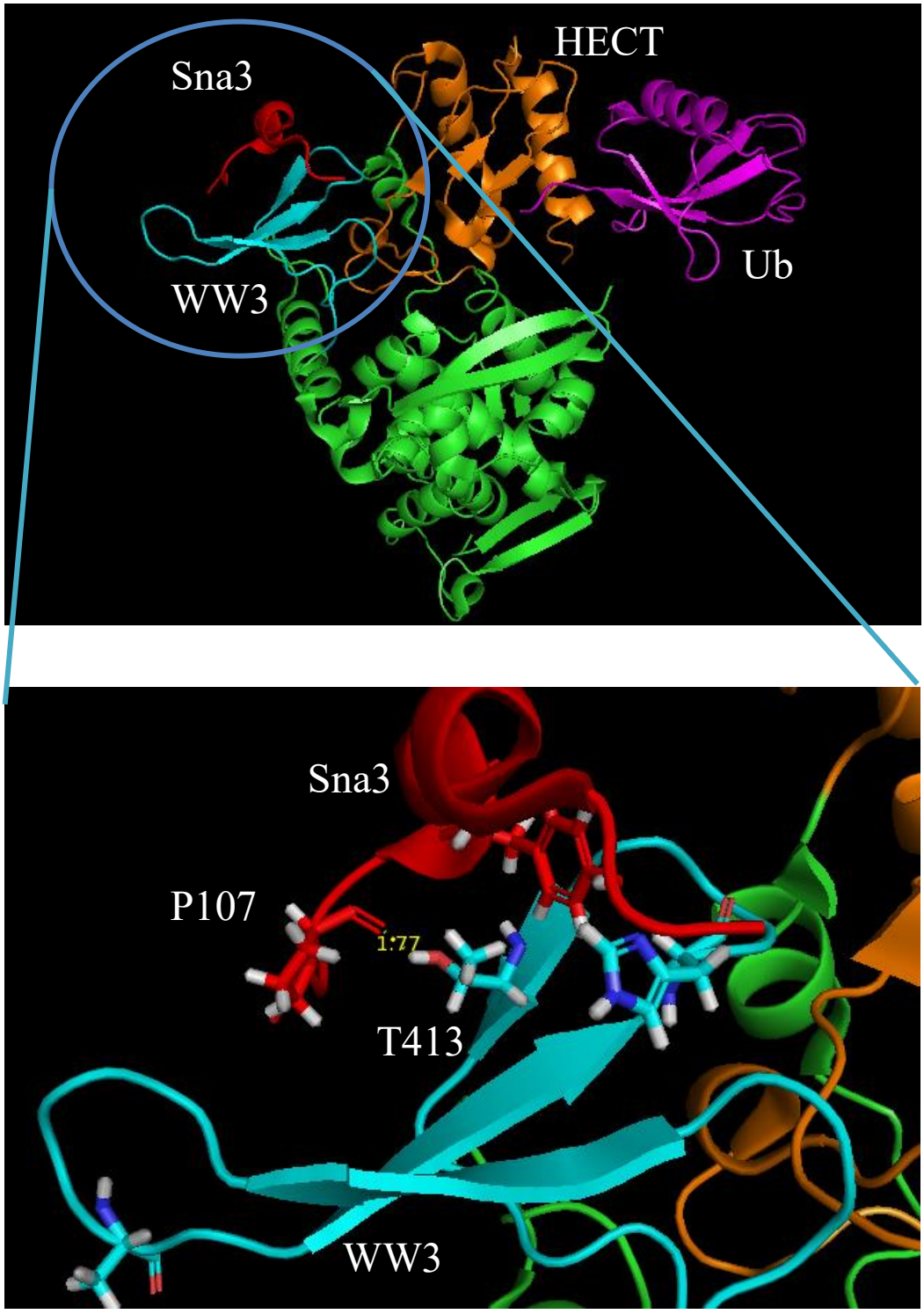

Figure 38. Predicted hydrogen bonding between hydroxyl group of Thr413 in the WW3 domain of Rsp5 and carbonyl group of Pro107 in the PPXY motif of an Rsp5 adaptor protein Sna3 (PDB: 4LCD)

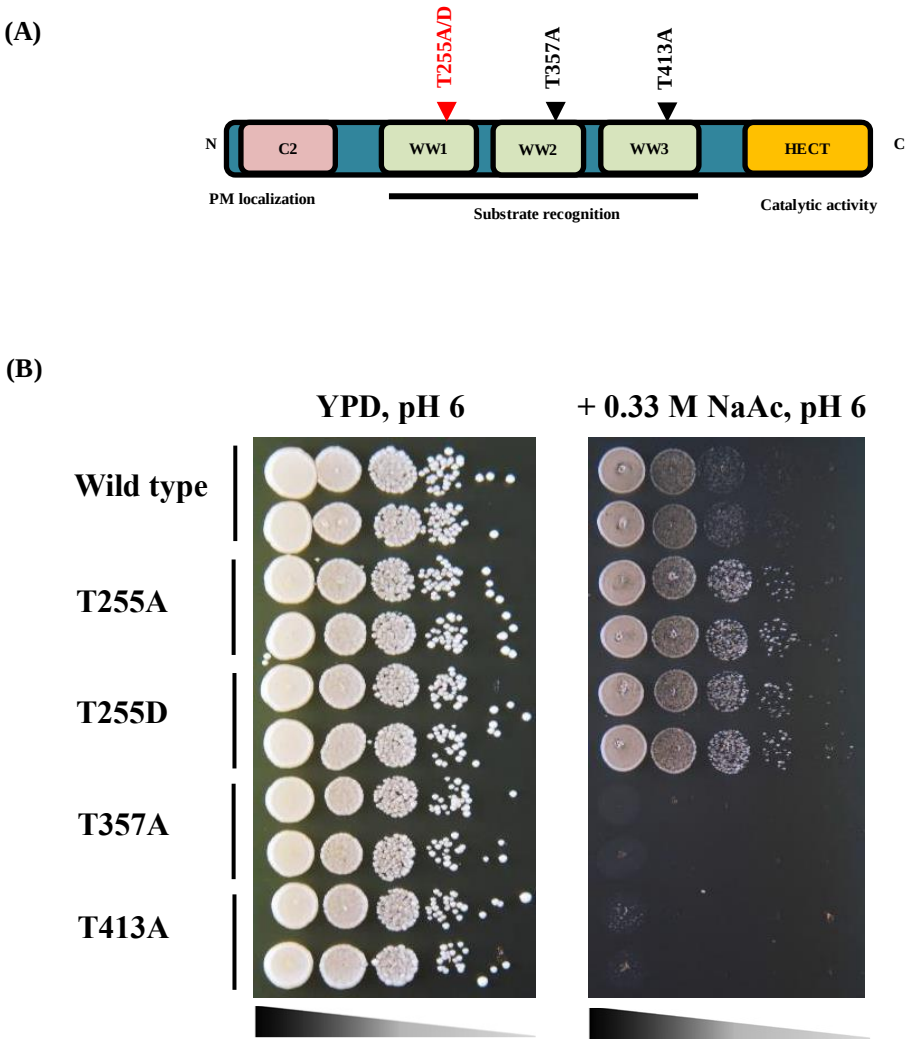

Figure 39. Conserved Thr residues in Rsp5 are important for NaAc stress responses.
(A) Schematic diagram represents corresponding mutations in *RSP5* gene including T255A or T255D (phosphorylation-mimic mutation) in the WW1 domain, T357A in the WW2 domain, and T413A in the WW3 domain. (B) Spot test of *S. cerevisiae* BY4741 wild-type, *rsp5*^{T255A} (T255A), *rsp5*^{T255D} (T255D), *rsp5*^{T357A} (T357A), and *rsp5*^{T413A} (T413A) cells on NaAc stress. Approximately, 1 OD_{600} cells were 10-fold serially diluted to 10^{-4} (from left to right), spotted on YPD at pH 6 (control) and YPD containing 0.33 M NaAc at pH 6 (NaAc stress), and incubated at 30˚C for approximately 2 days.

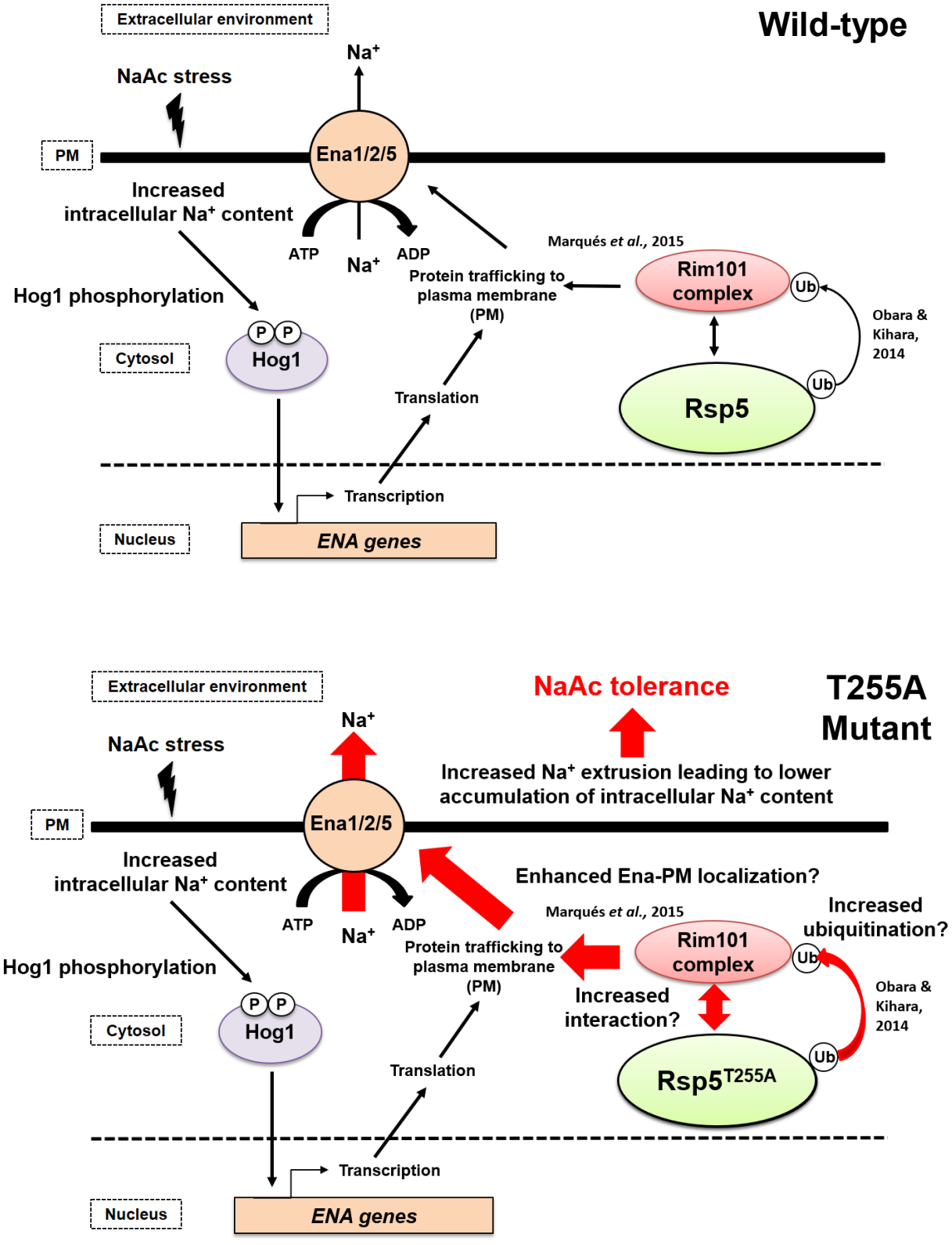

Figure 40. Proposed model for molecular mechanism of NaAc tolerance caused by the T255A mutant.

ACKNOWLEDGEMENTS

I would like to express my sincere gratitude to my supervisor Prof. Hiroshi Takagi for his scientific guidance, helps, encouragement, invaluable advice and instruction throughout this thesis. I am deeply thankful to Assist. Prof. Watanabe Daisuke for his kindness, supportive comments and ideas, scientific discussion, valuable instruction, and lots of encouragement throughout my study. I deeply thank my co-advisors Prof. Hisaji Maki and Prof. Kazuhiro Shiozaki for their critical comments and suggestion. In addition, I am really thankful to Assist. Prof. Keisuke Obara for providing me plasmids expressing Rim8-3HA and its mutants.

I am very thankful to Dr. Indah Wijayanti for constructing BY4741 *rsp5*^{T255A}*-kanMX6* mutant strain used in this study and to Miss Hiromi Yamada for her kindness and supports. I would like to confer my appreciation to former and current ubiquitin group members for their fun, joy, and discussion. My thanks also convey to all members in Takagi's laboratory.

I also would like to confer my gratitude to Graduate School of Biological Sciences, NAIST, MEXT, and JASSO for their financial supports throughout my study. This study is financially supported in part by Nagase Science and Technology Foundation.

Finally, I would like to express my deepest gratitude to my parents and family members for happiness, kindness, insight understanding, encouragement and patience throughout my study.

Watcharawipas Akaraphol

REFERENCES

Alepuz, P. M., Cunningham, K. W., & Estruch, F. (1997). Glucose repression affects ion homeostasis in yeast through the regulation of the stress-activated *ENA1* gene *Molecular Microbiology 26*(1), 91-98.

Almeida, J. R. M., Modig, T., Petersson, A., Hähn-Hägerdal, B., Lidén, G., & Gorwa-Grauslund, M. F. (2007). Increased tolerance and conversion of inhibitors in lignocellulosic hydrolysates by *Saccharomyces cerevisiae*. *Journal of Chemical Technology & Biotechnology, 82*(4), 340-349.

Altheim, B. A., & Schultz, M. C. (1999). Histone modification governs the cell cycle regulation of a replication-independent chromatin assembly pathway in *Saccharomyces cerevisiae Proceedings of the National Academy of Sciences, 96*, 1345-1350.

Ariño, J., Ramos, J., & Sychrova, H. (2010). Alkali metal cation transport and homeostasis in yeasts. *Microbiology and Molecular Biology Reviews, 74*(1), 95-120.

Arnason, T. G., Pisclevich, M. G., Dash, M. D., Davies, G. F., & Harkness, T. A. A. (2005). Novel interaction between Apc5p and Rsp5p in an intracellular signaling pathway in *Saccharomyces cerevisiae*. *Eukaryotic Cell, 4*(1), 134-146.

Balat, M., Balat, H., & Öz, C. (2008). Progress in bioethanol processing. *Progress in Energy and Combustion Science, 34*(5), 551-573.

Banuelos, M. A., Sychrova, H., Bleykasten-Grosshans, C., Souciet, J., & Potier, S. (1998). The Nha1 antiporter of *Saccharomyces cerevisiae* mediates sodium and potassium efflux *Microbiology, 144*, 2749-2758.

Beaudenon, S. L., Huacani, M. R., Wang, G., Mcdonnell, D. P., & Huibregtse, J. M. (1999). Rsp5 ubiquitin-protein ligase mediates DNA damage-induced degradation of the large subunit of RNA polymerase II in *Saccharomyces cerevisiae Molecular and Cellular Biology, 19*(10), 6972-6979.

Beck, T., Schmidt, A., & Hall, M. N. (1999). Starvation induces vacuolar targeting and degradation of the tryptophan permease in yeast. *The Journal of Cell Biology, 146*(6), 1227-1237.

Bellissimi, E., van Dijken, J. P., Pronk, J. T., & van Maris, A. J. A. (2009). Effects of acetic acid on the kinetics of xylose fermentation by an engineered, xylose-isomerase-based *Saccharomyces cerevisiae* strain. *FEMS Yeast Research, 9*(3), 358-364.

Casal, M., Paiva, S., Queirós, O., & Soares-Silva, I. (2008). Transport of carboxylic acids in yeasts. *FEMS Microbiology Reviews, 32*(6), 974-994.

Cornet, M., & Gaillardin, C. (2014). pH signaling in human fungal pathogens: a new target for antifungal strategies. *Eukaryotic Cell, 13*(3), 342-352.

Crespo, J. L., Daicho, K., Ushimaru, T., & Hall, M. N. (2001). The GATA transcription factors GLN3 and GAT1 link TOR to salt stress in *Saccharomyces cerevisiae*. *Journal of Biological Chemistry, 276*(37), 34441-34444.

Cullen, P. J., Sabbagh Jr., W., Graham, E., Irick, M. M., Van Olden, E. K., Neal, C., et al. (2004). A signaling mucin at the head of the Cdc42- and MAPK-dependent filamentous growth pathway in yeast. *Genes and Development, 18*, 1695-1708.

De Nadal, E., Zapater, M., Alepuz, P. M., Sumoy, L., Mas, G., & Posas, F. (2004). The MAPK Hog1 recruits Rpd3 histone deacetylase to activate osmoresponsive genes. *Nature 427*, 370-374.

Dechant, R., Binda, M., Lee, S. S., Pelet, S., Winderickx, J., & Peter, M. (2010). Cytosolic pH is a second messenger for glucose and regulates the PKA pathway through V-ATPase. *The EMBO Journal, 29*(15), 2515-2526.

Ding, J., Bierma, J., Smith, M. R., Poliner, E., Wolfe, C., Hadduck, A. N., et al. (2013). Acetic acid inhibits nutrient uptake in *Saccharomyces cerevisiae*: auxotrophy confounds the use of yeast deletion libraries for strain improvement. *Applied Microbiology and Biotechnology, 97*(16), 7405-7416.

Dunn, R., & Hicke, L. (2001). Domains of the Rsp5 ubiquitin-protein ligase required for receptor-mediated and fluid-phase endocytosis. *Molecular Biology of the Cell, 12*, 421-435.

Dunn, R., Klos, D. A., Adler, A. S., & Hicke, L. (2004). The C2 domain of the Rsp5 ubiquitin ligase binds membrane phosphoinositides and directs ubiquitination of endosomal cargo. *The Journal of Cell Biology, 165*(1), 135-144.

Fang, N. N., Chan, G. T., Zhu, M., Comyn, S. A., Persaud, A., Deshaies, R. J., et al. (2014). Rsp5/Nedd4 is the main ubiquitin ligase that targets cytosolic misfolded proteins following heat stress. *Nature Cell Biology, 16*(12), 1227-1237.

Fernandes, A. R., Mira, N. P., Vargas, R. C., Canelhas, I., & Sá-Correia, I. (2005). *Saccharomyces cerevisiae* adaptation to weak acids involves the transcription factor Haa1p and Haa1p-regulated genes. *Biochemical and Biophysical Research Communications, 337*(1), 95-103.

Galan, J. M., Moreau, V., Andre, B., Volland, C., & Haguenauer-Tsapis, R. (1996). Ubiquitination mediated by the Npi1p/Rsp5p ubiquitin-protein ligase is required for endocytosis of the yeast uracil permease. *The Journal of Biological Chemistry 271*(18), 10946-10952.

Garciadeblas, B., Rubio, F., Quintero, F. J., Banuelos, M. A., Haro, R., & Rodriguez-Navarro, A. (1993). Differential expression of two genes encoding isoforms of the ATPase involved in sodium efflux in *Saccharomyces cerevisiae Molecular Genetics and Genomics, 236*, 363-368.

Gilbert, A., Sangurdekar, D. P., & Srienc, F. (2009). Rapid strain improvement through optimized evolution in the cytostat. *Biotechnology and Bioengineering, 103*(3), 500-512.

Gitan, R. S., & Eide, D. J. (2000). Zinc-regulated ubiquitin conjugation signals endocytosis of the yeast *ZRT1* zinc transporter. *Biochemical Journal, 346*, 329-336.

Gomez, M. J., Luyten, K., & Ramos, J. (1996). The capacity to transport potassium influences sodium tolerance in *Saccharomyces cerevisiae FEMS Microbiology Letters, 135*, 157-160.

Gupta, R., Kus, B., Fladd, C., Wasmuth, J., Tonikian, R., Sidhu, S., et al. (2007). Ubiquitination screen using protein microarrays for comprehensive identification of Rsp5 substrates in yeast. *Molecular Systems Biology, 3*.

Gwizdek, C., Hobeika, M., Kus, B., Ossareh-Nazari, B., Dargemont, C., & Rodriguez, M. S. (2005). The mRNA Nuclear Export Factor Hpr1 Is Regulated by Rsp5-mediated Ubiquitylation. *Journal of Biological Chemistry, 280*(14), 13401-13405.

Haitani, Y., Shimoi, H., & Takagi, H. (2006). Rsp5 regulates expression of stress proteins via post-translational modification of Hsf1 and Msn4 in *Saccharomyces cerevisiae*. *FEBS Letters, 580*(14), 3433-3438.

Haitani, Y., & Takagi, H. (2008). Rsp5 is required for the nuclear export of mRNA of *HSF1* and *MSN2/4* under stress conditions in *Saccharomyces cerevisiae*. *Genes to Cells, 13*(2), 105-116.

Harkness, T. A. A., Davies, G. F., Ramaswamy, V., & Arnason, T. G. (2002). The ubiquitin-dependent targeting pathway in *Saccharomyces cerevisiae* plays a critical role in multiple chromatin assembly regulatory steps. *Genetics, 162*, 615-632.

Haro, R., Garciadeblas, B., & Rodriguez-Navarro, A. (1991). A novel P-type ATPase from yeast involved in sodium transport *FEBS Letters, 291*(2), 189-191.

Haro, R., & Rodríguez-Navarro, A. (2002). Molecular analysis of the mechanism of potassium uptake through the *TRK1* transporter of *Saccharomyces cerevisiae*. *Biochimica et Biophysica Acta, 1564*, 114-122.

Hein, C., & Andre, B. (1997). A C-terminal di-leucine motif and nearby sequences are required for $NH4^{+}$-induced inactivation and degradation of the general amino acid permease, Gap1p, of *Saccharomyces cerevisiae*. *Molecular Microbiology, 24*(3), 607-616.

Helliwell, S. B., Losko, S., & Kaiser, C. A. (2001). Components of a ubiquitin ligase complex specify polyubiquitination and intracellular trafficking of the general amino acid permease. *The Journal of Cell Biology, 153*(4), 649-662.

Herrador, A., Herranz, S., Lara, D., & Vincent, O. (2009). Recruitment of the ESCRT machinery to a putative seven-transmembrane-domain receptor is mediated by an arrestin-related protein. *Molecular and Cellular Biology, 30*(4), 897-907.

Herrador, A., Leon, S., Haguenauer-Tsapis, R., & Vincent, O. (2013). A mechanism for protein monoubiquitination dependent on a trans-acting ubiquitin-binding domain. *Journal of Biological Chemistry, 288*(23), 16206-16211.

Herrador, A., Livas, D., Soletto, L., Becuwe, M., Leon, S., & Vincent, O. (2015). Casein kinase 1 controls the activation threshold of an arrestin by multisite phosphorylation of the interdomain hinge. *Molecular Biology of the Cell, 26*(11), 2128-2138.

Hershko, A., & Ciechanover, A. (1998). The ubiquitin system. *Annual Review of Biochemistry, 67*, 425-479.

Hettema, E. H., Valdez-Taubas, J., & Pelham, H. R. B. (2004). Bsd2 binds the ubiquitin ligase Rsp5 and mediates the ubiquitination of transmembrane proteins. *The EMBO Journal, 23*, 1279-1288.

Hohmann, S. (2002). Osmotic stress signaling and osmoadaptation in yeasts. *Microbiology and Molecular Biology Reviews, 66*(2), 300-372.

Hohmann, S. (2009). Control of high osmolarity signalling in the yeast *Saccharomyces cerevisiae*. *FEBS Letters, 583*(24), 4025-4029.

Holyoak, C. D., Stratford, M., McMullin, Z., Cole, M. B., Crimmins, K., Brown, A. J., et al. (1996). Activity of the plasma membrane H(+)-ATPase and optimal glycolytic flux are required for rapid adaptation and growth of *Saccharomyces cerevisiae* in the presence of the weak-acid preservative sorbic acid. *Applied and Environmental Microbiology, 62*(9), 3158-3164.

Hoshikawa, C., Shichiri, M., Nakamori, S., & Takagi, H. (2003). A nonconserved Ala401 in the yeast Rsp5 ubiquitin ligase is involved in degradation of Gap1 permease and stress-induced abnormal proteins. *Proceedings of the National Academy of Sciences, 100*(20), 11505-11510.

Huibregtse, J. M., Scheffner, M., Beaudenon, S., Howley, P. M., & (1995). A family of proteins structurally and functionally related to the E6-AP ubiquitin-protein ligase. *Proceedings of the National Academy of Sciences, 92*, 2563-2567.

Inaba, T., Watanabe, D., Yoshiyama, Y., Tanaka, K., Ogawa, J., Takagi, H., et al. (2013). An organic acid-tolerant *HAA1*-overexpression mutant of an industrial bioethanol strain of *Saccharomyces cerevisiae* and its application to the production of bioethanol from sugarcane molasses. *AMB Express 3*(74), 1-7.

Jackson, P. K., Eldridge, A. G., Freed, E., Furstenthal, L., Hsu, J. Y., Kaiser, B. K., et al. (2000). The lore of the RINGs: substrate recognition and catalysis by ubiquitin ligases. *Trends in Cell Biology, 10*, 429-439.

Janke, C., Magiera, M. M., Rathfelder, N., Taxis, C., Reber, S., Maekawa, H., et al. (2004). A versatile toolbox for PCR-based tagging of yeast genes: new fluorescent proteins, more markers and promoter substitution cassettes. *Yeast, 21*(11), 947-962.

Kaliszewski, P., & Zoladek, T. (2008). The role of Rsp5 ubiquitin ligase in regulation of diverse processes in yeast cells. *Acta Biochimica Polonica, 55*(4), 649-662.

Kamadurai, H. B., Qiu, Y., Deng, A., Harrison, J. S., Macdonald, C., Actis, M., et al. (2013). Mechanism of ubiquitin ligation and lysine prioritization by a HECT E3. *elife, 2*, 1-26.

Kane, P. M. (2007). The long physiological reach of the yeast vacuolar H^+-ATPase. *Journal of Bioenergetics and Biomembranes, 39*, 415-421.

Katzmann, D. J., Babst, M., & Emr, S. D. (2001). Ubiquitin-dependent sorting into the multivesicular body pathway requires the function of a conserved endosomal protein sorting complex, ESCRT-I. *Cell, 106*, 145-155.

Khan, Q. A., & Hadi, S. M. (1994). Inactivation and repair of bacteriophage lamda by furfural. *Biochemistry and Molecular Biology International Journal, 32*(2), 379-385.

Klinke, H. B., Thomsen, A. B., & Ahring, B. K. (2004). Inhibition of ethanol-producing yeast and bacteria by degradation products produced during pre-treatment of biomass. *Applied Microbiology and Biotechnology, 66*(1), 10-26.

Krampe, S., Stamm, O., Hollenberg, C. P., & Boles, E. (1998). Catabolite inactivation of the high-affinity hexose transporters Hxt6 and Hxt7 of *Saccharomyces cerevisiae* occurs in the vacuole after internalization by endocytosis. *FEBS Letters, 441*, 343-347.

Kwapisz, M. (2005). Rsp5 ubiquitin ligase modulates translation accuracy in yeast *Saccharomyces cerevisiae*. *Rna, 11*(11), 1710-1718.

Lamb, T. M., & Mitchell, A. P. (2003). The transcription factor Rim101p governs ion tolerance and cell differentiation by direct repression of the regulatory genes *NRG1* and *SMP1* in *Saccharomyces cerevisiae*. *Molecular and Cellular Biology, 23*(2), 677-686.

Lamb, T. M., Xu, W., Diamond, A., & Mitchell, A. P. (2000). Alkaline response genes of *Saccharomyces cerevisiae* and their relationship to the RIM101 pathway. *Journal of Biological Chemistry, 276*(3), 1850-1856.

Lapathitis, G., & Kotyk, A. (1998). Univalent cation fluxes in yeast *Biochemistry and Molecular Biology International 44*(2), 371-380.

Lauwers, E., Erpapazoglou, Z., Haguenauer-Tsapis, R., & Andre, B. (2010). The ubiquitin code of yeast permease trafficking. *Trends in Cell Biology, 20*(4), 196-204.

Leon, S., Erpapazoglou, Z., & Haguenauer-Tsapis, R. (2008). Ear1p and Ssh4p are new adaptors of the ubiquitin ligase Rsp5p for cargo ubiquitylation and sorting at multivesicular bodies. *Molecular Biology of the Cell, 19*(6), 2379-2388.

Léon, S., & Haguenauer-Tsapis, R. (2009). Ubiquitin ligase adaptors: Regulators of ubiquitylation and endocytosis of plasma membrane proteins. *Experimental Cell Research, 315*(9), 1574-1583.

Levin, D. E. (2011). Regulation of cell wall biogenesis in *Saccharomyces cerevisiae*: the cell wall integrity signaling pathway. *Genetics, 189*(4), 1145-1175.

Lin, C. H., MacGurn, J. A., Chu, T., Stefan, C. J., & Emr, S. D. (2008). Arrestin-related ubiquitin-ligase adaptors regulate endocytosis and protein turnover at the cell surface. *Cell, 135*(4), 714-725.

Liu, J., Sitaram, A., & Burd, C. G. (2007). Regulation of copper-dependent endocytosis and vacuolar degradation of the yeast copper transporter, Ctr1p, by the Rsp5 ubiquitin ligase. *Traffic, 8*(10), 1375-1384.

Liu, X. F., Supek, F., Nelson, N., & Culotta, V. C. (1997). Negative control of heavy metal uptake by the *Saccharomyces cerevisiae BSD2* gene. *The Journal of Biological Chemistry, 272*(18), 11763-11769.

Logg, K., Warringer, J., Hashemi, S. H., Käll, M., & Blomberg, A. (2008). The sodium pump Ena1p provides mechanistic insight into the salt sensitivity of vacuolar protein sorting mutants. *Biochimica et Biophysica Acta (BBA) - Molecular Cell Research, 1783*(6), 974-984.

Ludovico, P. (2002). Cytochrome c release and mitochondria involvement in programmed cell death induced by acetic acid in *Saccharomyces cerevisiae*. *Molecular Biology of the Cell, 13*(8), 2598-2606.

Maeda, T., Takekawa, M., & Saito, H. (1995). Activation of yeast PBS2 MAPKK by MAPKKKs or by binding of an SH3-containing osmosensor. *Science 269*, 554-558.

Marques, M. C., Zamarbide-Fores, S., Pedelini, L., Llopis-Torregrosa, V., & Yenush, L. (2015). A functional Rim101 complex is required for proper accumulation of the Ena1 Na^+-ATPase protein in response to salt stress in *Saccharomyces cerevisiae*. *FEMS Yeast Research, 15*(4), fov017-fov017.

Marquez, J. A., & Serrano, R. (1996). Multiple transduction pathways regulate the sodium-extrusion gene *PMR2/ENA1* during salt stress in yeast. *FEBS Letters, 382*, 89-92.

Martinez, P., & Persson, B. L. (1998). Identification, cloning and characterization of a derepressible Na^+-coupled phosphate transporter in *Saccharomyces cerevisiae*. *Molecular Genetics and Genomics 258*, 628-638.

Martinez-Munoz, G. A., & Kane, P. (2008). Vacuolar and plasma membrane proton pumps collaborate to achieve cytosolic pH homeostasis in yeast. *Journal of Biological Chemistry, 283*(29), 20309-20319.

Mas, A., Torija, M. J., García-Parrilla, M. d. C., & Troncoso, A. M. (2014). Acetic acid bacteria and the production and quality of wine vinegar. *The Scientific World Journal, 2014*, 1-6.

Medintz, I., Jiang, H., & Michels, C. A. (1998). The role of ubiquitin conjugation in glucose-induced proteolysis of *Saccharomyces* maltose permease. *The Journal of Biological Chemistry, 273*(51), 34454-34462.

Mendoza, I., Rubio, F., Rodriguez-Navarro, A., & Pardo, J. M. (1994). The protein phosphatase calcineurin is essential for NaCl tolerance of *Saccharomyces cerevisiae*. *The Journal of Biological Chemistry, 269*(12), 8792-8796.

Mira, N. P., Becker, J. D., & Sá-Correia, I. (2010). Genomic expression program involving the Haa1p-regulon in *Saccharomyces cerevisiae* response to acetic Acid. *OMICS: A Journal of Integrative Biology, 14*(5), 587-601.

Mira, N. P., Henriques, S. F., Keller, G., Teixeira, M. C., Matos, R. G., Arraiano, C. M., et al. (2011). Identification of a DNA-binding site for the transcription factor Haa1, required for *Saccharomyces cerevisiae* response to acetic acid stress. *Nucleic Acids Research, 39*(16), 6896-6907.

Modig, T., Liden, G., & Taherzadeh, M. J. (2002). Inhibition effects of furfural on alcohol dehydrogenase, aldehyde dehydrogenase and pyruvate dehydrogenase. *Biochemical Journal, 363*, 769-776.

Mollapour, M., & Piper, P. W. (2006). Hog1p mitogen-activated protein kinase determines acetic acid resistance in *Saccharomyces cerevisiae*. *FEMS Yeast Research, 6*(8), 1274-1280.

Mollapour, M., & Piper, P. W. (2007). Hog1 mitogen-activated protein kinase phosphorylation targets the yeast Fps1 aquaglyceroporin for endocytosis, thereby rendering cells resistant to acetic acid. *Molecular and Cellular Biology, 27*(18), 6446-6456.

Mollapour, M., Shepherd, A., & Piper, P. W. (2008). Novel stress responses facilitate *Saccharomyces cerevisiae* growth in the presence of the monocarboxylate preservatives. *Yeast, 25*(3), 169-177.

Mollapour, M., Shepherd, A., & Piper, P. W. (2009). Presence of the Fps1p aquaglyceroporin channel is essential for Hog1p activation, but suppresses Slt2(Mpk1)p activation, with acetic acid stress of yeast. *Microbiology, 155*(10), 3304-3311.

Mukhopadhyay, D., & Riezman, H. (2007). Proteasome-independent functions of ubiquitin in endocytosis and signaling. *Science, 315*, 201-205.

Murguía, J. R., Belles, J. M., & Serrano, R. (1996). The yeast *HAL2* nucleotidase is an *in vivo* target of salt toxicity. *The Journal of Biological Chemistry, 271*(46), 29029-29033.

Neumann, S., Petfalski, E., Brügger, B., Großhans, H., Wieland, F., Tollervey, D., et al. (2003). Formation and nuclear export of tRNA, rRNA and mRNA is regulated by the ubiquitin ligase Rsp5p. *EMBO reports, 4*(12), 1156-1162.

Nguyen, T. T. M., Iwaki, A., Ohya, Y., & Izawa, S. (2014). Vanillin causes the activation of Yap1 and mitochondrial fragmentation in *Saccharomyces cerevisiae*. *Journal of Bioscience and Bioengineering, 117*(1), 33-38.

Nikko, E., & Pelham, H. R. B. (2009). Arrestin-mediated endocytosis of yeast plasma membrane transporters. *Traffic, 10*(12), 1856-1867.

Novoselova, T. V., Zahira, K., Rose, R. S., & Sullivan, J. A. (2012). Bul proteins, a nonredundant, antagonistic family of ubiquitin ligase regulatory proteins. *Eukaryotic Cell, 11*(4), 463-470.

Obara, K., & Kihara, A. (2014). Signaling events of the Rim101 pathway occur at the plasma membrane in a ubiquitination-dependent manner. *Molecular and Cellular Biology, 34*(18), 3525-3534.

Orij, R., Urbanus, M. L., Vizeacoumar, F. J., Giaever, G., Boone, C., Nislow, C., et al. (2012). Genome-wide analysis of intracellular pH reveals quantitative control of cell division rate by pHc in *Saccharomyces cerevisiae*. *Genome Biology, 13*, 1-15.

O'Rourke, S. M., & Herskowitz, I. (2004). Unique and redundant roles for HOG MAPK pathway components as revealed by whole-genome expression analysis. *Molecular Biology of the Cell, 15*(2), 532-542.

Paiva, S., Vieira, N., Nondier, I., Haguenauer-Tsapis, R., Casal, M., & Urban-Grimal, D. (2009). Glucose-induced ubiquitylation and endocytosis of the yeast Jen1 transporter: ROLE OF LYSINE 63-LINKED UBIQUITIN CHAINS. *Journal of Biological Chemistry, 284*(29), 19228-19236.

Palmqvist, E., & Hahn-Hägerdal, B. (2000). Fermentation of lignocellulosic hydrolysates. II: inhibitors and mechanisms of inhibition. *Bioresource Technology, 74*, 25-33.

Pampulha, M. E., & Loureire-Dias, M. C. (1989). Combined effect of acetic acid, pH and ethanol on intracellular pH of fermenting yeast. *Applied Microbiology and Biotechnology, 31*, 547-550.

Pearce, A. K., Booth, I. R., & Brown, A. J. (2001). Genetic manipulation of 6-phosphofructo-1-kinase and fructose 2,6-bisphosphate levels affects the extent to which benzoic acid inhibits the growth of *Saccharomyces cerevisiae*. *Microbiology, 147*, 403-410.

Peña, P. V., Glasker, S., & Srienc, F. (2013). Genome-wide overexpression screen for sodium acetate resistance in *Saccharomyces cerevisiae*. *Journal of Biotechnology, 164*(1), 26-33.

Piper, P. W. (2011). Resistance of yeasts to weak organic acid food preservatives. *Advances in Applied Microbiology, 77*, 97-113.

Platara, M., Ruiz, A., Serrano, R., Palomino, A., Moreno, F., & Arino, J. (2006). The transcriptional response of the yeast Na^+-ATPase *ENA1* gene to alkaline stress involves three main signaling pathways. *Journal of Biological Chemistry, 281*(48), 36632-36642.

Polymenis, M., Jarmoszewicz, K., Łukasiak, K., Riezman, H., & Kaminska, J. (2012). Rsp5 ubiquitin ligase is required for protein trafficking in *Saccharomyces cerevisiae* COPI mutants. *PLoS ONE, 7*(6), e39582.

Posas, F., & Saito, H. (1997). Osmotic activation of the HOG MAPK pathway via Ste11p MAPKKK: scaffold role of Pbs2p MAPKK. *Science, 276*(5319), 1702-1705.

Posas, F., Witten, E. A., & Saito, H. (1998). Requirement of STE50 for osmostress-induced activation of the STE11 mitogen-activated protein kinase kinase kinase in the high-osmolarity glycerol response pathway. *Molecular and Cellular Biology, 18*(10), 5788-5796.

Proft, M., & Serrano, R. (1999). Repressors and upstream repressing sequences of the stress-regulated *ENA1* gene in *Saccharomyces cerevisiae*: bZIP protein Sko1p confers HOG-dependent osmotic regulation. *Molecular and Cellular Biology, 19*(1), 537-546.

Proft, M., & Struhl, K. (2002). Hog1 kinase converts the Sko1-Cyc8-Tup1 repressor complex into an activator that recruits SAGA and SWI/SNF in response to osmotic stress. *Molecular Cell, 9*, 1307-1317.

Raitt, D. C., Posas, F., & Saito, H. (2000). Yeast Cdc42 GTPase and Ste20 PAK-like kinase regulate Sho1-dependent activation of the Hog1 MAPK pathway. *The EMBO Journal, 19*(17), 4623-4631.

Reggiori, F., & Pelham, H. R. B. (2001). Sorting of proteins into multivesicular bodies: ubiquitin-dependent and -independent targeting. *The EMBO Journal, 20*(18), 5176-5186.

Reid, J., & Svejstrup, J. Q. (2004). DNA damage-induced Def1-RNA polymerase II interaction and Def1 requirement for polymerase ubiquitylation in vitro. *Journal of Biological Chemistry, 279*(29), 29875-29878.

Reiser, V., Raitt, D. C., & Saito, H. (2003). Yeast osmosensor Sln1 and plant cytokinin receptor Cre1 respond to changes in turgor pressure. *The Journal of Cell Biology, 161*(6), 1035-1040.

Reiser, V., Salah, S. M., & Ammerer, G. (2000). Polarized localization of yeast Pbs2 depends on osmostress, the membrane protein Sho1 and Cdc42. *Nature Cell Biology, 2*, 620-627.

Rodriguez, M. S., Gwizdek, C., Haguenauer-Tsapis, R., & Dargemont, C. (2003). The HECT ubiquitin ligase Rsp5p is required for proper nuclear export of mRNA in *Saccharomyces cerevisiae*. *Traffic, 4*, 566-575.

Rotin, D., & Kumar, S. (2009). Physiological functions of the HECT family of ubiquitin ligases. *Nature Reviews Molecular Cell Biology, 10*(6), 398-409.

Rotin, D., & Staub, O. (2012). Nedd4-2 and the regulation of epithelial sodium transport. *Frontiers in Physiology, 3*.

Ruiz, A., & Arino, J. (2007). Function and regulation of the *Saccharomyces cerevisiae* ENA sodium ATPase system. *Eukaryotic Cell, 6*(12), 2175-2183.

Saito, H. (2001). Histidine phosphorylation and two-component signaling in eukaryotic cells. *Chemical Reviews, 101*, 2497-2509.

Saito, H. (2003). The Sln1-Ypd1-Ssk1 multistep phosphorelay system that regulates an osmosensing MAP kinase cascade in yeast. In *Histidine Kinases in Signal Transduction*, M. Inouye, and R. Dutta, eds. (San Diego: Academic Press), pp. 397–419.

Sánchez, Ó. J., & Cardona, C. A. (2008). Trends in biotechnological production of fuel ethanol from different feedstocks. *Bioresource Technology, 99*(13), 5270-5295.

Sasaki, T., & Takagi, H. (2013). Phosphorylation of a conserved Thr357 in yeast Nedd4-like ubiquitin ligase Rsp5 is involved in down-regulation of the general amino acid permease Gap1. *Genes to Cells, 18*(6), 459-475.

Serrano, R. (1996). Salt tolerance in plants and microorganisms: toxicity targets and defense responses. *International Review of Cytology, 165*, 1-52.

Serrano, R., Ruiz, A., Bernal, D., Chambers, J. R., & Arino, J. (2002). The transcriptional response to alkaline pH in *Saccharomyces cerevisiae*: evidence for calcium-mediated signalling. *Molecular Microbiology, 46*(5), 1319-1333.

Shcherbik, N., Kee, Y., Lyon, N., Huibregtse, J. M., & Haines, D. S. (2004). A single PXY motif located within the carboxyl terminus of Spt23p and Mga2p mediates a physical and functional interaction with ubiquitin ligase Rsp5p. *Journal of Biological Chemistry, 279*(51), 53892-53898.

Shcherbik, N., Zoladek, T., Nickels, J. T., & Haines, D. S. (2003). Rsp5p is required for ER bound Mga2p120 polyubiquitination and release of the processed/tethered transactivator Mga2p90. *Current Biology, 13*(14), 1227-1233.

Shiga, T., Yoshida, N., Shimizu, Y., Suzuki, E., Sasaki, T., Watanabe, D., et al. (2014). Quality control of plasma membrane proteins by *Saccharomyces cerevisiae* Nedd4-like ubiquitin ligase Rsp5p under environmental stress conditions. *Eukaryotic Cell, 13*(9), 1191-1199.

Simoes, T., Mira, N. P., Fernandes, A. R., & Sa-Correia, I. (2006). The *SPI1* gene, encoding a glycosylphosphatidylinositol-anchored cell wall protein, plays a prominent role in the development of yeast resistance to lipophilic weak-acid food preservatives. *Applied and Environmental Microbiology, 72*(11), 7168-7175.

Smardon, A. M., & Kane, P. M. (2014). Loss of vacuolar H^+-ATPase activity in organelles signals ubiquitination and endocytosis of the yeast plasma membrane proton pump Pma1p. *Journal of Biological Chemistry, 289*(46), 32316-32326.

Soetens, O., De Craene, J. O., & Andre, B. (2001). Ubiquitin is required for sorting to the vacuole of the yeast general amino acid permease, Gap1. *Journal of Biological Chemistry, 276*(47), 43949-43957.

Springael, J. Y., De Craene, J. O., & Andre, B. (1999a). The yeast Npi1/Rsp5 ubiquitin ligase lacking its N-terminal C2 domain is competent for ubiquitination but not for subsequent endocytosis of the Gap1 permease. *Biochemical and Biophysical Research Communications, 257*, 561-566.

Springael, J. Y., Galan, J. M., Haguenauer-Tsapis, R., & Andre, B. (1999b). NH_4^+-induced down-regulation of the *Saccharomyces cerevisiae* Gap1p permease involves its ubiquitination with lysine-63-linked chains. *Journal of Cell Science, 112*, 1375-1383.

Stawiecka-Mirota, M., Pokrzywa, W., Morvan, J., Zoladek, T., Haguenauer-Tsapis, R., Urban-Grimal, D., et al. (2007). Targeting of Sna3p to the endosomal pathway depends on its interaction with Rsp5p and multivesicular body sorting on its ubiquitylation. *Traffic, 8*(9), 1280-1296.

Stimpson, H. E., Lewis, M. J., & Pelham, H. R. (2006). Transferrin receptor-like proteins control the degradation of a yeast metal transporter. *The EMBO Journal, 25*, 662-672.

Strasser, K., Masuda, S., Mason, P., Pfannstiel, J., Oppizzi, M., Rodriguez-Navarro, S., et al. (2002). TREX is a conserved complex coupling transcription with messenger RNA export. *Nature, 417*(304-308).

Stratford, M., Nebe-von-Caron, G., Steels, H., Novodvorska, M., Ueckert, J., & Archer, D. B. (2013). Weak-acid preservatives: pH and proton movements in the yeast *Saccharomyces cerevisiae*. *International Journal of Food Microbiology, 161*(3), 164-171.

Stukey, J. E., McDonough, V. M., & Martin, C. E. (1989). Isolation and characterization of *OLE1*, a gene affecting fatty acid desaturation from *Saccharomyces cerevisiae*. *The Journal of Biological Chemistry, 264*(28), 16537-16544.

Sudol, M. (1996). Structure and function of the WW domain. *Progress in Biophysics and Molecular Biology 65*, 113-132.

Sullivan, J. A., Lewis, M. J., Nikko, E., & Pelham, H. R. B. (2007). Multiple interactions drive adaptor-mediated recruitment of the ubiquitin ligase Rsp5 to membrane proteins in vivo and in vitro. *Molecular Biology of the Cell, 18*(7), 2429-2440.

Tanaka, K., Ishii, Y., Ogawa, J., & Shima, J. (2012). Enhancement of acetic acid tolerance in *Saccharomyces cerevisiae* by overexpression of the *HAA1* gene, encoding a transcriptional activator. *Applied and Environmental Microbiology, 78*(22), 8161-8163.

Tanaka, K., Tatebayashi, K., Nishimura, A., Yamamoto, K., Yang, H. Y., & Saito, H. (2014). Yeast osmosensors Hkr1 and Msb2 activate the Hog1 MAPK cascade by different mechanisms. *Science Signaling, 7*(314), 1-10.

Ullah, A., Orij, R., Brul, S., & Smits, G. J. (2012). Quantitative analysis of the modes of growth inhibition by weak organic acids in *Saccharomyces cerevisiae*. *Applied and Environmental Microbiology, 78*(23), 8377-8387.

Urbanowski, J. L., & Piper, R. C. (2001). Ubiquitin sorts proteins into the intralumenal degradative compartment of the late-endosome/vacuole. *Traffic, 2*, 622-630.

Van Wuytswinkel, O., Reiser, V., Siderius, M., Kelders, M. C., Ammerer, G., Ruis, H., et al. (2000). Response of *Saccharomyces cerevisiae* to severe osmotic stress: evidence for a novel activation mechanism of the HOG MAP kinase pathway. *Molecular Microbiology, 37*(2), 382-397.

Vilela-Moura, A., Schuller, D., Mendes-Faia, A., Silva, R. D., Chaves, S. R., Sousa, M. J., et al. (2011). The impact of acetate metabolism on yeast fermentative performance and wine quality: reduction of volatile acidity of grape musts and wines. *Applied Microbiology and Biotechnology, 89*(2), 271-280.

Wadskog, I., Forsmark, A., Rossi, G., Konopka, C., Oyen, M., Goksor, M., et al. (2006). The yeast tumor suppressor homologue Sro7p is required for targeting of the sodium pumping ATPase to the cell surface. *Molecular Biology of the Cell, 17*(12), 4988-5003.

Wang, G., Yang, J., & Huibregtse, J. M. (1999). Functional domains of the Rsp5 ubiquitin-protein ligase. *Molecular and Cellular Biology, 19*(1), 342-352.

Watanabe, D., Murai, H., Tanahashi, R., Nakamura, K., Sasaki, T., & Takagi, H. (2015). Cooperative and selective roles of the WW domains of the yeast Nedd4-like ubiquitin ligase Rsp5 in the recognition of the arrestin-like adaptors Bul1 and Bul2. *Biochemical and Biophysical Research Communications, 463*(1-2), 76-81.

Wieland, J., Nitsche, A. M., Strayle, J., Steiner, H., & Rudolph, H. K. (1995). The *PMR2* gene cluster encodes functionally distinct isoforms of a putative Na^+ pump in the yeast plasma membrane. *The EMBO Journal, 14*(16), 3870-3882.

Wijayanti, I., Watanabe, D., Oshiro, S., & Takagi, H. (2014). Isolation and functional analysis of yeast ubiquitin ligase Rsp5 variants that alleviate the toxicity of human α-synuclein. *Journal of Biochemistry, 157*(4), 251-260.

Winston, F. (1993). *RSP5* alleles can suppress *SPT3* mutations. *Personal Communication to SGD*.

Yashiroda, H., Oguchi, T., Yasuda, Y., Toh-e, A., & Kikuchi, Y. (1996). Bul1, a new protein that binds to the Rsp5 ubiquitin ligase in *Saccharomyces cerevisiae*. *Molecular and Cellular Biology*, *16*(7), 3255-3263.

Young, B. P., Shin, J. J., Orij, R., Chao, J. T., Li, S. C., Guan, X. L., et al. (2010). Phosphatidic acid is a pH biosensor that links membrane biogenesis to metabolism. *Science*, *329*(5995), 1085-1088.

Zenklusen, D., Vinciguerra, P., Wyss, J. C., & Stutz, F. (2002). Stable mRNP formation and export require cotranscriptional recruitment of the mRNA export factors Yra1p and Sub2p by Hpr1p. *Molecular and Cellular Biology*, *22*(23), 8241-8253.

Zhang, S., Skalsky, Y., & Garfinkel, D. J. (1999). *MGA2* or *SPT23* is required for transcription of the D9 fatty acid desaturase gene, *OLE1*, and nuclear membrane integrity in *Saccharomyces cerevisiae*. *Genetics, 151*, 473-483.

Zhao, Y., MacGurn, J. A., Liu, M., & Emr, S. D. (2013). The ART-Rsp5 ubiquitin ligase network comprises a plasma membrane quality control system that protects yeast cells from proteotoxic stress. *eLife, 2*, 1-18.

Zaldivar, J., Nielsen, J., & Olsson, L. (2001). Fuel ethanol production from lignocellulose: a challenge for metabolic engineering and process integration. *Applied Microbiology and Biotechnology*, *56*(1), 17-34.